e-ISSN:2687-6698

Turkish Journal of Analytical Chemistry

2019

Volume 3
Issue 1
June 2021

www.turkjac.org

e-ISSN: 2687-6698

https://dergipark.org.tr/tr/pub/turkjac

Turkish Journal of Analytical Chemistry

TurkJAC

Volume 3
Issue 1
June 2021

Publication Type: Peer-reviewed scientific journal
Publication Date: June 29, 2021
Publication Language: English
Published two times in a year (June, December)

Authorship, Originality, and Plagiarism: The authors accept that the work is completely original and that the works of others have been appropriately cited or quoted in the text with the necessary permissions. The authors should avoid plagiarism. It is recommended that they check the article using appropriate software such as Ithenticate and CrossCheck. The responsibility for this matter rests entirely with the authors. All authors will be notified when the manuscript is submitted. If a change of author is needed, the reason for the change should be indicated. Once the manuscript is accepted, no author changes can be made.

Aims and Scope

"Turkish Journal of Analytical Chemistry" publishes original full-text research articles and reviews covering a variety of topics in analytical chemistry. Original research articles may be improved versions of known analytical methods. However, studies involving new and innovative methods are preferred. Topics covered include:

- Analytical materials
- Atomic methods
- Biochemical methods
- Chromatographic methods
- Electrochemical methods
- Environmental analysis
- Food analysis
- Forensic analysis
- Optical methods
- Pharmaceutical analysis
- Plant analysis
- Theoretical calculations
- Nanostructures for analytical purposes
- Chemometric methods

ETHICAL GUIDELINES

TurkJAC follows ethical tasks and responsibilities are defined by the Committee on Publication Ethics (COPE) in publication procedure. Based on this guide, the rules regarding publication ethics are presented in the following sections.

Ethical Approval

Ethics committee approval must be obtained for studies on clinical and experimental regarding human and animals that require an ethical committee decision, this approval must be stated in the article and documented in the submission. In such articles, the statement that research and publication ethics are complied with should include. Information about the approval such as committee name, date, and number should be included in the method section and also on the first/last page of the article.

Editors

1. In the preliminary evaluation of a submission, the editor of the journal evaluates the article's suitability for the purpose and scope of the journal, whether it is similar to other articles in the literature, and whether it meets the expectations regarding the language of writing. When it meets the mentioned criteria, the scientific evaluation process is started by assigning a section editor if necessary.
2. A peer-reviewed publication policy is employed in all original studies, taking into full account of possible problems due to related or conflicting interests.
3. Section editors work on the articles with a specific subject and their suggestion is effective in the journal editor's decision about acceptance or rejection of the article.
4. No section editor contacts anyone except the authors, reviewers, and the journal editor about articles in the continued evaluation process.
5. In the journal editor's decision to accept or reject an article, in the addition of section editor's suggestion in consequence of scientific reviewing, the importance of the article, clarity and originality are decisive. The final decision, in this case, belongs to the journal editor.

Authors

1. The authors should actively contribute to the design and execution of the work. Authorship should not be given to a person who does not have at least one specific task in the study.
2. Normally all authors are responsible for the content of the article. However, in interdisciplinary studies with many authors, the part that each author is responsible for should be explained in the cover letter.
3. Before the start of the study, it would be better to determine the authors, contributors, and who will be acknowledged in order to avoid conflict in academic credits.
4. The corresponding author is one of the authors of the article submitted to the journal for publication. All communications will be conducted with this person until the publication of the article. The copyright form will be signed by the corresponding author on all the authors' behalf.
5. It is unacceptable to submit an article that has already been published entirely or partly in other publication media. In such situation, the responsibility lies with all authors. It is also unacceptable that the same article has been sent to TurkJAC and another journal simultaneously for publication. Authors should pay attention to this situation in terms of publication ethics.
6. Plagiarism from others' publications or their own publications and slicing of the same study is not acceptable.
7. All authors agree that the data presented in the article are real and original. In case of an error in the data presented, the authors have to be involved in the withdraw and correction process.
8. All authors must contribute to the peer-reviewed procedure.

Reviewers

1. Peer reviewers worked voluntarily are external experts assigned by editors to improve the submitted article.
2. It is extremely important that the referee performs the review on time so that the process does not prolong. Therefore, when the invitation is agreed upon, the reviewer is expected to do this on time. Also, the reviewer agrees that there are no conflicts of interest regarding the research, the authors, and/or the research funders.
3. Reviewers are expected not to share the articles reviewed with other people. The review process should be done securely.
4. Reviewers are scored according to criteria such as responding to the invitations, whether their evaluations are comprehensive and acting in accordance with deadlines, and the article submissions that they can make to TurkJAC are handled with priority.

Contents

Reviews

Research Articles

*Author of correspondence:

e-ISSN: 2687-6698 **Review**

Turkish Journal of Analytical Chemistry

TurkJAC www.turkjac.org 2019

A review on recent electroanalytical methods for the analysis of antiviral COVID-19 drugs

Deniz Emre[1], Nuran Özaltın[2], Selehattin Yılmaz[3]*

[1]Çanakkale Onsekiz Mart University, School of Health, Pharmacy Services Program 17100 Çanakkale, Turkey
[2]Hacettepe University, Faculty of Pharmacy, Department of Analytical Chemistry, 06100, Ankara, Turkey
[3]Çanakkale Onsekiz Mart University, Faculty of Science and Arts, Department of Chemistry, 17100 Çanakkale, Turkey

Abstract

Currently, there are no specific drugs for the severe acute respiratory syndrome coronavirus 2 (SARS-CoV-2) infection, designated as coronavirus disease 2019 (COVID-19). Several therapeutic options, including antiviral, antithrombotic, immunosuppressive, and anti-rheumatic drugs, are researched worldwide. Analytical methods are needed in every step of the innovation, research, development, and manufacturing process of pharmaceuticals. Therefore, new analytical methods for pharmaceuticals are developed and validated increasingly over time. In this review, recent reports on electroanalytical techniques for the determination of selected COVID-19 drugs, favipiravir (FAV), remdesivir (REM), lopinavir (LOP) / ritonavir (RIT), hydroxychloroquine (HCQ), chloroquine (CQ), ribavirin (RIB), and sofosbuvir (SOF) were emphasized. Electroanalysis of antiviral active pharmaceutical ingredients carried out at various modified or non-modified electrodes by cyclic voltammetry (CV), linear sweep voltammetry (LSV), differential pulse voltammetry (DPV), square wave voltammetry (SWV), square-wave adsorptive stripping voltammetry (SWAdSV), differential pulse stripping voltammetry (DPSV); adsorptive stripping differential pulse voltammetry (AdSDPV), chronocoulometry (CC) and chronoamperometry (CA) were compiled from the literature. The effects of supporting electrolyte and pH on the current and potential of the analytical signal were evaluated. Scan rate results obtained by the CV method showed whether the redox process of the drug active ingredient diffusion or adsorption controlled at the electrode used in the selected solvent-supporting electrolyte and pH systems. Linearity range and the limit of detection (LOD) of applied electroanalytical methods were compared by combining the results obtained from drug active ingredients given in references.

Keywords: Antiviral drugs, pandemic, coronavirus, Covid-19, analysis, determination, electroanalytical methods

1. Introduction

There are no specific drugs and tests for the treatment of acute respiratory syndrome coronavirus 2 (SARS-CoV-2) infection, designated as the COVID-19 [1]. Repurposing (or repositioning) of existing drugs, such as antivirals for other viruses, anti-rheumatics, corticosteroids, anticoagulants, and other drugs have been used for COVID-19 treatment [2-4].

Although pharmacopeias include many standard methods of analysis, they do not include all pharmaceutical substances. Therefore, developing and validating new analytical methods for pharmaceutical analysis is always needed. This approach makes numerous studies in the literature in a short period, which is hard to follow all of them regularly. That is why reviews are useful; they provide an overview of many methods in a single article, as well as suggest future research directions [5].

After brief information on COVID-19, existing COVID-19 drug regimens, and mechanisms of drug action; this review is focused on recent electroanalytical methods for the analysis of antiviral COVID-19 drugs.

1.1. Coronavirus Infection (COVID-19)

COVID-19 disease, which is caused by a new coronavirus called SARS-CoV-2, is identified by the World Health Organization (WHO) on 31 Dec 2019, following a cluster of case reports on viral pneumonia in Wuhan, China. In a short time, the disease has spread worldwide, and WHO declared the COVID-19 pandemic [6-9].

Citation: D. Emre, N. Özaltın, S. Yılmaz, A review on recent electroanalytical methods for the analysis of antiviral COVID-19 drugs, Turk J Anal Chem, 3(1), 2021, 1-8.

https://doi.org/10.51435/turkjac.935765

***Author of correspondence:** seletyilmaz@hotmail.com
Tel: +90 286 218 00 18
Fax +90 286 218 05 33
Received: May 10, 2021
Accepted: June 06, 2021

According to WHO COVID-19 Dashboard, as of 6 May 2021, there have been 155,506,494 confirmed cases of COVID-19, including 3,247,228 deaths worldwide reported to WHO, and as of 4 May 2021, a total of 1,170,942,729 vaccine doses have been administered. There are no specific drugs for the treatment of COVID-19 but, several APIs, including REM, LOP + RIT combinations, CQ, and HCQ, were suggested in the WHO's Solidarity Therapeutics Trial [6,7,10-12]. Despite the initial reports of success, a recent interim report released by the WHO's Solidarity Therapeutics Trial concluded that REM, HCQ, LOP + RIT, and interferon regimens have little or no effect on 28-day mortality or the hospitalization course of COVID-19 patients and some APIs are under clinical trials [10-14].

Coronaviruses are single-stranded RNA viruses. Six types of coronaviruses, which cause infection in humans, have been reported since the 1960s. For example, SARS-CoV-2 is a type of coronavirus that causes COVID-19. This respiratory illness is defined as various known symptoms containing cough, fever, difficulty breathing, fatigue, conjunctivitis, sore throat, headache changes in the sense of taste and smell. A few antiviral drugs are approved for different infections, or new alternative APIs are under trials for COVID-19 treatment [6,15-22].

1.2. COVID-19 Drugs

SARS-CoV-2 has high contagiousness that causes a considerable risk for the health system. Therefore, many studies are undergoing on a few antiviral drugs, which have been approved for various infections, and tested in different countries [6,9,15-22]. Analytical methods play an important role in these studies, and electroanalytical methods are also of great importance too. A list of some electroactive antiviral compounds used for the treatment of COVID-19 was given in Table 1.

1.3. General information on selected electroactive antiviral Covid-19 drugs

General information on COVID-19 drugs selected for this review is summarized below.

1.3.1. Favipiravir (FAV)

FAV (6-fluoro-3-hydroxy-2-pyrazincarboxamide) is an inhibitor of RNA replication from an RNA template catalyzed by RNA polymerase enzyme [1]. FAV was approved as an antiviral for influenza viruses (avian flu and others) in Japan in 2014. It has been used to treat COVID-19 disease [1,6,23].

1.3.2. Remdesivir (REM)

REM is a new antiviral drug belonging to the class of nucleotide analogues [24,25]. The clinical trials have confirmed the efficiency of REM [26,27]. It manifested exclusive efficiency and activity against COVID-19 in patients with mild and moderate symptoms. It was the first EU-approved drug against COVID-19 [27-31]. Moreover, as it contains a nitrile group, it may show high toxicity if taken in excess [32-35]. REM has been previously administered to West African Ebola virus patients [27]. The mechanism of action of REM is based on viral RNA-dependent RNA polymerase inhibition. REM is a phosphoramidate prodrug of an analogue of adenine-C-nucleoside structure. REM is metabolized into its active form, which is a competitive inhibitor of RNA synthesis [35].

1.3.3. Lopinavir + Ritonavir (LOP + RIT)

LOP + RIT is an inhibitor of the human immunodeficiency virus (HIV) protease, whose main structure is different from the SARS-CoV-2 counterpart (3CLpro) [26,27,32]. This state would affect the inhibition efficiency of LOP+RIT and raise doubt on the efficacy of LOP + RIT for COVID-19 treatment [26,27,36,37], and WHO has discontinued LOP + RIT use in COVID-19 treatment [2,38].

1.3.4. Hydroxychloroquine (HCQ) and Chloroquine (CQ)

HCQ and CQ are used in the treatment of malaria, discoid lupus erythematosus, and rheumatoid arthritis. In addition, they have been used as antivirals in the treatment of COVID-19 disease [7, 39-41]. HCQ and CQ were thought to be inhibiting the pre-entry step of the viral cycle by interfering with viral particles binding to their cellular cell surface receptors. It was also thought that the intracellular site of SARS-CoV-2 budding was determined by the localization of its membrane M proteins that accumulate in the Golgi complex beyond the site of virion budding, suggesting a possible action of HCQ or CQ at this step of the replication cycle of the virus [7]. However, according to a study on mortality outcomes with HCQ in COVID-19, it is found that HCQ is associated with increased mortality in COVID-19 patients. Also, there is no benefit of CQ [13]. Therefore, WHO has discontinued HCQ and CQ use in COVID-19 treatment [2,38]. Nowadays, in some countries such as Turkey, HCQ use in COVID-19 treatment was discontinued [42].

HCQ had been previously used as an antiviral agent in COVID-19 treatment [7], and has been discontinued nowadays [2,13,38]. But, HCQ has been analyzed by electroanalytical methods recently [39-41]. These methods can be used in further studies, such as toxicological studies on patients who had used HCQ in the past. Therefore, electroanalytical studies on HCQ are included in this review.

Table 1. Antiviral COVID-19 drugs included in this review

Active pharmaceutical ingredient (API)	Therapeutic group	Mechanism of action	Chemical structure	References
FAV	Antiviral	Viral RNA polymerase inhibitor	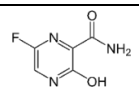	[6,23]
REM	Antiviral	Viral RNA polymerase inhibitor	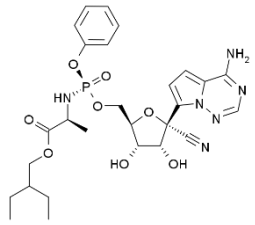	[24,25]
LOP + RIT	Antiretroviral	Protease inhibitor	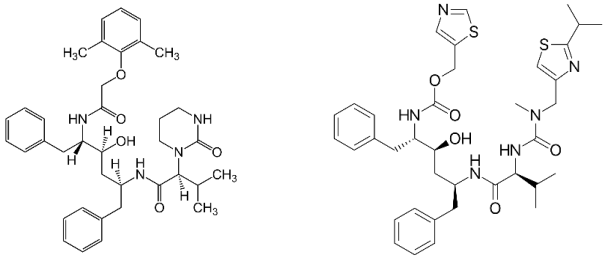 LOP RIT	[26,27]
CQ, HCQ	Antirheumatic and antiviral	Cytokine storm inhibitor, viral-cellular binding inhibitor, and viral replication inhibitor	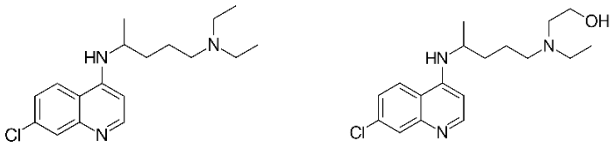 CQ HCQ	[7,38-42]
RIB	Antiviral	Viral RNA polymerase inhibitor	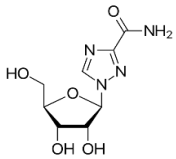	[4]
SOF	Antiviral	Viral RNA polymerase inhibitor	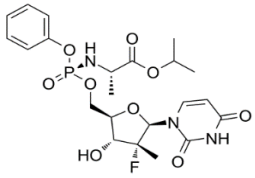	[4]

1.3.5. Ribavirin (RIB)

Some nucleotide analogues terminate RNA synthesis catalyzed by polymerases of coronaviruses. Computational chemistry studies, including sequence analysis, modeling, and molecular docking experiments, showed that some nucleotide analogue antiviral drugs can be used to prevent viral replication in infected cells. RIB is one of the RNA-dependent RNA polymerase enzyme inhibitors, which is used for the treatment of hepatitis C virus infections. RIB can also be used against other RNA viruses, such as zika virus and coronaviruses [4].

1.3.6. Sofosbuvir (SOF)

SOF is another nucleotide derivative that is used against Hepatitis C Virus and also SARS-CoV-2. SOF competes with physiological nucleotide for RNA-dependent RNA polymerase enzyme active site, competitively inhibits viral RNA polymerase, and by the way, it prevents viral replication of SARS-CoV-2 in infected cells [4].

2. Electrochemical behavior and determination of antiviral COVID-19 drugs

This current review reported the most recent and relevant literature dealing with the electroanalytical determination of COVID-19 antiviral drugs in pharmaceutical preparations and biological samples (such as urine and plasma). Thus, selective and sensitive electroanalytical methods are needed for these complicated samples [1].

Recent developments in technology make electroanalytical determinations more selective, sensitive, rapid, and easy than other methods and applicable for most pharmaceutical and chemical analysis fields. As a result, electrochemical methods

nowadays enable trace analysis for pharmaceuticals with a sufficient degree of precision, accuracy, selectivity, sensitivity, and reproducibility.

Electroanalytical determination of drugs can be used for understanding their pharmacokinetic properties (adsorption, distribution, metabolism, and elimination). In addition, the determination of APIs in biologic samples is useful for new drug development, bio-equivalence, toxicology, and drug-monitoring studies [43,44].

In this review, various electro-analytical methods for the determination of COVID-19 drugs in different samples available literature are summarized as below:

2.1. FAV

Investigation of the literature revealed that three studies had been carried out for the quantification of FAV by High-Performance Liquid Chromatography (HPLC) with ultraviolet (UV) detector [6,45], spectrofluorimetric [6,46], and electroanalytical methods [6]. Electroanalytical techniques are versatile analytical techniques that can easily solve many problems of pharmaceutical interest. Varieties of techniques are available to researchers to study the electrochemistry of electroactive species in solution. Particularly voltammetry is a practical electroanalytical technique that offers high sensitivity, selectivity, precision, and accuracy, a wide linear range, and low-cost instrumentation and time.

The electrochemical behavior and determination of FAV were carried out first time in pharmaceutical and biological samples at Boron Doped Diamond (BDD) electrode by CV and SWAdSV [6]. Some of the analysis parameters, such as concentration range and LOD values, were given in Table 2.

2.2. REM

Electroanalytical methods studied on similar molecular structures with the analyte can be useful when the analyte does not have a validated electroanalytical method. A theoretically evaluated electrochemical determination of REM by correspondent mathematical model analysis, made by linear stability theory and bifurcation analysis, has been studied on an anodic process using a Squaraine Dye-Ag_2O_2 composite. In this theoretical study, it was reported that the composite has electroanalytical efficiency as an electrode modifier [25]. The calculated LOD value was given in Table 2.

2.3. LOP + RIT

Simultaneous determination of RIT and some other antivirals in human plasma, using HPLC with combined ultraviolet absorbance and electrochemical (potentiometric) detector was studied [47].

Electrochemical Impedance Spectroscopy (EIS) was studied with nanomaterial-modified biosensors, which can be used in biosensing probes to determine the interaction between SARS-CoV-2 spike protein and drugs. SARS-CoV-2 enters human cells by binding its spike protein to the cell expressing angiotensin-converting enzyme 2 (ACE2). Some ACE2 inhibitors, as ramiprilat and perindoprilat, are found to be effective for inhibition of spike protein-ACE2 binding. EIS is concluded to be useful for developing biosensors for screening of modulators for S-protein-ACE2 binding [11]. A similar screening assay based on EIS was developed for the determination of protease inhibitors at picomolar levels, including LOP + RIT. The method was based on the immobilization of the thiol terminated ferrocene (Fc)-pepstatin conjugate on a single-walled carbon nanotube/gold nanoparticle modified gold electrode. The estimated inhibition constant (Ki) was reported for LOP + RIT as Ki = 20 ± 3 pmol/L [48]. A similar assay can be studied for SARS-CoV-2 protease inhibitors. Some of the analysis parameters, such as concentration range and LOD values, were given in Table 2.

2.4. HCQ

The sensitive electrochemical sensor was improved by the modification of a glassy carbon electrode (GCE) with a new Schiff base [41].

The electrochemical properties of HCQ in the existence of uric acid (UA) at the surface of the modified electrode were studied by the DPV technique. In addition, the effect of pH, scan rate on the current and potential signal of HCQ was studied. Finally, the nanosensor was economically developed for the analysis of actual samples [41]. So far, some electrochemical techniques applied for the analysis of HCQ and CQ are summarized in Table 2 [40,49-51].

CV and DPV methods containing accumulation and stripping steps were developed for the determination of CQ on modified carbon paste electrodes. Accumulation and trace measurement were carried on dsDNA modified carbon paste surface, which allowed a preconcentration step for CQ. Modification of the carbon paste electrode achieved higher sensitivity compared with the bare surface. The linear range was 1.0×10^{-7} - 1.0×10^{-5} mol/L and LOD was 3.0×10^{-8} mol/L at the dsDNA-modified electrode. The method was applied on serum, without sample pretreatment [52,53].

CV and DPV methods were developed for the determination of CQ using GCE electrode modified with reduced graphene oxide on tungsten disulfide WS2 quantum dots. A hydrothermal method was used for the WS_2 quantum dots synthesis.

Table 2. Summary of electrochemical studies of antiviral COVID-19 drugs

Drug name	Linear range	Limit of detection (LOD)	Method	Application media	Ref.
FAV	0.01 - 0.10 µg/Ml (6.4×10^{-8} - 6.4×10^{-7} M)	0.0028 µg/mL (1.8×10^{-8} M)	CV and SW-AdSV-BDD Electrode	Pharmaceutical tablets, Human urine	[6]
FAV	0.10 - 20.00 µg/mL (6.4×10^{-7} - 1.3×10^{-4} M)	0.023 µg/mL (1.5×10^{-7} M)	CV and SW-AdSV-BDD Electrode	Pharmaceutical tablets, Human urine	[6]
REM	(Theoretical study without experimental results)	(Theoretical study without experimental results)	EO-Squaraine Dye -Ag_2O_2 Composite	(Theoretical study without experimental results)	[25]
RIT	250 - 5000 ng/mL	12 ng/mL	HPLC-EC	Human plasma	[47]
LOP + RIT	20 - 1000 pmol/mL	10 pmol/mL	EIS- SWCNT/AuNP-Modified Gold Electrode	Clinical drug capsules	[48]
HCQ	2.00×10^{-5} - 5.00×10^{-4} mg/mL	11.29 mg/mL	DPV-GCE	Malaria drug (Plaquenil)	[40]
CQ	0.068 - 6.88 mg/mL	0.01 mg/mL	DPV-$Cu(OH)_2$ Nanowire-Modified CPE	Pharmaceutical tablet	[49]
HCQ	0.10 - 1.90 mmol/L	0.06 mmol/L	SWV-Cathodically Pretreated BDD Electrode	Spiked human blood serum	[50]
HCQ	0.01 - 0.25 µmol/L	2.00 nmol/L	SWV- Cathodically Pretreated BDD Electrode	Commercial pharmaceutical samples	[50]
HCQ	0.10 - 10.0 µmol/L	0.03 µmol/L	SWV-dsDNA/CPE	Commercial pharmaceutical samples	[50]
HCQ	0.13 - 13.30 µmol/L	0.02 µmol/L	SWV-CuNW/CPE	Commercial pharmaceutical samples	[50]
HCQ	1.0×10^{-5} - 1.0×10^{-2} mol/L 1.0×10^{-6} - 1.0×10^{-2} mol/L	7.90×10^{-6} mol/L 5.00×10^{-6} mol/L	ISE- PME and Modified-CPE	Pharmaceutical preparations and human urine	[51]
CQ	1.0×10^{-7} - 1.0×10^{-5} M	3.0×10^{-8} M	CV and DPSV- CPE modified with dsDNA	Human serum	[52,53]
CQ	0.5 - 82 µM	40 - 120 nM	CV and DPV- Modified GCE with rGO/ WS_2 Quantum Dots	Human serum and pharmaceutical formulations	[52,54]
HCQ	5.7×10^{-8} - 1.0×10^{-4} M	6.0 nM	AdSDPV,CV,CC and CA-MWCNTs/CPE	Pharmaceutical formulations and biological fluids	[52,55]
RIB	10.0-7.5×10^2 ng/mL	No data available	CV-APBA/ERGO/GCE	Pharmaceutical injections	[56]
RIB	1.0×10^{-10} - 2.0×10^{-7} mol/L	2.02×10^{-10} mol/L	SWASV-HMDE	Pharmaceutical dosage form, urine, and serum	[57]
SOF	1 - 400 nM	0.36 nM	CV and DPV-N,S@GQDs Electrode	Human plasma	[58,59]

DPV: Differential Pulse Voltammetry; SWV: Square Wave Voltammetry; CV: Cyclic Voltammetry; SWAdSV: Square-Wave Adsorptive Stripping Voltammetry; SWASV: Square-Wave Adsorptive Stripping Voltammetry; DPSV: Differential Pulse Stripping Voltammetry; AdSDPV: Adsorptive Stripping Differential Pulse Voltammetry; CC: Chronocoulometry; CA: Chronoamperometry; EO: Electrochemical Oscillations; ISE: Ion Selective Electrode, HPLC-EC: High Performance Liquid Chromatography-Electrochemical Detector; EIS: Electrochemical Impedance Spectroscopy; BDD: Boron-Doped Diamond; CPE : Carbon Paste Electrode; GCE : Glassy Carbon Electrode; PME: Polymeric Membrane Electrode; CuNW/CPE: Copper Nanowires/Carbon Paste Electrode; dsDNA/CPE: Double-Stranded DNA/Carbon Paste Electrode; SWCNT/AuNP-Modified Gold Electrode: Single-Walled Carbon Nanotube/Gold Nanoparticle Modified Gold Electrode; APBA/ERGO/GCE: 3-Aminophenylbornic Acid Electrochemically Reduced Graphene Oxide Modified Glassy Carbon Electrode; HMDE: Hanging Mercury Drop Electrode; N,S@GQDs: N,S co-doped graphene quantum dots electrode; CPE modified with dsDNA: Carbon Paste Electrode Modified with Double Stranded Deoxyribonucleic Acid; Modified-GCE with rGO/WS_2QDs: Modified Glassy Carbon Electrode with Reduced Graphene Oxide Layers Containing Tungsten Disulphite Quantum Dots; MWCNTs/CPE : Multiwalled Carbon Nanotubes/ Carbon Paste Electrode

The resulting composite material, containing WS2 quantum dots on reduced graphene oxide sheets, was deposited on a GCE to enhance electroactivity. CQ potential maximum was at 1.2 V (vs. AgCl/Ag) on the modified GCE. The linear range was 0.5 µM - 82 µM for CQ, and LOD was 40 - 120 nM (at S/N = 3). The method was applied to human serum and pharmaceutical formulations [52,54].

The determination of HCQ was carried on AdSDPV with multiwall carbon nanotube-modified carbon paste electrode. CV, CC, and CA were also studied on HCQ. Linear range was 5.7×10^{-8} M - 1×10^{-4} M, and LOD was 6.0 nM (S/N = 3) [52,55].

2.5. RIB

It was reported that RIB was not electrochemically active. Therefore, RIB was determined by an indirect electrochemical method, using boronic acid-functionalized modified GCE. Modification of the GCE was carried out by 3-aminophenylboronic acid-electrochemically reduced graphene oxide. CV reduction peak current of $[Fe(CN)_6]^{3-/4-}$ was measured

before and after the addition of RIB. After the modified GCE was immersed in RIB solution, complexation of RIB with boronic acid groups on the surface of the modified GCE caused steric effects, and CV reduction peak current of $[Fe(CN)_6]^{3-/4-}$ was decreased. The optimal reaction time between RIB and modified GCE surface was reported to be 10 min, pH was 7.5 and temperature was 15 °C. The linear range was 10.0 - 7.5 × 10^2 ng/mL. The developed method was applied on the determination of RIB in an injection and results were reported to be comparable with the standard HPLC method described in the Chinese Pharmacopoeia Commission [56].

SWAdSV was applied for the determination of RIB in pharmaceutical formulations and biological samples (urine and serum). The developed method was based on the reduction of RIB at hanging mercury drop electrode in Britton Robinson buffer at pH 10, after accumulation for 30 s at 50 mV potential, the peak was observed at 880 mV. The linear range was 1.0 × 10^{-10} - 2.0 × 10^{-7} mol/L and LOD was 2.02 × 10^{-10} mol/L [57]. Some of the analysis parameters, such as concentration range and LOD values, were given in Table 2.

2.6. SOF

A molecularly imprinted polymer was proposed for the electrochemical determination of SOF. The sensor was obtained by polymerization of p-amino thiophenol on N,S co-doped graphene quantum dots in the presence of gold nanoparticles to form a gold-sulfur covalent network. It was reported that the quantum dots improved the electron transfer rate, enhanced surface activity, and amplified the signal. DPV and CV were applied with the developed sensor. SOF linear concentration range was found to be 1 - 400 nM, and the LOD was 0.36 nM. SOF spiked human plasma was studied [58,59]. Some of the analysis parameters, such as concentration range and LOD values, were given in Table 2.

3. Conclusions

The main aim of pharmaceuticals is to make humans free from potential illness or prevent them from getting ill. There are no specific drugs against COVID-19. Therefore, drug repurposing is a useful method for COVID-19 treatment. Antiviral drugs, which were used against other viruses with similar mechanisms of viral replication, may also be effective against SARS-CoV-2. Studies in various fields focusing on this approach need electroanalytical methods for antiviral COVID-19 drugs. This review is focused on the electroanalytical methods developed for the analysis of antiviral COVID-19 drugs in pharmaceutical forms and biological samples such as in human serum and urine. The methods studied with various modified or non-modified electrodes were compiled from the literature. Quantitative analysis of antiviral COVID-19 drug active ingredients was investigated in terms of some validation parameters such as linearity range, LOD, and sensitivity. The review also highlights the advantages of the applied electroanalytical techniques. It is concluded that electroanalytical methods and electrochemical sensors offer some unique advantages over other analytical methods, and more electroanalytical studies on antiviral COVID-19 drugs are recommended for further research. Due to the lack of electroanalytical methods for the analysis of antiviral COVID-19 drugs in the literature, this review will shed light on new research studies by giving brief information about existing studies.

Disclosure statement

No potential conflict of interest was reported by the authors.

References

[1] M.A. Acquavia, L. Foti, R. Pascale, A. Nicolò, V. Brancaleone, T.R.I. Cataldi, G. Martelli, L. Scrano, G. Bianco, Detection and quantification of Covid-19 antiviral drugs in biological fluids and tissues, Talanta, 224, 2021, 121862.

[2] WHO solidarity trial consortium, repurposed antiviral drugs for COVID-19-interim who solidarity trial results, New Engl J Med, 384(6), 2021, 497-511.

[3] S. Dotolo, A. Marabotti, A. Facchiano, R. Tagliaferri, A review on drug repurposing applicable to COVID-19, Brief Bioinform, 22(2), 2021, 726-741.

[4] A.A. Elfiky, Anti-HCV, nucleotide inhibitors, repurposing against COVID-19, Life Sci, 248, 2020, 117477.

[5] S. Ahmed, M.S. Islam, B. Ullah, S. Kanti Biswas, M.A. Samad Azad, M.S. Hossain, A review article on pharmaceutical analysis of pharmaceutical industry according to pharmacopoeias, Orient J Chem, 36, 2020, 01-10.

[6] S. Allahverdiyeva, O. Yunusoğlu, Y. Yardım, Z. Şentürk, First electrochemical evaluation of favipiravir used as an antiviral option in the treatment of COVID-19: A study of its enhanced voltammetric determination in cationic surfactant media using a boron-doped diamond electrode, Anal Chim Acta, 1159, 2021, 338418.

[7] C.A. Devaux, J.-M. Rolain, P. Colson, D. Raoult, New insights on the antiviral effects of chloroquine against coronavirus: What to expect for COVID-19?, Int J Antimicrob Agents, 55, 2020, 105938.

[8] World Health Organization, Questions and Answers: What is COVID-19?, 2020, https://www.who.int/news-room/q-a-detail/coronavirus-disease-covid-19

[9] C. Sohrabi, Z. Alsafi, N. O'Neill, M. Khan, A. Kerwan, A. Al-Jabir, C. Iosifidis, R. Agha, World Health Organization declares global emergency: A review of the 2019 novel coronavirus (COVID-19), Int J Surg, 76, 2020, 71-76.

[10] E. Dong, H. Du, L. Gardner, An interactive web-based dashboard to track COVID-19 in real time, Lancet Infect Dis, 20 ,2020, 533-534.

[11] L.V. Kiew, C.Y. Chang, S.Y. Huang, P.W. Wang, C.H. Heh, C.T. Liu, C.H. Cheng, Y.X. Lu, Y.C. Chen, Y.X. Huang, S.Y. Chang, H.Y. Tsai, Y.A. Kung, PN. Huang, M.-H. Hsu, B.F. Leo, Y.Y. Foo,

C.H. Su, K.C. Hsu, P.H. Huang, C.J. Ng, A. Kamarulzaman, C.J. Yuan, D.B. Shieh, S.R. Shih, L.Y. Chung, C.C. Chang, Development of flexible electrochemical impedance spectroscopy-based biosensing platform for rapid screening of SARS-CoV-2 inhibitors, Biosens Bioelectron, 183, 2021, 113213.

[12] C. Harrison, Coronavirus puts drug repurposing on the fast track, Nat Biotechnol, 38, 2020, 379-381.

[13] C. Axfors, A.M. Schmitt, P. Janiaud, J. Van'T Hooft, S. Abd-Elsalam, E.F. Abdo, B.S. Abella, J. Akram, R.K. Amaravadi, D.C. Angus, Y.M. Arabi, S. Azhar, L.R. Baden, A.W. Baker, L. Belkhir, T. Benfield, M.A.H. Berrevoets, C.-P. Chen, T.-C. Chen, S.-H. Cheng, C.-Y. Cheng, W.-S. Chung, Y.Z. Cohen, L.N. Cowan, O. Dalgard, F.F. De Almeida E Val, M.V.G. De Lacerda, G.C. De Melo, L. Derde, V. Dubee, A. Elfakir, A.C. Gordon, C.M. Hernandez-Cardenas, T. Hills, A.I.M. Hoepelman, Y.-W. Huang, B. Igau, R. Jin, F. Jurado-Camacho, K.S. Khan, P.G. Kremsner, B. Kreuels, C.-Y. Kuo, T. Le, Y.-C. Lin, W.-P. Lin, T.-H. Lin, M.N. Lyngbakken, C. Mcarthur, B.J. Mcverry, P. Meza-Meneses, W.M. Monteiro, S.C. Morpeth, A. Mourad, M.J. Mulligan, S. Murthy, S. Naggie, S. Narayanasamy, A. Nichol, L.A. Novack, S.M. O'Brien, N.L. Okeke, L. Perez, R. Perez-Padilla, L. Perrin, A. Remigio-Luna, N.E. Rivera-Martinez, F.W. Rockhold, S. Rodriguez-Llamazares, R. Rolfe, R. Rosa, H. Røsjø, V.S. Sampaio, T.B. Seto, M. Shehzad, S. Soliman, J.E. Stout, I. Thirion-Romero, A.B. Troxel, T.-Y. Tseng, N.A. Turner, R.J. Ulrich, S.R. Walsh, S.A. Webb, J.M. Weehuizen, M. Velinova, H.-L. Wong, R. Wrenn, F.G. Zampieri, W. Zhong, D. Moher, S.N. Goodman, J.P.A. Ioannidis, L.G. Hemkens, Mortality outcomes with hydroxychloroquine and chloroquine in COVID-19 from an international collaborative meta-analysis of randomized trials, Nat Commun, 12, 2021, 2349.

[14] H. Pan, R. Peto, Q.A. Karim, M. Alejandria, A.M. Henao-Restrepo, C.H. García, M.-P. Kieny, R. Malekzadeh, S. Murthy, M.-P. Preziosi, S. Reddy, M.R. Periago, V. Sathiyamoorthy, J.-A. Røttingen, S. Swaminathan, Repurposed antiviral drugs for COVID-19 -interim WHO SOLIDARITY trial results, MedRxiv, 2020.

[15] A.R. Fehr, S. Perlman, Coronaviruses: An Overview of Their Replication and Pathogenesis, Methods in Molecular Biology, Editors: H. Maier, E. Bickerton, P. Britton, 2015, 1-23, USA, New-York.

[16] C.C. Lai, T.P. Shih, W.C. Ko, H.J. Tang, P.R. Hsueh, Severe acute respiratory syndrome coronavirus 2 (SARS-CoV-2) and coronavirus disease-2019 (COVID-19): The epidemic and the challenges, Int J Antimicrob Agents, 55, 2020, 105924.

[17] S.J. Chen, S.C. Wang, Y.C. Chen, Novel Antiviral Strategies in the Treatment of COVID-19: A Review, Microorganisms, 8, 2020, 1259.

[18] Y.A. Helmy, M. Fawzy, A. Elaswad, A. Sobieh, S.P. Kenney, A.A. Shehata, The COVID-19 Pandemic: A Comprehensive Review of Taxonomy, Genetics, Epidemiology, Diagnosis, Treatment, and Control, J Clin Med, 9, 2020, 1225.

[19] B. Udugama, P. Kadhiresan, H.N. Kozlowski, A. Malekjahani, M. Osborne, V.Y.C. Li, H. Chen, S. Mubareka, J.B. Gubbay, W.C.W. Chan, Diagnosing COVID-19, The Disease and Tools for Detection, ACS Nano, 14, 2020, 3822-3835.

[20] Y. Jin, H. Yang, W. Ji, W. Wu, S. Chen, W. Zhang, G. Duan, Virology, Epidemiology, Pathogenesis, and Control of COVID-19, Viruses, 12, 2020, 372.

[21] WHO Coronavirus Disease (COVID-2019) Dashboard, 2021, https://covid19.who.int.

[22] Y. Furuta, K. Takahashi, K. Shiraki, K. Sakamoto, D.F. Smee, D.L. Barnard, B.B. Gowen, J.G. Julander, J.D. Morrey, T-705 (favipiravir) and related compounds: Novel broad-spectrum inhibitors of RNA viral infections, Antivir Res, 82, 2009, 95-102.

[23] Y. Du, X. Chen, Favipiravir: pharmacokinetics and concerns about clinical trials for 2019-nCoV infection, Clin Pharmacol Ther, 108, 2020, 242-247.

[24] S. Bagheri Novir, M.R. Aram, Quantum mechanical studies of the adsorption of Remdesivir, as an effective drug for treatment of COVID-19, on the surface of pristine, COOH-functionalized and S-, Si- and Al- doped carbon nanotubes, Physica E, 129, 2021, 114668.

[25] V.V. Tkach, M.V. Kushnir, S.C. Oliveira, J.G. Ivanushko, A.V. Velyka, A.F. Molodianu, P.I. Yagodynets, Z.O. Kormosh, , L.V. Reis, O.V. Luganska, K.V. Palamarek, Y.L. Bredikhina, Theoretical Description for Anti-COVID-19 Drug Remdesivir Electrochemical Determination, Assisted by Squaraine Dye-Ag_2O_2 Composite, Biointerface Res Appl Chem, 11, 2021, 9201-9208.

[26] Cao, Y. Wang, D. Wen, W. Liu, J. Wang, G. Fan, L. Ruan, B. Song, Y. Cai, M. Wei, X. Li, J. Xia, N. Chen, J. Xiang, T. Yu, T. Bai, X. Xie, L. Zhang, C. Li, Y. Yuan, H. Chen, H. Li, H. Huang, S. Tu, F. Gong, Y. Liu, Y. Wei, C. Dong, F. Zhou, X. Gu, J. Xu, Z. Liu, Y. Zhang, H. Li, L. Shang, K. Wang, K. Li, X. Zhou, X. Dong, Z. Qu, S. Lu, X. Hu, S. Ruan, S. Luo, J. Wu, L. Peng, F. Cheng, L. Pan, J. Zou, C. Jia, J. Wang, X. Liu, S. Wang, X. Wu, Q. Ge, J. He, H. Zhan, F. Qiu, L. Guo, C. Huang, T. Jaki, F.G. Hayden, P.W. Horby, D. Zhang, C. Wang, A Trial of Lopinavir–Ritonavir in Adults Hospitalized with Severe Covid-19, New Engl J Med, 382, 2020, 1787-1799.

[27] M. Costanzo, M.A.R. Giglio, G.N. Roviello, SARS-CoV-2: Recent reports on antiviral therapies based on lopinavir/ritonavir, darunavir/umifenovir, hydroxychloroquine, remdesivir, favipiravir and other drugs for the treatment of the new coronavirus, Curr Med Chem, 27, 2020, 4536-4541.

[28] R.T. Eastman, J.S. Roth, K.R. Brimacombe, A. Simeonov, M. Shen, S. Patnaik, M.D. Hall, Remdesivir: A Review of its discovery and development leading to emergency use authorization for treatment of COVID-19, ACS Cent Sci, 6, 2020, 672-683.

[29] J. Grein, N. Ohmagari, D. Shin, G. Diaz, E. Asperges, A. Castagna, T. Feldt, G. Green, M.L. Green, F.-X. Lescure, E. Nicastri, R. Oda, K. Yo, E. Quiros-Roldan, A. Studemeister, J. Redinski, S. Ahmed, J. Bernett, D. Chelliah, D. Chen, S. Chihara, S.H. Cohen, J. Cunningham, A. D'Arminio Monforte, S. Ismail, H. Kato, G. Lapadula, E. L'Her, T. Maeno, S. Majumder, M. Massari, M. Mora-Rillo, Y. Mutoh, D. Nguyen, E. Verweij, A. Zoufaly, A.O. Osinusi, A. Dezure, Y. Zhao, L. Zhong, A. Chokkalingam, E. Elboudwarej, L. Telep, L. Timbs, I. Henne, S. Sellers, H. Cao, S.K. Tan, L. Winterbourne, P. Desai, R. Mera, A. Gaggar, R.P. Myers, D.M. Brainard, R. Childs, T. Flanigan, Compassionate Use of Remdesivir for Patients with Severe Covid-19, New Engl J Med, 382, 2020, 2327-2336.

[30] J.H. Beigel, K.M. Tomashek, L.E. Dodd, A.K. Mehta, B.S. Zingman, A.C. Kalil, E. Hohmann, H.Y. Chu, A. Luetkemeyer, S. Kline, D. Lopez De Castilla, R.W. Finberg, K. Dierberg, V. Tapson, L. Hsieh, T.F. Patterson, R. Paredes, D.A. Sweeney, W.R. Short, G. Touloumi, D.C. Lye, N. Ohmagari, M.-D. Oh, G.M. Ruiz-Palacios, T. Benfield, G. Fätkenheuer, M.G. Kortepeter, R.L. Atmar, C.B. Creech, J. Lundgren, A.G. Babiker, S. Pett, J.D. Neaton, T.H. Burgess, T. Bonnett, M. Green, M. Makowski, A. Osinusi, S. Nayak, H.C. Lane, Remdesivir for the Treatment of Covid-19-Final Report, New Engl J Med, 383, 2020, 1813-1826.

[31] S.C.J. Jorgensen, R. Kebriaei, L.D. Dresser, Remdesivir: review of pharmacology, pre-clinical data, and emerging clinical experience for COVID-19, Pharmacotherapy, 40, 2020, 659-671.

[32] V. Avataneo, A. De Nicolò, J. Cusato, M. Antonucci, A. Manca, A. Palermiti, C. Waitt, S. Walimbwa, M. Lamorde, G. Di Perri, A. D'Avolio, Development and validation of a UHPLC-MS/MS method for quantification of the prodrug remdesivir and its metabolite GS-441524: a tool for clinical pharmacokinetics of SARS-CoV-2/COVID-19 and Ebola virus disease, J Antimicrob Chemoth, 75, 2020, 1772-1777.

[33] T.P. Sheahan, A.C. Sims, S.R. Leist, A. Schäfer, J. Won, A.J. Brown, S.A. Montgomery, A. Hogg, D. Babusis, M.O. Clarke, J.E. Spahn, L. Bauer, S. Sellers, D. Porter, J.Y. Feng, T. Cihlar, R. Jordan, M.R. Denison, R.S. Baric, Comparative therapeutic efficacy of

remdesivir and combination lopinavir, ritonavir, and interferon beta against MERS-CoV, Nat Commun, 11, 2020, 1-14.
[34] C.J. Gordon, E.P. Tchesnokov, E. Woolner, J.K. Perry, J.Y. Feng, D.P. Porter, M. Götte, Remdesivir is a direct-acting antiviral that inhibits RNA-dependent RNA polymerase from severe acute respiratory syndrome coronavirus 2 with high potency, J Biol Chem, 295, 2020, 6785-6797.
[35] M. Sisay, Available evidence and ongoing clinical trials of remdesivir: Could it be a promising therapeutic option for COVID-19?, Front Pharmacol, 11, 2020, 1-6.
[36] Q. Wang, Y. Zhao, X. Chen, A. Hong, Virtual screening of approved clinic drugs with main protease (3CLpro) reveals potential inhibitory effects on SARS-CoV-2, J Biomol Struct Dyn. 2020, 1-11, 1817786.
[37] Y.W. Chen, C.P.B. Yiu, K.Y. Wong, Prediction of the SARS-CoV-2 (2019-nCoV) 3C-like protease (3CLpro) structure: virtual screening reveals velpatasvir, ledipasvir, and other drug repurposing candidates, F1000Research, 9, 2020, 129.
[38] WHO discontinues hydroxychloroquine and lopinavir/ritonavir treatment arms for COVID-19, 2020, https://www.who.int/news/item/04-07-2020-who-discontinues-hydroxychloroquine-and-lopinavir-ritonavir-treatment-arms-for-covid-19.
[39] A. Shrivastava, Analytical methods for the determination of hydroxychloroquine in various matrices, Int J Appl Pharm, 12, 2020, 55-61.
[40] M.L.P.M. Arguelho, J.F. Andrade, N.R. Stradiotto, Electrochemical study of hydroxychloroquine and its determination in Plaquenil by differential pulse voltammetry, J Pharmaceut Biomed, 32, 2003, 269-275.
[41] A. Khoobi, S.M. Ghoreishi, M. Behpour, Sensitive and selective determination of hydroxychloroquine in the presence of uric acid using a new nanostructure self-assembled monolayer modified electrode: optimization by multivariate data analysis, Analyst, 139, 2014, 4064-4072.
[42] Republic of Turkey, Ministry of Health, Discontiues hydroxychloroquine treatment in COVID-19 in guide for treatment of adult patients with COVID-19, 2021, https://covid19.saglik.gov.tr/Eklenti/40719/0/covid-19rehberieriskinhastayonetimivetedavipdf.pdf.
[43] J.S. Kang, M.H. Lee, Overview of Therapeutic Drug Monitoring, Korean J Intern Med, 24, 2009, 1.
[44] N.M. Cassiano, V.V. Lima, R.V. Oliveira, A.C. De Pietro, Q.B. Cass, Development of restricted-access media supports and their application to the direct analysis of biological fluid samples via high-performance liquid chromatography, Anal Bioanal Chem, 384, 2006, 1462-1469.
[45] I. Bulduk, HPLC-UV method for quantification of favipiravir in pharmaceutical formulations, Acta Chromatogr, 33, 2020, 209-215.
[46] S.M. Megahed, A.A. Habib, S.F. Hammad, A.H. Kamal, Experimental design approach for development of spectrofluorimetric method for determination of favipiravir; a potential therapeutic agent against COVID-19 virus: Application to spiked human plasma, Spectrochim Acta A, 249, 2021, 119241.
[47] E. Marchei, R. Pacifici, G. Tossini, R. Di Fava, L. Valvo, P. Zuccaro, Simultaneous liquid chromatographic determination of indinavir, saquinavir, and ritonavir in human plasma with combined ultraviolet absorbance and electrochemical detection, J Liq Chromatogr R T, 24, 2001, 2325-2336.
[48] K.A. Mahmoud, J.H.T. Luong, Impedance method for detecting hiv-1 protease and screening for its inhibitors using ferrocene–peptide conjugate/Au nanoparticle/single-walled carbon nanotube modified electrode, Anal Chem, 80, 2008, 7056-7062.
[49] M.H. Mashhadizadeh, M. Akbarian, Voltammetric determination of some anti-malarial drugs using a carbon paste electrode modified with $Cu(OH)_2$ nano-wire, Talanta, 78, 2009, 1440-1445.
[50] P.B. Deroco, F.C. Vicentini, G.G. Oliveira, R.C. Rocha-Filho, O. Fatibello-Filho, Square-wave voltammetric determination of hydroxychloroquine in pharmaceutical and synthetic urine samples using a cathodically pretreated boron-doped diamond electrode, J Electroanal Chem, 719, 2014, 19-23.
[51] M.M. Khalil, Y.M. Issa, G.A. El Sayed, Modified carbon paste and polymeric membrane electrodes for determination of hydroxychloroquine sulfate in pharmaceutical preparations and human urine, RSC Adv, 5, 2015, 83657-83667.
[52] C. Saka, Analytical methods on determination in pharmaceuticals and biological materials of chloroquine as available for the treatment of COVID-19, Crit Rev Anal Chem, 2020, 1-16.
[53] A. Radi, Accumulation and trace measurement of chloroquine drug at DNA-modified carbon paste electrode, Talanta, 65, 2004, 271-275.
[54] M. Srivastava, P. Tiwari, V.K. Mall, S.K. Srivastava, R. Prakash, Voltammetric determination of the antimalarial drug chloroquine using a glassy carbon electrode modified with reduced graphene oxide on WS2 quantum dots, Microchim Acta, 186, 2019, 415.
[55] S.M. Ghoreishi, A.M. Attaran, A.M. Amin, A. Khoobi, Multiwall carbon nanotube-modified electrode as a nanosensor for electrochemical studies and stripping voltammetric determination of an antimalarial drug, RSC Adv, 5, 2015, 14407-14415.
[56] X. Wang, W. Shen, X. Zhang, S. Guo, Y. Gao, X. Li, F. Feng, G. Yang, Indirect Electrochemical Determination of Ribavirin Using Boronic Acid-Diol Recognition on a 3-Aminophenylboronic Acid-Electrochemically Reduced Graphene Oxide Modified Glassy Carbon Electrode (APBA/ERGO/GCE), Anal Lett, 52, 2019, 1900-1913.
[57] A.A.A. Gaber, S.A. Ahmed, A.M.A. Rahim, Cathodic adsorptive stripping voltammetric determination of Ribavirin in pharmaceutical dosage form, urine and serum, Arab J Chem, 10, 2017, 2175-2181.
[58] A.M. Mahmoud, M.M. El-Wekil, M.H. Mahnashi, M.F.B. Ali, S.A. Alkahtani, Modification of N,S co-doped graphene quantum dots with p-aminothiophenol-functionalized gold nanoparticles for molecular imprint-based voltammetric determination of the antiviral drug sofosbuvir, Microchim Acta, 186 ,2019, 617.
[59] O. Selcuk, Y. Demir, C. Erkmen, S. Yıldırım, B. Uslu, Analytical methods for determination of antiviral drugs in different matrices: recent advances and trends, Crit Rev Anal Chem, 2021, 1-32.

e-ISSN: 2687-6698 **Review**

Turkish Journal of Analytical Chemistry

TurkJAC www.turkjac.org 2019

The recent studies about the interaction of phthalocyanines with DNA

Esra Bağda[1]*, Efkan Bağda[2]

[1]Sivas Cumhuriyet University, Faculty of Pharmacy, Department of Basic Pharmaceutical Sciences, Analytical Chemistry Division, 58140, Sivas, Turkey

[2] Sivas Cumhuriyet University, Faculty of Science, Department of Molecular Biology and Genetics, 58140, Sivas, Turkey

Abstract

Cancer is one of the major diseases affecting all humanity with high mortality rates worldwide. Photodynamic therapy offers one of the most important and promising treatment methods, especially in recent years. Photodynamic therapy takes the steps of administering the photo-sensitizing compound to the body and stimulating it with a light of an appropriate wavelength after its accumulation in the target tissue. With the formation of complex processes that take place in the target area with the reactive oxygen species formed by the stimulated compounds, death or the inhibition of the proliferation of the cells causes situations such as the destruction of the target tissue.

Phthalocyanines constitute an important group of photo-sensitizers with their strong absorption close to the therapeutic window. With large Π systems, they can bind with many biological macromolecules with high affinity by many mechanisms, including the Π - Π stacking.

This review article describes the last three years of studies in the WOS (Web of Science) database about the interactions of phthalocyanines with DNA. The interactions of phthalocyanines with DNA are important as they can make differences in the proliferation of tumour cells. On the other hand, DNA replication and transcription have increased due to the increased metabolic rate of these cells. The DNA double-strand opened during replication, and gene expression allows the formation of different secondary structures such as hairpin, triple and G-quadruplex. The interaction of G-quadruplex DNA structures with these compounds, which can be formed in the guanine-rich regions of the DNA has been described in studies.

Keywords: G-quadruplex, DNA, phthalocyanine, interaction

1. Introduction

Phthalocyanines are synthetic dyes and composed of four benzoid nuclei joined by four nitrogen atoms [1, 2]. These compounds have very important advantages such as definite chemical structure, repeatable synthesis, strong absorption in the near-infrared region, tunable photophysical and photochemical properties, and inherent biodegradability [3]. The free and metallated phthalocyanines have characteristic bands on the ultraviolet-visible absorption spectrum: a broad Soret band at 300-425 nm and Q band at 550-750 nm [4].

Apart from usage as photosensitizers for photodynamic therapy, phthalocyanines have been used in the different technological fields such as solar cell materials [5, 6, 7, 8], non-linear optical materials [9, 10, 11].

Genome integrity is essential for proper cell proliferation. Genetic instability can result in the inhibition of proliferation and some diseases [12]. Deoxyribonucleic acid (DNA) is a very important biopolymer that acts as a target for a large number of drugs, therefore, investigation of interactions of DNA with small molecules which are potential drugs is important for designing new types of pharmaceuticals [13]. The investigation of the interaction of drugs with DNA is a very important task in pharmacology as DNA is often the target for the majority of anticancer and antibiotic drugs [14].

G-quadruplexes DNA (G-Q) are four-stranded secondary DNA structures forming in guanine-rich nucleic acids regions of the genome, which can be found in some important parts of the genome such as promoter regions [15]. G-Q structures stabilized by Hoogsteen hydrogen bonding between a tetrad of guanine bases [16]. The G-quadruplex structure has essential roles in many biological processes such as translation, telomere maintenance, transcription, and replication [17, 18, 19]. According to De Magis et al., G-quadruplexes DNA and R loops are non-canonical DNA structures, and they can

Citation: E. Bağda, E. Bağda, The recent studies about the interaction of phthalocyanine with DNA, Turk J Anal Chem, 3(1), 2021, 9-18.

https://doi.org/10.51435/turkjac.938781

***Author of correspondence:** esraer@cumhuriyet.edu.tr
Tel: +90 346 219 10 10
Fax +90 346 219 16 34

Received: May 18, 2021
Accepted: June 13, 2021

regulate basic nuclear processes and trigger DNA damage, genome instability, and cell killing [20].

The important roles of DNA and G-quadruplex DNA structures in the cell cycle have made these structures targets for cancer drugs. Molecules that bind effectively to DNA structures can alter the normal process of the cell. This situation is very promising for cancer treatment.

In this review, phthalocyanines, molecules that can bind with B-DNA and G-quadruplex DNA, were investigated.

When searching WOS with "phthalocyanine" and "DNA" keywords (topic), 528 studies were found (Access date to WOS 12.05.2021). According to the WOS categories, out of 528 studies, 128 belongs to the "chemistry multidisciplinary" category, 123 belongs to the "biochemistry, molecular biology" category, 60 belongs to the "biophysics" category, 51 belongs to the "chemistry physical" category, 39 belongs to "chemistry inorganic nuclear" category, 36 belongs to "chemistry analytical" category, 31 belongs to "oncology" category.

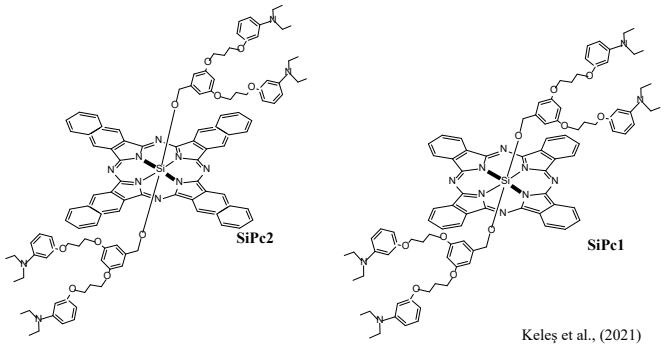

Figure 1. The structure of silicon phthalocyanines used in the study of Keleş et al. [21]

When the studies are evaluated according to the years they were published, there are most studies in 2020 (42), 37 in 2018, 30 in 2019, 29 in 2017, and 28 in 2016.

According to document types, 475 documents are articles, 30 documents are proceeding papers and 30 reviews.

When the studies grouped into funding agencies, 64 of them funded by the National Natural Science Foundation of China (NSFC), 45 of them funded by the United States Department Of Health Human Services, 44 of them funded by the National Institutes of Health (NIH) USA, 33 of them funded by (NIH) National Cancer Institute (NCI), 24 of them funded by Grants in Aid for Scientific Research Kakenhi, 24 of them funded by Japan Society for the Promotion of Science, 24 of them funded by Ministry of Education Culture Sports Science and Technology Japan (MEXT), 23 of them funded by The Scientific and Technological Research Council of Turkey (TUBITAK), 18 of them funded by European Commission, 14 of them funded by Conselho Nacional De Desenvolvimento Cientifico E Tecnologico (CNPQ).

When the studies are evaluated according to "organization-enhanced", 30 documents from Karadeniz Technical University, 24 from Case Western Reserve University, 22 from Chinese Academy Of Sciences, 15 from Istanbul Technical University, 15 from Russian Academy of Sciences, 15 from Universidade De Sao Paulo, 12 from Gebze Technical University, 12 from Centre National De La Recherche Scientifique CNRS, 10 from Institute of Chemical Biology Fundamental Medicine Siberian Branch of The Ras, and 10 from University of Sherbrooke.

2. Literature Survey

The studies obtained from the research in WOS and belonging to the last three years can be briefly summarized as follows.

Keleş et al., have synthesized and characterized the water-soluble and non-aggregated silicon (IV) phthalocyanines and naphthalocyanines containing (3,5-bis{3-[3(diethylamino)phenoxy]propoxy}phenyl)-methoxy groups to investigate their anticancer potential (Fig. 1) [21]. They conducted the experiments to investigate the ct-DNA interaction of the compounds and the binding constant (K_b) values of **SiPc1a** and **SiNc2a** were found as 6.85 ± (0.35) × 10^6 and 1.72 ± (0.16) × 10^4 M^{-1}. It is also reported that the ΔT_m values of **SiPc1a** and **SiNc2a** were calculated as 6.45 and 2.50 °C, respectively. They concluded from the all obtained experimental results that **SiPc1a** is a promising candidate as an anticancer agent [21].

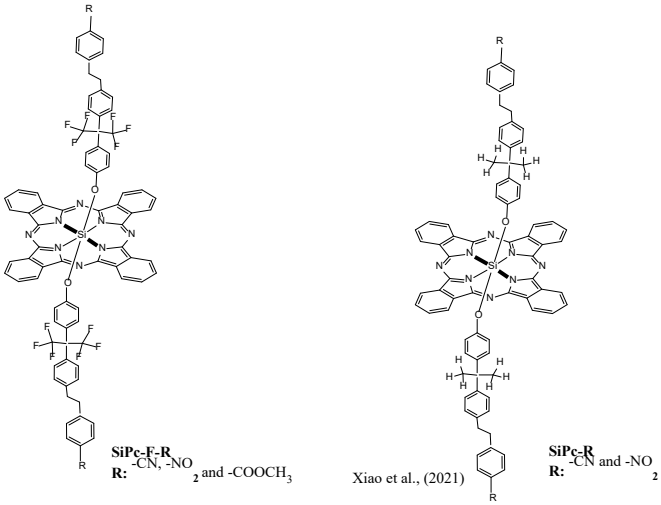

Figure 2. The structure of silicon phthalocyanines used in the study of Xiao et al. [22]

Xiao et al., have synthesized and characterized two series of fluorinated and non-fluorinated dendritic silicon (IV) phthalocyanines with cyano/nitro/ester terminal functionalities (Fig. 2) [22]. They used an

amphiphilic diblock copolymer polyethylene glycol monomethyl ether–polycaprolactone to encapsulate these silicon phthalocyanines to form fluorinated and non-fluorinated dendritic silicon phthalocyanines nanoparticles to endow water-soluble and biocompatibility of the compounds. The binding constants (K_a) between the fluorinated dendritic silicon nanoparticles and DNA were 3.569 × 10^3 for **MPEG@SiPc-F-CN**, 3.887 × 10^3 for **MPEG@SiPc-F-NO$_2$**, and 4.629 × 10^3 M^{-1} for **MPEG@SiPc-F-COOCH$_3$**. to support the binding experiments results in the competition binding sites experiment was also conducted by Xiao et al., and they concluded that the interaction between the DNA with nanoparticles could be explained that the interaction between "positive charge" of fluorinated dendritic silicon phthalocyanines and the negative phosphate backbone of DNA [22].

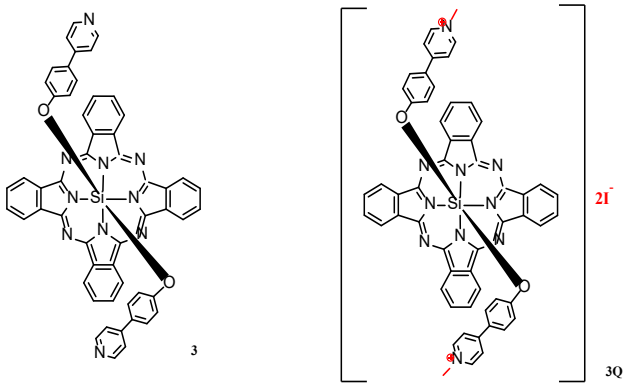

Figure 3. The structure of silicon phthalocyanine used in the study of Al-Raqa et al. [23]

Al-Raqa et al., synthesized and characterized axially the novel bis[4-(4-pyridinyl)phenol] substituted silicon(IV) phthalocyanine (**3**) and its quaternized derivative (**3Q**) (Fig. 3) [23]. The binding constants (K_b) between the quaternized derivative (**3Q**) and ct-DNA was 3.09 × 10^6 M^{-1}, the binding stoichiometry (n) was found as 1.57. They stated that the presence of an isosbestic point at 703 nm supports the intercalation mode of interaction between **3Q** and ct-DNA [23].

A study conducted by our research group was about the interaction of a water-soluble quaternized non-peripherally gallium(III)phthalocyanine chloride (**GaPc**) bearing 2-mercapto-N-methylpyridinium groups with different G- quadruplex DNA and ct-DNA. We found that the **GaPc** complex has a higher affinity to G-quadruplex DNA structures [24]. The binding constants were found as 1.9 ×10^6 M^{-1}, 1.1 ×10^6 M^{-1}, 8.5 ×10^5 M^{-1} for c-MYC, AS1411, Tel21, and it was found as 2.9 ×10^4 M^{-1} for ct-DNA.

Uchiyama et al., studied the interaction between an all parallel-stranded tetrameric G-quadruplex formed from a heptanucleotide d(TTAGGGT) ([d(TTAGGGT)]4) and Ga(III) phthalocyanine (Pc) derivative bearing eight N-methylpyridinium groups at peripheral β-positions (2,3,6,7,10,11,14,15-octakis-[N-methyl-(4-methylpyridinium-3-yloxy) phthalocyaninato] chloro gallium(III) iodide (GaPc)) (Fig. 4) [25]. They stated that **GaPc** exhibits stepwise binding to the G-quadruplex DNA to form a 2:1 **GaPc**-DNA complex. The binding constans for the first and second steps were found as (21 ± 2) × 10^6 and (0.09 ± 0.06) × 10^6 M^{-1}. They found that **GaPc** exhibits high binding affinity to the A3G4 step of [d(TTAGGGT)]4 through the electrostatic interactions of its positively-charged side chains with the negatively-charged phosphate groups, in addition to the π-π stacking interaction. They concluded that the polarity of the binding site alters the **GaPc**-binding affinity to the DNA [25].

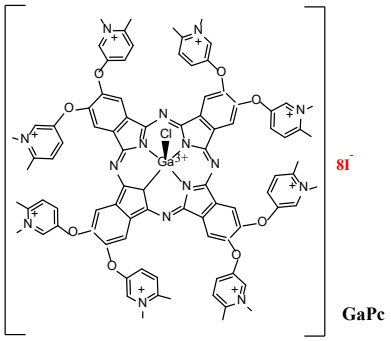

Figure 4. The structure of Ga(III) phthalocyanine used in the study of Uchiyama et al. [25]

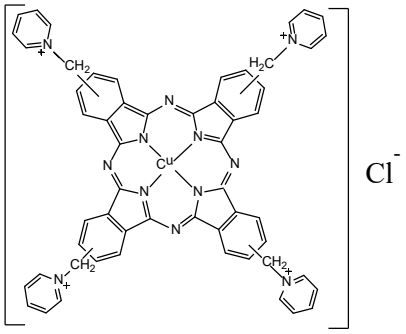

Figure 5. The structure of Cu(II) phthalocyanine used in the study of Macii et al. [26]

Macii et al., investigated the binding mechanism of a is a well know dye, copper phthalocyanine (Alcian Blue-tetrakis(methylpyridinium) chloride, **ABTP**) (Fig. 5), to natural ct-DNA, G-quadruplexes (G4), and synthetic RNA polynucleotides in the form of double polyriboadenylic·polyribouridylic acid (poly(A)·poly(U)) or triple strands polyriboadenylic·2polyribouridylic acid (poly(A)·2poly(U)). K_{app} is the binding constant and in the presence of NaCl 0.1 M, NaCa 2.5 mM, pH 7.0 and 25 °C they calculated the values as K_{app}(**ABTP**/ct-DNA) = (5.0 ± 1.1) × 10^3 M^{-1}, K_{app}(**ABTP**/polyA·polyU) = (1.2 ± 0.6) × 10^4 M^{-1} and K_{app}(**ABTP**/polyA·2polyU) = (6.2 ± 3.2) × 10^3 M^{-1} [26]. They also conducted the titrations experiments in the range of 15-46 °C and calculated the

thermodynamic parameters. They stated that magnitude for enthalpy changes lies at the boundaries between groove binding (low negative or positive ΔH) and intercalation (highly negative ΔH). They also conducted melting studies and concluded that the significant helix stabilization observed upon **ABTP** binding (at **CABTP**/Cpoly = 1.25, ΔTm > 15 °C for both **ABTP**/polyA·polyU and **ABTP**/polyA·2polyU. They also conducted similar experiments with G-quadruplexes and the apparent binding constants were calculated as K_{app} (**ABTP**/Tel23) = (3.7 ± 1.2) × 10^5 M^{-1}, K_{app} (**ABTP**/c-myc) = (3.6 ± 1.1) × 10^5 M^{-1} and K_{app} (**ABTP**/CTA22) = (6.1 ± 2.1) × 10^5 M^{-1} (KCl 0.1 M, LiCac 2.5 mM, pH 7.0, 25.0 °C). They concluded from the thermodynamic studies that the low values of ΔH_{app} agree with externally binding. Interestingly, the CD experiments strongly indicate dye intercalation in the case of **ABTP** with ct-DNA [26].

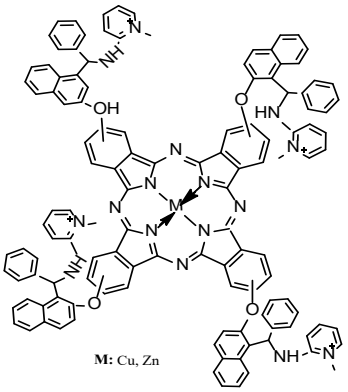

Figure 6. The structure of phthalocyanines used in the study of Amitha and Vasudevan [27]

Amitha and Vasudevan synthesized Betti base substituted zinc and copper phthalocyanines (**ZnBBPc** and **CuBBPc**) and their quaternized derivatives **qZnBBPc** and **qCuBBPc** were and characterized (Fig. 6) [27]. The DNA binding activities of **qZnBBPc** and **qCuBBPc** against ct-DNA were investigated and intercalative mode of interaction with K_b of the order of 10^5 M^{-1} was found. They finally assumed that the preferred mode of interaction was intercalative and the activity followed the order **qCuBBPc** > **qZnBBPc** [27].

Çoban et al., investigated some biological applications such as ct-DNA binding and supercoiled plasmid pBR322 DNA cleavage of zinc (II) phthalocyanine bearing ferrocene groups (**Pc-Zn**) [28]. They calculated the binding constant (K_b) value of the Pc-Zn as 1.80 ± (0.37) × 10^4 M^{-1} and hypochromicity % as 29.71 ± 3.45. They concluded the binding mechanism as groove binding because the binding constant of **Pc-Zn** found lower than 10^5 - 10^9 M^{-1} which are the K_b values of intercalation [28].

Barut et al., synthesized the peripherally and non-peripherally tetra substituted water-soluble zinc(II) phthalocyanines (**5a** and **5b**), and their ct-DNA binding behavior was investigated as well as other biological applications (Fig. 7) [29]. The binding constants were found to be 2.92 ± (0.20) × 10^5 and 1.30 ± (0.16) × 10^6 M^{-1} for **5a** and **5b**. They concluded that compound **5b** interacted with DNA 10 times stronger than **5a**.

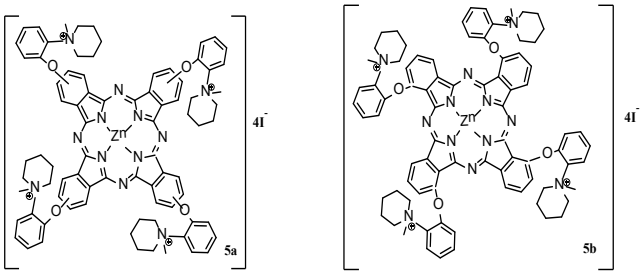

Figure 7. The structure of Zn(II) phthalocyanines used in the study of Barut et al. [29]

Khezami et al., synthesized two new tetra- or octa-substituted zinc(II) phthalocyanines (**1** and **2**) bearing 3-(morpholinomethyl)phenyl groups [30]. They also converted **1** and **2** to their water-soluble derivatives (**1Q** and **2Q**) by quaternization. They investigated the interaction of **1Q** and **2Q** with ct-DNA as well as BSA. They found the K_b values as 6.3 × 10^4 and 1.5 × 10^5 M^{-1}.

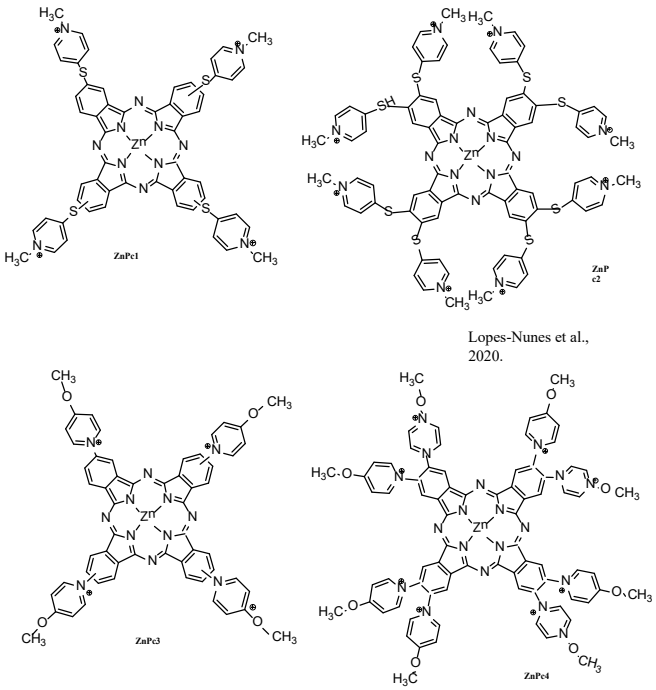

Figure 8. The structure of Zn(II) phthalocyanines used in the study of Lopes-Nunes et al. [31]

Lopes-Nunes et al., studied the interactions of four Zn(II) phthalocyanines (thiopyridinium **ZnPcs 1** and **2**, and methoxypyridinium **ZnPcs 3** and **4**) (Fig. 8) with the G-quadruplex forming AS1411 aptamer and its derived sequences AT11, -L0 and -B0 [31]. They calculated the dissociation constants and concluded that **ZnPc 4** has the highest affinity for all G4s aptamers; this is due to a compromise between the eight positive charges and

their hindered location in the methoxypyridinium moieties.

Ballı et al., reported the ct-DNA binding properties of tetra phenoxy-3-methoxybenzoic acid substituted Co(II) (**4**) and Cu(II) (**5**) metal phthalocyanines (Fig. 9) [32]. They found the binding constants as 1.85 × 10^6 and 2.22 ×10^6. They assumed that both two phthalocyanine compounds bound to the ct-DNA using the intercalation binding mechanism. Ballı et al, found the Tm value of bare calf thymus DNA as 74.63 °C and 79.48 °C and 80.75 °C. They suggested that the melting temperature also demonstrated intercalation binding mechanism for the compound **4** and **5** [32].

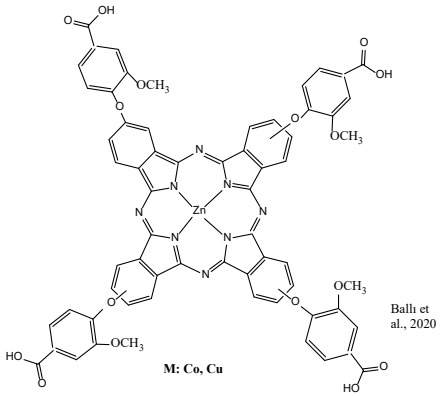

Figure 9. The structure of phthalocyanines used in the study of Ballı et al. [32]

Uchiyama et al., investigated the G-quadruplex DNA binding behavior of 2,9(10),16(17),23(24)-tetrakis(carboxyl)phthalocyanine copper(II) complex (**CuTCPc**) (Fig. 10) [33]. The compound, **CuTCPc**, is an anionic phthalocyanine and the researchers found that binds this anionic phthalocyanine compound selectively to the 3′-terminal G-quartet, i.e., G6 G-quartet, of the all parallel-stranded tetrameric G-quadruplex of d(TTAGGG). The addition of an extra T at the 3′-terminal of the constituent sequence inhibited the specific binding of **CuTCPc** to G6 G-quartet. They concluded that the inhibition of specific binding is most likely due to the electrostatic repulsion between the carboxylate groups of **CuTCPc** and the negatively-charged phosphate of the phosphodiester bond at the G6T7 step of the G-quadruplex DNA [33].

Yalazan et al., synthesized tosylated 4-morpholinoaniline units fused peripherally tetra-substituted free-base (**5**), copper(II) (**6**), zinc(II) (**7**), cobalt(II) (**8**), and magnesium(II) (**9**) (Fig. 11) phthalocyanine compounds [34]. The DNA interaction of **7** was investigated and the intrinsic binding constant was determined as 2.45 ± (0.20) × 10^4 M^{-1}. 25.98% of hypochromic effect was observed for compound **7** without any shift upon the addition of ct-DNA. The authors concluded from the results that compound (**7**) bound to ct-DNA via non-covalent interaction [34].

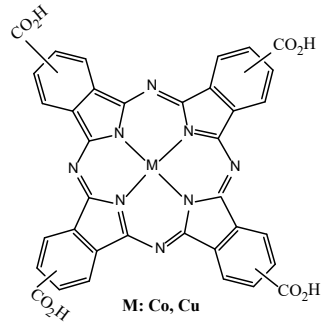

Figure 10. The structure of phthalocyanines used in the study of Uchiyama et al. [33]

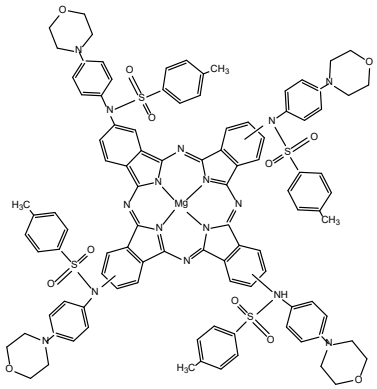

Figure 11. The structure of Mg(II) phthalocyanine used in the study of Yalazan et al. [34]

Yan et al., investigated the photodynamic therapy with a zinc phthalocyanine (**ZnPc**) photosensitizer coupled with 2,4,6-tris (N, N-dimethylaminomethyl) phenoxy (TAP), termed as **ZnPc(TAP)$_4$** (Fig. 12) [35]. They investigated the ct-DNA binding and they found the K_b, intrinsic binding constant as 3.2 × 10^6. They commented that the intrinsic binding constant for **ZnPc(TAP)4** is higher than that of ethidium bromide (K_b = 1.23 × 10^5) showing that **ZnPc(TAP)4** has a strong affinity to ct-DNA.

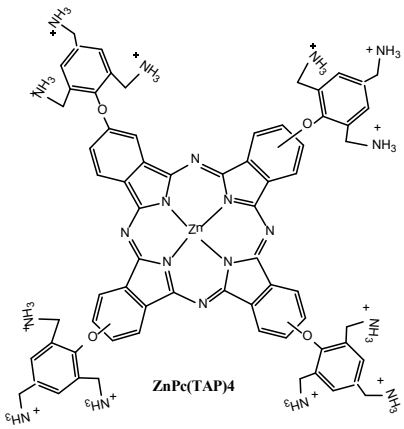

Figure 12. The structure of Zn(II) phthalocyanine used in the study of Yan et al. [35]

Wang et al., studied the specific binding of the anionic phthalocyanine 3,4′,4′′,4′′′-tetrasulfonic acid

(**APC**) (Fig. 13) to the human hybrid (3 + 1) G4s [36]. They investigated the binding at the atomic level using molecular docking and molecular dynamics simulations. They suggested that **APC** preferred the end-stacking binding with the telomere hybrid type II G4 and the groove binding with the hybrid type I G4. They also commented that the electrostatic interaction and the polar solvation effect made unfavorable and favorable contributions respectively to the binding of **APC** and hybrid G4s [36].

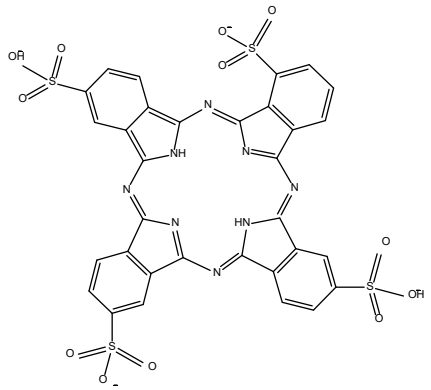

Figure 13. The structure of phthalocyanine used in the study of Wang et al. [36]

A tetra substituted neutral zinc phthalocyanine (**ZnPc-4**) (Fig. 14) bearing 4-phenylazophenoxy group at the periphery had been prepared by [37]. The interaction between ct-DNA and **ZnPc-4** was investigated. They concluded from the electronic spectrum results as well as the planar shape of the compound that intercalation mode of binding with ct-DNA. They calculated the binding constant as 1.58 x 10^5 M^{-1}.

Baran et al., synthesized three phthalocyanine derivatives (Zn (**3a**), Co (**3b**), and metal-free (**3c**)) were synthesized (Fig. 15) [38]. The ct-DNA binding studies conducted with **3a**. the binding constant of **3a** calculated as 5.2 (± 0.52) 10^3 M^{-1}. They concluded from the spectral data that the existence of non-intercalative interactions between the synthesized **Pcs** and ct-DNA.

Kasyanenko et al., investigated the ct-DNA interaction of cobalt phthalocyanine disodium disulfonate (**CoPc)** (Fig. 16) [39]. The authors claimed that two types of **CoPc** binding to DNA were observed. For the first binding, fast **CoPc** interactions with DNA via external binding to DNA phosphates backbone were accompanied by the formation of stack-type phthalocyanine structures on the periphery of the DNA helix (binding constant was found as (4.8 ± 0.4) × 10^4 M^{-1}. The authors stated that the second binding manifests itself in a certain period of time. It can be associated with the reorganization of ligands and second binding does not affect the first complexes, that is **CoPc** binding with DNA phosphates [39].

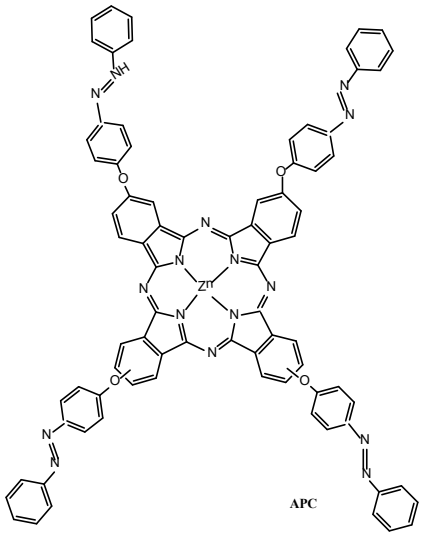

Figure 14. The structure of Zn(II) phthalocyanine used in the study of Amita and Vasudevan [37]

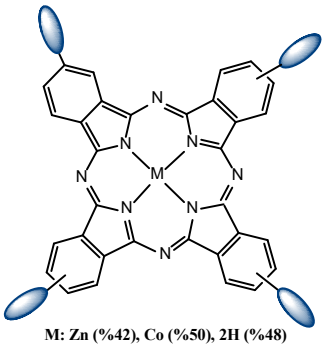

Figure 15. The structure of phthalocyanines used in the study of Baran et al. [38]

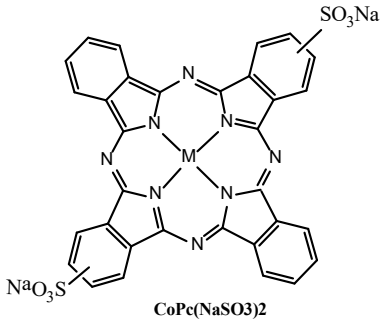

Figure 16. The structure of phthalocyanine used in the study of Kasyanenko et al. [39]

McRae et al., have studied the interaction of two cationic zinc phthalocyanines (**Pc1** and **Pc2**) with several DNA secondary structures (ss-DNA, ds-DNA, and G4-DNA structures) [40]. They suggested that according to the spectrophotometric titration experiment there are strong interactions between both phthalocyanine compounds and ss-DNA, ds-DNA, and G4-DNA and consistent with non-specific interactions with the phosphodiester backbone.

Keleş et al., have synthesized axially [3,5-bis(3-pyridin-4-ylpropoxy)phenyl]methoxy groups substituted silicon (IV) phthalocyanine **2**,

napthalocyanine **3** and their water-soluble derivatives **2a**, **3a** (Fig. 17) [41]. They found that the **3a** and **3b** interacted to ct-DNA via intercalation with a binding constant of $3.94 \pm (0.15) \times 10^6$ and $1.08 \pm (0.10) \times 10^5$ M^{-1}. They concluded from electronic absorption spectral changes (hypochromism, redshift and isosbestic points) are indicators of a non-covalent binding mode via intercalation due to strong interactions between chromophore and DNA base pairs [41].

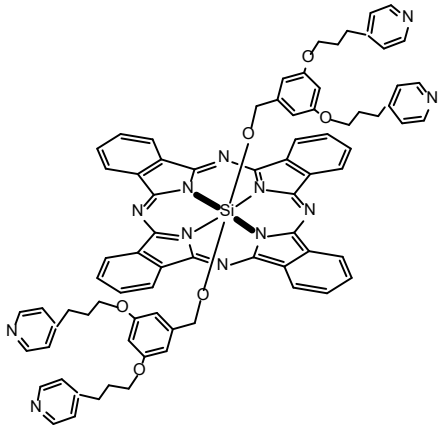

Figure 17. The structure of Si phthalocyanine used in the study of Keleş et al. [41]

Uslan et al., have synthesized new Zinc(II) (5), indium(III) (6), and lutetium(III) (7) phthalocyanines (**Pcs**) (Fig. 18) peripherally substituted with poly (ethylene glycol) (PEG) monomethyl ether 2000 (PEGME-2000) blocks [42]. The binding constant was calculated from the titration data for 5, 6 and 7 as 9×10^5, 11×10^5, and 10×10^5, respectively. The authors also calculated the thermodynamic parameters and concluded from the results that the binding mode of three phthalocyanines with ct-DNA could be attributed as non-specific, hydrophobic, entropy-controlled, and spontaneous [42].

Figure 18. The structure of phthalocyanines used in the study of Uslan et al. [42]

Demirbaş et al., have synthesized triazol compound 3-methyl-4-(3-morpholinopropyl)-1H-1,2,4-triazol-5(4H)-one (**3**), phthalonitrile compound 4-(3-methyl-4-(3-morpholinopropyl)-5-oxo-4,5-dihydro-1H-1,2,4-triazol-1-yl)phthalonitrile (**5**), peripherally tetra substituted zinc(II) (**6**) and copper(II) (**7**) phthalocyanines and their water-soluble quaternized derivatives (**6a**) and (**7a**) (Fig. 19) [43]. The binding constant for ct-DNA interaction was calculated as $6.53 \pm (0.04) \times 10^4$ M^{-1} and $1.14 \pm (0.02) \times 10^4$ M^{-1} for **6a** and **6b**. They also found that the ΔT_m values as 7.55 °C and 5.75 °C. The authors concluded that the spectral characteristics, that is observed hypochromicities with redshifts suggest that both compounds interact with ct-DNA via intercalation or minor groove binding mode [43].

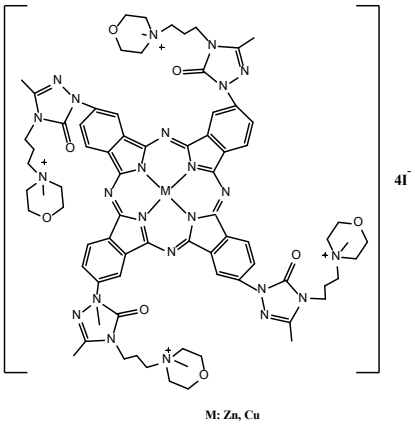

Figure 19. The structure of phthalocyanines used in the study of Demirbaş et al. [43]

Ramos et al., have studied the interaction of four phthalocyanine compounds, with four positive charges and with eight positive charges (**ZnPc1** and **ZnPc3** contain four positive charges, **ZnPc2** and **ZnPc4** contain eight positive charges) (Fig. 20) with different DNA structures (tetramolecular G-quadruplex, unimolecular G-quadruplex, salmon sperm DNA, and 5GC small double-strand DNA) [44]. They found that **ZnPc1** and **ZnPc4** have high selectivity and affinity for G-quadruplex over duplex structures. Ramos et al. have also concluded some important inferences about the structure-activity relationship: They have explained that the existence of a high number of positive charges results in a better affinity but lacks its selectivity towards DNA and the position of the positive charge is important for the interactions; a balance between the number and position of the positive charges, is a fundamental attribute for selectivity of ligands towards G-quadruplex structures [44].

Demirbaş has synthesized peripherally tetra 4-(1-phenoxypropan-2-yloxy)-substituted novel zinc(II) phthalocyanine (**4**) (Fig. 21) [45]. He has found the ct-DNA binding constant of compound **4** as $1.73 \pm 0.50 \times 10^4$ M^{-1}. A hypochromic effect (27.97%) after the addition of ct-DNA has been observed. The author also concluded from spectrophotometric titration and ethidium bromide competitive binding experiments that

phthalocyanine **4** interacted with ct-DNA strongly via non-intercalation mode [45].

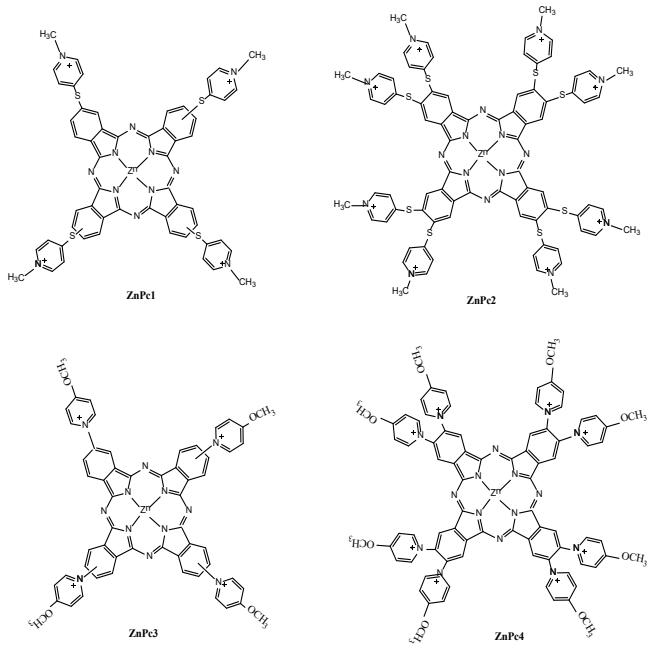

Figure 20. The structure of zinc phthalocyanines used in the study of Ramos et al. [44]

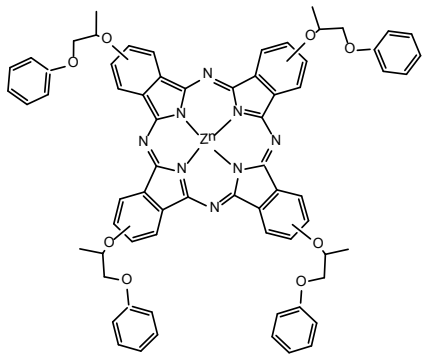

Figure 21. The structure of zinc phthalocyanines used in the study of Demirbaş [45]

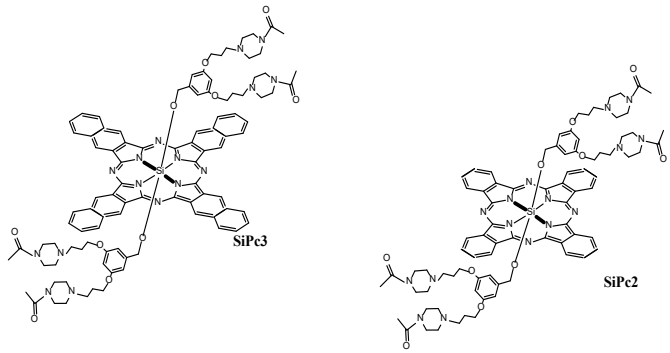

Figure 22. The structure of zinc phthalocyanine used in the study of Baş et al. [46]

Baş et al., have synthesized axially 1-acetylpiperazine substituted silicon (IV) phthalocyanine, naphthalocyanine **2**, **3**, and their water-soluble derivatives (**2a** and **2b**) (Fig. 22) [46]. They studied the ct-DNA interaction of **2a** and **2b**. The binding constans have been calculated as 1.25 ± (0.01) × 10^4 and 1.13 ± (0.03) × 10^4 M^{-1}. The 50.03% and 44.98% hypochromisms and redshifts of 1 nm and 5 nm have been observed for the interaction of **2a** and **3a** with DNA. The changes in melting temperatures have been found as 4.25 °C and 3.75 °C for **2a** and **3a** [46].

3. Conclusion

Investigating the interactions of molecules targeting DNA and G-quadruplex DNA with these structures is very important for drug development studies. Drugs targeting these structures are very important for the treatment of many diseases, including cancer. The ability of phthalocyanines to be synthesized differently to have different properties, to have high absorption in the near IR region, to form species such as singlet oxygen by activating light made these molecules compatible with photodynamic therapy. Until now, important studies have been carried out on this subject and in the light of the obtained data, new compounds more specific to the target will be synthesized.

References

[1] K. L. M. Santos, R. M. Barros, D. P. da Silva Lima, A. M. A. Nunes, M. R. Sato, R. Faccio, J. A. O. Junior, Prospective application of phthalocyanines in the photodynamic therapy against microorganisms and tumor cells: a mini-review, Photodiagn Photodyn, 2020,102032.

[2] M. Soncin, C. Fabris, A. Busetti, D. Dei, D. Nistri, G. Roncucci, G. Jori, Approaches to selectivity in the Zn (II)-phthalocyanine-photosensitized inactivation of wild-type and antibiotic-resistant Staphylococcus aureus, Photoch Photobiol Sci, 1(10), 2002, 815-819.

[3] B. D. Zheng, Q. X. He, X. Li, J. Yoon, J. D. Huang, Phthalocyanines as contrast agents for photothermal therapy, Coordin Chem Rev, 426, 2021, 213548.

[4] C. P. Ribeiro, L. M. Lourenço, Overview of cationic phthalocyanines for effective photoinactivation of pathogenic microorganisms, J Photoch Photobio C, 2021, 100422.

[5] Z. Dalkılıç, C. B. Lee, H. Choi, I. Nar, N. K. Yavuz, A. K. Burat, Tetra and octa substituted Zn (II) and Cu (II) phthalocyanines: Synthesis, characterization and investigation as hole-transporting materials for inverted type-perovskite solar cells, J Organomet Chem, 922, 2020, 121419.

[6] M. V. Martínez-Díaz, M. Ince, T. Torres, Phthalocyanines: colorful macroheterocyclic sensitizers for dye-sensitized solar cells, Monatsh Chem, 142(7), 2011, 699-707.

[7] A. C. Yüzer, G. Kurtay, T. İnce, S. Yurtdaş, E. Harputlu, K. Ocakoglu, M. İnce, Solution-processed small-molecule organic solar cells based on non-aggregated zinc phthalocyanine derivatives: A comparative experimental and theoretical study, Mat Sci Semicon Proc, 129, 2021, 105777.

[8] S. W. Kim, G. Kim, C. S. Moon, T. Y. Yang, J. Seo, Metal-free phthalocyanine as a hole transporting material and a surface passivator for efficient and stable perovskite solar cells, Small Methods, 2021, 2001248.

[9] A. Husain, A. Ganesan, M. Sebastian, S. Makhseed, Large ultrafast nonlinear optical response and excellent optical limiting

behaviour in pyrene-conjugated zinc (II) phthalocyanines at a near-infrared wavelength, Dyes Pigments, 184, 2021, 108787.
[10] S. I. Qashou, E. F. M. El-Zaidia, A. A. A. Darwish, T. A. Hanafy, Methylsilicon phthalocyanine hydroxide doped PVA films for optoelectronic applications: FTIR spectroscopy, electrical conductivity, linear and nonlinear optical studies, Physica B, 571, 2019, 93-100.
[11] A. Y. Tolbin, M. S. Savelyev, A. Y. Gerasimenko, L. G. Tomilova, N. S. Zefirov, Thermally stable J-type phthalocyanine dimers as new non-linear absorbers for low-threshold optical limiters, Phys Chem Chem Phys, 18(23), 2016, 15964-15971.
[12] I. M. Del Mundo, K. M. Vasquez, G. Wang, Modulation of DNA structure formation using small molecules, Bba-Mol Cell Res, 1866(12), 2019, 118539.
[13] A. R. Jalalvand, Chemometrics in investigation of small molecule-biomacromolecule interactions: A review, Int J Biol Macromol, 181, 2021, 478-493.
[14] A. Rescifina, Zagni, C. M. G. Varrica, V. Pistarà, A. Corsaro, Recent advances in small organic molecules as DNA intercalating agents: Synthesis, activity, and modeling, Eur J Med Chem, 74, 2014, 95-115.
[15] A. Awadasseid, X. Ma, Y. Wu, W. Zhang, G-quadruplex stabilization via small-molecules as a potential anti-cancer strategy, Biomed Pharmacother, 139, 2021, 111550.
[16] J. L. Huppert, S. Balasubramanian, Prevalence of quadruplexes in the human genome, Nucleic Acids Res, 33(9), 2005, 2908-2916.
[17] P. A. Summers, B. W. Lewis, J. Gonzalez-Garcia, R. M. Porreca, A. H. Lim, P. Cadinu, R. Vilar, Visualising G-quadruplex DNA dynamics in live cells by fluorescence lifetime imaging microscopy, Nat Commun, 12(1), 2021, 1-11.
[18] M. L. Bochman, K. Paeschke, V. A. Zakian, DNA secondary structures: stability and function of G-quadruplex structures, Nat Rev Genet, 13(11), 2012, 770-780.
[19] S. Neidle, Quadruplex nucleic acids as targets for afnticancer therapeutics, Nat Rev Chem, 1(5), 2017, 1-10.
[20] A. De Magis, S. G. Manzo, M. Russo, J. Marinello, R. Morigi, O. Sordet, G. Capranico, DNA damage and genome instability by G-quadruplex ligands are mediated by R loops in human cancer cells, Proc Natl Acad Sci, 116(3), 2019, 816-825.
[21] T. Keleş, B. Barut, A. Özel, Z. Biyiklioglu, Design, synthesis and biological evaluation of water soluble and non-aggregated silicon phthalocyanines, naphthalocyanines against A549, SNU-398, SK-MEL128, DU-145, BT-20 and HFC cell lines as potential anticancer agents, Bioorg Chem, 107, 2021, 104637.
[22] W. Xiao, X. Guan, B. Huang, T. Q. Ye, Zhang, K. Chen, F. Fu, Fluorinated dendritic silicon (IV) phthalocyanines nanoparticles: Synthesis, photoinduced intramolecular energy transfer and DNA interaction, Dyes Pigments, 186, 2021, 109013.
[23] S. Y. Al-Raqa, K. Khezami, E. N. Kaya, M. Durmuş, A novel water soluble axially substituted silicon (IV) phthalocyanine bearing quaternized 4-(4-pyridinyl) phenol groups: synthesis, characterization, photophysicochemical properties and BSA/DNA binding behavior, Polyhedron, 194, 2021, 114937.
[24] E. Bağda, E. Bağda, A. Kocak, M. Durmuş, Investigation of Binding behaviour of a water-soluble gallium (III) phthalocyanine with double-stranded and G-quadruplex DNA via experimental and computational methods, J Mol Struct, 1240, 2021, 130536.
[25] M. Uchiyama, A. Momotake, T. Ikeue, Y. Yamamoto, Stepwise binding of a cationic phthalocyanine derivative to an all parallel-stranded tetrameric G-quadruplex DNA, J Inorg Biochem, 213, 2020, 111270.
[26] F. Macii, C. Perez-Arnaiz, L. Arrico, N. Busto, B. Garcia, T. Biver, Alcian blue pyridine variant interaction with DNA and RNA polynucleotides and G-quadruplexes: changes in the binding features for different biosubstrates, J Inorg Biochem, 212, 2020, 111199.
[27] G. S. Amitha, S. Vasudevan, DNA binding and cleavage studies of novel Betti base substituted quaternary Cu (II) and Zn (II) phthalocyanines, Polyhedron, 190, 2020, 114773.
[28] Ö. Çoban, B. Barut, C. Ö. Yalçın, A. Özel, Z. Bıyıklıoğlu, Development and in vitro evaluation of BSA-coated liposomes containing Zn (II) phthalocyanine-containing ferrocene groups for photodynamic therapy of lung cancer, J Organomet Chem, 925, 2020, 121469.
[29] B. Barut, C. Ö. Yalçın, Ü. Demirbaş, H. T. Akçay, H. Kantekin, A. Özel, The novel Zn (II) phthalocyanines: Synthesis, characterization, photochemical, DNA interaction and cytotoxic/phototoxic properties, J Mol Struct, 1218, 2020, 128502.
[30] K. Khezami, K. Harmandar, E. Bağda, E. Bağda, G. Şahin, N. Karakodak, M. Durmuş, The new water soluble zinc (II) phthalocyanines substituted with morpholine groups-synthesis and optical properties, J Photoch Photobio A, 401, 2020, 112736.
[31] J. Lopes-Nunes, J. Carvalho, J. Figueiredo, C. I. Ramos, L. M. Lourenço, J. P. Tomé, C. Cruz, Phthalocyanines for G-quadruplex aptamers binding, Bioorg Chem, 100, 2020, 103920.
[32] Z. Ballı, A. Arslantaş, D. G. Solğun, M. S. Ağırtaş, DNA binding studies of the 2, 10, 16, 24–tetrakis (phenoxy-3-methoxybenzoic acid) phthalocyaninato) Co (II) and Cu (II) compounds, SN Appl Sciences, 2(5), 2020, 1-10.
[33] M. Uchiyama, A. Momotake, N. Kobayashi, Y. Yamamoto, Specific binding of an anionic phthalocyanine derivative to G-quadruplex DNAs, Chem Lett, 49(5), 2020, 530-533.
[34] H. Yalazan, B. Barut, B. Ertem, C. Ö. Yalçın, Y. Ünver, A. Özel, H. Kantekin, DNA interaction and anticancer properties of new peripheral phthalocyanines carrying tosylated 4-morpholinoaniline units, Polyhedron, 177, 2020, 114319.
[35] S. Yan, H. Guo, J. Su, J. Chen, X. Song, M. Huang, Z. Chen, Effects of hydroxyl radicals produced by a zinc phthalocyanine photosensitizer on tumor DNA, Dyes Pigments, 173, 2020, 107894.
[36] Z. Wang, J. Li, J. Liu, L. Wang, Y. Lu, J. P. Liu, Molecular insight into the selective binding between human telomere G-quadruplex and a negatively charged stabilizer, Clin Exp Pharmacol P, 47(5), 2020, 892-902.
[37] G. S. Amitha, S. Vasudevan, DNA/BSA binding studies of peripherally tetra substituted neutral azophenoxy zinc phthalocyanine, Polyhedron, 175, 2020, 114208.
[38] A. Baran, S. Col, E. Karakılıç, F. Özen, Photophysical, photochemical and DNA binding studies of prepared phthalocyanines, Polyhedron, 175, 2020, 114205.
[39] N. A. Kasyanenko, R. A. Tikhomirov, V. M. Bakulev, V. N. Demidov, E. V. Chikhirzhina, E. B. Moroshkina, DNA complexes with cobalt (II) phthalocyanine disodium disulfonate, ACS Omega, 4(16), 2019. 16935-16942.
[40] E. K. McRae, D. E. Nevonen, S. A. McKenna, V. N. Nemykin, Binding and photodynamic action of the cationic zinc phthalocyanines with different types of DNA toward understanding of their cancer therapy activity, J Inorg Biochem, 199, 2019, 110793.
[41] T. Keleş, B. Barut, A. Özel, Z. Biyiklioglu, Synthesis of water soluble silicon phthacyanine, naphthalocyanine bearing pyridine groups and investigation of their DNA interaction, topoisomerase inhibition, cytotoxic effects and cell cycle arrest properties, Dyes Pigments, 164, 2019, 372-383.
[42] C. Uslan, B. Köksoy, M. Durmuş, N. D. İşleyen, Y. Öztürk, Z. P. Çakar, B. S. Sesalan, The synthesis and investigation of photochemical, photophysical and biological properties of new lutetium, indium, and zinc phthalocyanines substituted with PEGME-2000 blocks, J Biol Inorg Chem, 24(2), 2019, 191-210.
[43] Ü. Demirbaş, B. Barut, A. Özel, F. Çelik, H. Kantekin, K. Sancak, Synthesis, characterization and DNA interaction properties of the novel peripherally tetra 4-(3-methyl-4-(3-morpholinopropyl)-5-oxo-4, 5-dihydro-1H-1, 2, 4-triazol-1-yl) substituted water soluble Zn (II) and Cu (II) phthalocyanines, J Mol Struct, 1177, 2019, 571-578.

[44] C. I. V. Ramos, S. P. Almeida, L. M. Lourenço, P. M. Pereira, R. Fernandes, M. A. F. Faustino, M. G. P. M. S. Neves, Multicharged phthalocyanines as selective ligands for G-quadruplex DNA structures, Molecules, 24(4), 2019, 733.

[45] Ü. Demirbaş, Synthesis, characterization, and investigation of singlet oxygen, DNA interaction, and topoisomerase I inhibition properties of novel zinc (II) phthalocyanine, Turk J Chem, 43(6), 2019, 1646-1655.

[46] H. Baş, B. Barut, Z. Biyiklioglu, A. Özel, Synthesis, DNA interaction, topoisomerase I, II inhibitory and cytotoxic effects of water soluble silicon (IV) phthalocyanine and napthalocyanines bearing 1-acetylpiperazine units, Dyes Pigments, 160, 2019, 136-144.

e-ISSN: 2687-6698 Research Article

Turkish Journal of Analytical Chemistry
TurkJAC
www.turkjac.org
2019

Three species of *Verbascum* L. from Northwest Anatolia of Turkey as a source of biological activities

Nurcihan Hacıoğlu Doğru[1]*, Neslihan Demir[1], Özer Yılmaz[2]

[1]Çanakkale Onsekiz Mart University, Faculty of Science and Arts, Department of Biology, 17020, Çanakkale, Turkey
[2]Uludağ University, Faculty of Science and Arts, Department of Biology, 16240, Bursa, Turkey

Abstract

Phytochemical constituents and some biological activities i.e., antimutagenicity, DNA damage protecting, antioxidant, antibacterial, and antibiofilm of ethanolic extracts of three *Verbascum* plants (*Verbascum mucronatum* Lam., *V. bombyciferum* Boiss., *V. vacillans* Murb.) were studied. This paper is the first comprehensive research on *V. mucronatum*, *V. bombyciferum*, *V. vacillans* biological activities. *V. vacillans* ethanol extract has been determined to be the lowest plant for phytochemical contents. In 2,2-diphenyl-1-picrylhydrazyl (DPPH) free radical scavenging activity and the Cu(II) ion reducing antioxidant capacity (CUPRAC) of three plant extracts showed concentration-dependent antioxidant capacity. *V. mucronatum* and *V. bombyciferum* extracts exhibited a strong antimutagenic effect on *Salmonella typhimurium* TA98 and TA100 strains. *Verbascum* extracts showed DNA damage protection potential in tested concentrations. However, the lowest concentration (0.5 µM) of the *V. bombyciferum* species Form III were observed and almost completely disintegrate DNA in this concentration. Three *Verbascum* plants were showed strong antibacterial activities with inhibition zones at 9.0 - 19.0 mm and a significant reduction in biofilm formation. It was observed that these plants are potential sources of various biological activities.

Keywords: Antibacterial, antimutagenicity, antioxidant activity, *Verbascum mucronatum*, *V. bombyciferum*, *V. vacillans*

1. Introduction

The genus *Verbascum* L. (Scrophulariaceae), knowing as mullein, has approximately 360 species, which are distributed in Europe, Asia, and Northeast Africa [1]. Turkey is one of the richest countries in the world with circa 250 species, and nearly 80% of this species is endemic to Anatolia [2,3,4]. The genus *Verbascum* has been divided in the flora of Turkey into thirteen artificial groups from A to M. The species which have chosen for this study belong to group E (*Verbascum bombyciferum* Boiss.) and group K (*V. mucronatum* Lam., *V. vacillans* Murb.). Except *V. mucronatum*, they have local distributions. *V. mucronatum* has a wide distribution, but to be found rare in their habitats, in west Anatolia. Also, this species is growing only in Crete, outside Turkey. While *V. bombyciferum* is an endemic around to Bursa and Yalova provinces, *V. vacillans* is confined to the south part of Kazdağı Mountain in Balıkesir, and also has been reported from Lesbos [5-6].

Verbascum plant species are a group used in traditional and modern medicine for respiratory diseases, dysentery infection antimicrobial, anti-inflammatory, sedative, diuretic, sudorific, expectorant, and antidiarrheal [7,8,9]. It is very important to investigate the medicinal components and effects of herbs as natural and alternative medicine sources. Some of the biological activities such as antimicrobial, antimalarial, antiviral, antioxidant, anti-inflammatory, antitumoral, cytotoxic, antinociceptive, immunomodulatory, antiulcerogenic, antihepatotoxic, antihyperlipidemic, antinociceptive, antitussive, anthelminthic, and antigermination of genus *Verbascum* have been also previously reviewed [7,10,11,12,13,14,15]. However, in the literature, it has been determined that biological activity studies especially from these three plant species are insufficient. As far as we know, there are not comprehensive investigations on phytochemical content, antioxidant, antimutagenicity, DNA damage protection, antibacterial and antibiofilm activities with the *V. mucronatum*, *V. bombyciferum*, and *V. vacillans* plant species. Therefore, the present study is about the comparison of three *Verbascum* species in terms of these biological activities.

Citation: N. Hacıoğlu Doğru, N. Demir, Ö. Yılmaz, Three species of *Verbascum* L. from Northwest Anatolia of Turkey as a source of biological activities, Turk J Anal Chem, 3(1), 2021, 19-26.

https://doi.org/10.51435/turkjac.886692

***Author of correspondence:** nhacioglu@comu.edu.tr
Tel: +90 (286) 218 00 18
Fax: +90 (286) 218 05 33
Received: February 25, 2021
Accepted: May 21, 2021

2. Material and Methods

2.1. Plant materials

The specimens belong to *V. mucronatum*, *V. bombyciferum*, and *V. vacillans* were collected from Bursa and Balıkesir provinces (NW Anatolia) in 2017, respectively. The specimens were identified with the aid of flora of Turkey [2,5,16,17] and other relevant publications [18,19,20] by Dr. Özer Yılmaz. Also samples of the three species kept in the herbarium BULU (University of Uludağ, Bursa, Turkey) (Table 1).

2.2. Preparation of plant extracts

Dried plant materials (15 g) were ground mechanically in aseptic condition and extracted with 150 mL ethanol (80%) by using Soxhlet (Wisd-WiseTherm) [21], then filtered extracts were evaporated with rotary evaporator equipment.

2.3. Qualitative phytochemical screening

The phytochemical screening was performed for the presence of seven phytochemicals; coumarins, cardiac glycosides, phlabotannins, quinones, flavanones, anthocyanins, and proteins using the standard procedures as described by Harborne (1973), Raaman (2006), Evans (2009) [22,23,24].

2.4. Evaluation of antioxidant activity

2.4.1. DPPH free-radical scavenging assay

The antioxidant activity of the extracts was measured by using 2,2-diphenyl-1-picrylhydrazyl (DPPH) following the procedure described by Brand-Williams [25]. The absorbance values of the samples were measured at 517 nm. The radical scavenging activity of each sample was calculated using the following formula and the results were expressed as % inhibition.

$$Inhibition\ (\%) = \frac{Abs_{control} - Abs_{sample}}{Abs_{control}} \times 100 \qquad (1)$$

2.4.2. Cu(II) ion reducing antioxidant capacity (CUPRAC)

The Cu(II) ion reducing the antioxidant capacity of *Verbascum* species was performed using Apak [26] method. The samples were incubated for half an hour at room temperature; absorbance was measured at 450 nm by spectrophotometer.

2.5. Antimutagenicity assay

The antimutagenic activity of *Verbascum* extracts has been investigated by Ames/*Salmonella* test system [27]. The experiment was carried out using *Salmonella typhimurium* auxotroph mutant strains TA98 (frame-shift mutation) and TA100 (base-pair substitution) strains. The positive controls, 4-nitro-*o*-phenylenediamine (NPD, 10 µg/plate) for TA98 strain and the sodium azide (SA, 1 µg/plate) for the TA100 strain were used. In the negative control, the solvents of the extracts were used for both strains. The inhibition rates of extracts were calculated according to the formula given by Hong and Lyu [28].

$$Inhibition\ Rate\ (\%) = \frac{A - B}{A - C} \times 100 \qquad (2)$$

A is the number of revertant colonies in the presence of mutagen/plate, B is the number of revertant colonies in the presence of extract/plate, C is the number of spontaneous colony/plate.

As a result of antimutagenicity studies, it was considered non-antimutagenic when the inhibitory effect of the extracts tested was below 25%. The 25 - 40% inhibition rate is moderate and more than 40% is defined as a strong antimutagenic effect [29, 30]

2.6. DNA damage protecting activity

DNA damage protecting activity was performed using supercoiled pBR322 DNA plasmid by agarose gel electrophoresis. Plasmid DNA in Tris-HCl buffer was treated with the extracts of different *Verbascum* species at 37 °C for 3 h. To determine the mechanism of damage protecting activity H_2O_2 was added to the mixture as an oxidant. After incubation samples were electrophoresis for 1 h at 60 V on 1% agarose gel in TAE buffer according to Russo et al. [31] with some modifications. Then, the DNA bands were visualized under UV light and photographed (Quantum ST4 gel imagining system, Vilbar Lourmat).

2.7. Screening antibacterial activities

The standard disc diffusion method [32] was used for screening antibacterial activities of three *Verbascum* extracts against some Gram-negative and positive bacteria (Table 4). Reference antibiotic [Penicillin (P10)] was used to compare afterward with plant extracts. Minimal inhibition concentration (MIC) and minimal bactericidal concentration (MBC) were investigated as recommended instruction of the Clinical and Laboratory Standards Institute [33,34].

2.8. Biofilm inhibition assay

The microplate biofilm method [35] was used to evaluate the inhibition of biofilm formation by *Verbascum* plant extracts against test bacteria. The measurement of the antibiotic effect of the extracts was made by the percentage reduction formulation.

Table 1. Voucher specimens used in this study.

Species	Locality	Collectors
V. mucronatum	Balıkesir: Edremit, Akçay-Küçükkuyu, 39°35′27′′N-26°53′37′′E, 29 July 2017.	A. Yılmaz and Ö. Yılmaz 1933 (BULU)
V. bombyciferum	Bursa: Nilüfer, Çalı-Atlas, 242 m, 40°09′28′′N-28°54′58′′E, 26 April 2017.	Ö. Yılmaz 1860 (BULU)
V. vacillans	Balıkesir: Edremit, Zeytinli-Beyoba, 39°38′07′′N-26°55′52′′E, 30 July 2017.	A. Yılmaz and Ö. Yılmaz 1934 (BULU)

$$Inhibition\ (\%) = \frac{A_{control} - A_{sample}}{A_{sample}} \times 100 \qquad (3)$$

$A_{control}$: Absorbance of the control (containing 100 µL Mueller Hinton Broth instead of plant extract) reaction, A_{sample}: Absorbance of the test compounds

3. Results and discussions

3.1. Qualitative phytochemical analysis

This study revealed that the ethanol extracts of three *Verbascum* species contained coumarins, cardiac glycosides, phlorotannins quinones, flavanones, anthocyanins, and proteins (Table 2).

Table 2. Phytochemical analysis of *Verbascum* species

Phytochemical contents	*Verbascum* plant species		
	V1	V2	V3
Coumarins	-	+	+
Cardiac glycosides	+	-	-
Phlabotannins	+	++	-
Quinones	+	-	-
Flavanones	+	+	++
Anthocyanins	+	-	-
Proteins (Biuret test)	-	+	-

V1: *V. mucronatum*, V2: *V. bombyciferum*, V3: *V. vacillans*; +: low intensity reaction, ++: strong intensity reaction; -: Not Detected

However, cardiac glycosides, quinones anthocyanins were detected only in *V. mucronatum* (V1); proteins were detected only in *V. bombyciferum* (V2); only flavanones were detected in all three *Verbascum* species. *V. vacillans* ethanol extract also has been determined to be the lowest plant for phytochemical contents.

Phytochemicals are natural bioactive including alkaloids, terpenoids, steroids, polyphenols, and flavonoids have rational uses and are found in varying amounts in different organisms [36]. Plants are an important source of these bioactive compounds and elucidation of these phytochemicals is important in revealing the benefits for human health [37].

The members of the *Verbascum* species are known to be rich in saponins, tannins, terpenoids, phenylethanoid glycosides, flavonoids contained in the *Verbascum* species are responsible for biological activities [38,39]. It can be said that not only a single substance but the different substances they contain affect the activity [39]. The presence of alkaloids, tannins, flavonoids, flavones, anthraquinones, cardiac glycosides *V. thapsus* were determined by phytochemical analysis [40]. In the present study, phytochemical analysis of *Verbascum* species showed the presence of various bioactive constituents. This variety can be explained by that the secondary metabolite profile in plants can be determined by different factors. The genotypic characteristics and phenology of the species are the basic elements that determine the phytochemical profile [41]. Biotic (pathogens and herbivorous organisms) and abiotic factors (light, temperature, nutrients, water condition, and geographical conditions) can directly affect the secondary metabolite chemical composition of the plant [42,43].

There is no report about the phytochemical contents of three *Verbascum* species except *V. mucronatum* [44]. This is the first study that report phytochemical contents of *V. mucronatum*, *V. bombyciferum*, and *V. vacillans* ethanol extracts. Flavonoids were detected as common the phytochemical content in three plant extracts. It is important that flavonoids constitute the largest plant phenolic group that makes up more than half of the natural phenolic compounds [45].

3.2. Antioxidant activity

3.2.1. DPPH free radical scavenging activity

Free radical scavenging activity of the ethanolic extracts of *Verbascum* species was measured by DPPH assay at five varying concentrations (10, 20, 40, 60, and 80 µg/mL). DPPH free scavenging activity of each plant extracts was increased in a concentration-dependent. The highest concentration of 80 µg/mL extract of *V. mucronatum* shown the best antioxidant activity (75.06%), followed by *V. vacillans* (73.16%), *V. bombyciferum* (72.79%), and synthetic antioxidant butylhydroxytoluene (BHT) (68.89%), respectively (Fig. 1). The IC_{50} value, which indicates the amount of sample needed to inhibit 50% of the radical. According to the results, all the extract was found strongly active in the range of 10-50 µg/mL [46]. The IC_{50} value of *Verbascum* extracts were; *V. vacillans* (24.84 µg/mL), *V. bombyciferum* (27.84 µg/mL), and *V. mucronatum* (35.22 µg/mL).

3.2.2. Cu(II) ion reducing antioxidant capacity

The Cu(II) ion reducing the antioxidant capacity of *Verbascum* plant species, especially *V. vacillans* showed strong antioxidant capacity at the highest concentration of 80 µg/mL as same as a positive control (Fig. 2).

Free radicals are drawn in many disorders like neurodegenerative diseases, cancer, and AIDS. Antioxidants due to their scavenging activity are useful for the management of these diseases and this explains

the curative effects of medicinal plants having antioxidant effect [24].

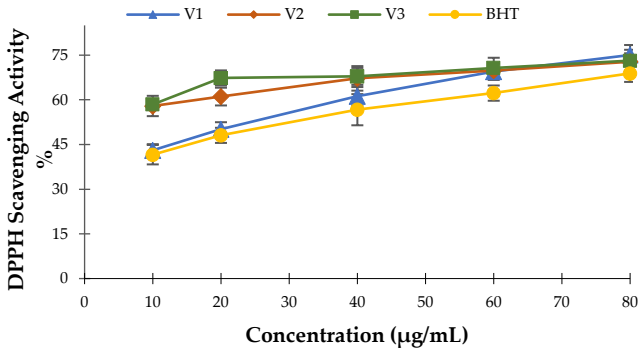

Figure 1. DPPH free scavenging activity of *Verbascum* species. V1: *V. mucronatum*, V2: *V. bombyciferum*, V3: *V. vacillans*. Values are means of three experiments ± SD

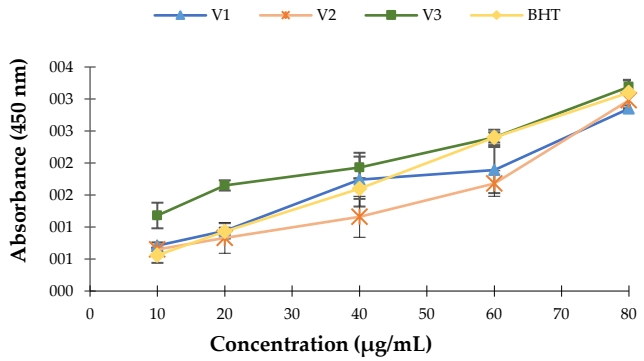

Figure 2. The Cu(II) ion reducing antioxidant capacity of *Verbascum* species. V1: *V. mucronatum*, V2: *V. bombyciferum*, V3: *V. vacillans*. Values are means of three experiments ± SD

It has been determined that the biological activities of the extracts can vary depending on the season, the type of the solvent, the dose, and the application time. Studies have emphasized that there is a linear correlation between the total phenolic content of plant extracts and antioxidant efficiency values. Considering the crude extracts of these plants have plenty of constituents it becomes tough to praise the antioxidant property selectively to any group of them without more investigations [47].

DPPH is a stable free radical. It is purple in color and this color can be absorbed in 517 nm. When DPPH free radicals are captured by an antioxidant, their color changes from purple to yellow. This color change is observed because DPPH transforms into 2,2-diphenyl-1-picryl hydrazine by interacting with antioxidant substances [25]. The antioxidant activity of *Verbascum* species was evaluated using different extracts such as the methanol and acetone extracts of *V. pinetorum* besides methanol (IC_{50} = 65.4 ± 0.5 µg/mL) and water (IC_{50} = 235.6 ± 0.5 µg/mL) extracts of *V. mucronatum* showed high free radical scavenging activity by DPPH assay [48,49] and *V. pinetorum* acetone, methanol, and water extracts showed high activity by CUPRAC test [49]. Georgiev et al. [8] studied *V. xanthophoeniceum* leaves and reported that have strong antioxidant activities and active constituents (forsythoside B, verbascoside and leucosceptoside B) showed IC_{50} values of 21-44 µg/mL DPPH radical scavenging activities. In this study, the ethanolic extracts of *Verbascum* species were evaluated for the antioxidant activity for DPPH free radical scavenging and Cu(II) ion reducing antioxidant capacity. Our results supported the previous findings that *Verbascum* extracts had concentration-dependent antioxidant capacity.

3.3. Antimutagenicity assay

In this study, the antimutagenicity of the *Verbascum* extracts was investigated using *S. typhimurium* TA98 and TA100 mutant strains. Findings obtained as a result of antimutagenicity activity were shown in Table 3.

V. mucronatum extract showed a strong antimutagenic effect (inhibition rate > 40 %) at all concentrations on *S. typhimurium* TA98 strain. *V. bombyciferum* was found to have a moderate antimutagenic effect (32.83 %) at 0.5 ppm concentration and strong antimutagenic activity (45.48 % and 48.03 %) at concentrations of 1 and 2 ppm, respectively on TA98 strains. *V. vacillans* extract did not prevent frameshift mutation except the higher concentration of 2 ppm (28.37%). The results obtained from the TA100 strain showed strong antimutagenic effect of *V. mucronatum* and *V. bombyciferum* extracts of all concentrations while the *V. vacillans* extract did not prevent base-pair mutation at any concentrations.

It is known that many plants or plant products consumed contain a variety of the antimutagenic agents and are also capable of inactivating environmental mutagens or carcinogens. Therefore, it is important to determine antimutagenic activities of extracts obtained from plants. In this study, the potential *in vitro* effects of *Verbascum* extracts on genetic material was investigated by the Ames test. As a result of the antimutagenicity study, *Verbascum* species generally found to have moderate or strong antimutagenic effects at different concentrations. Probably chemical contents of the *Verbascum* species play an active role in the antimutagenic activity. There is no report about *Verbascum* plant species antimutagenic effects. Makhafola et al. [50] have examined 31 plant extracts for antimutagenic activity, and it was found that most plants have potential antimutagenic activity and also a close relationship between antioxidant activities. Mutagenic and antimutagenic activities of medically used *Salacia crassifolia* root shell fractions (hexane, ethyl acetate, and hydroalcoholic) were investigated using *S. typhimurium* TA98 and TA100 strains. There was no mutagenic effect

and high antimutagenic activity was present in hexane of strain TA100 [51].

Table 3. The antimutagenic effects of different concentration of *Verbascum* extract on *S. typhimurium* TA98 and TA100 strains

Extracts		Conc. (ppm)	Number of his+ revertant colony/Plate TA98 Mean ± SD	Inh. %	TA100 Mean ± SD	Inh. %
Positive control	NPD		894± 17.1			
	SA				1033± 21.1	
V1		0.5	545±9.8	40.6	461±6.9	61.6
		1	520±6.3	43.5	453±9.2	62.4
		2	514±7.6	44.2	422±11.0	65.8
V2		0.5	480±8.3	32.8	568±8.5	50.1
		1	502±10.2	45.5	556±6.5	51.4
		2	611±9.6	48.0	515±10.3	55.8
V3		0.5	776±13.6	13.7	857±4.9	18.9
		1	701±11.2	22.4	804±7.5	24.7
		2	650±14.1	28.4	812±8.3	23.8
Negative control			43±2.9		112±4.3	
Spontaneous control			34±3.9		104±6.1	

V1: *V. mucronatum*, V2: *V. bombyciferum*, V3: *V. Vacillans*, NPD: 4-nitro-o-phenylene-diamine, SA: sodium azide, Conc.: Concentration, Inh.: Inhibition, Values were expressed as mean ± standard deviation of three experiments.

Sutherlandia frutescens (L.) is an endemic species used in the treatment of cancer and diabetes in Southern Africa. Mutagenic and antimutagenic activities were tested with Ames test using ethyl acetate and 50% methanol extracts. No mutagenic activity was observed, ethyl acetate extract showed an antimutagenic effect in all concentrations and bacterial strains (TA97a, TA98, TA100, and TA102) [52]. The antimutagenicity findings obtained in our study support previous studies.

3.4. DNA damage protection potential

In the presence of an oxidizing agent (H_2O_2), *Verbascum* plant ethanol extracts showed DNA damage protection potential in tested concentrations. However, the lowest concentration (0.5 µM) of the *V. bombyciferum* species Form III were observed and almost completely disintegrate DNA in this concentration (Fig. 3). Form I indicated supercoiled, Form II relaxed circular, and Form III linear form of plasmid DNA. These forms act at different speeds in agarose gel electrophoresis. Because the load density is high and the volume is low, Form I moves fastest in the gel, and Form II is the slower moving band in gel.

The DNA damage protection potential results showed that the treatment of pBR322 plasmid DNA with H_2O_2 did not result in changes in plasmid conformation. Only, the lowest concentration (0.5 µM) of the *V. bomyciferum* species changed the plasmid DNA conformation. However, Boğa et al. [49] found that methanol extracts of *V. pinetorum* did not show a significant protection activity of DNA.

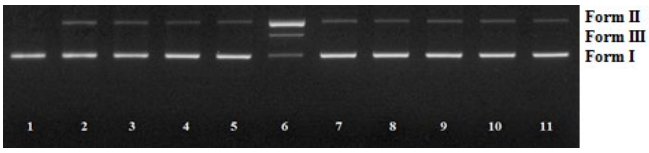

Figure 3. DNA damage protection potential of *Verbascum* species. 1. Plazmid DNA, 2. DNA+ H_2O_2, 3. DNA+ 0,5 µM V1+ H_2O_2, 4. DNA+ 1 µM V1+ H_2O_2, 5. DNA+ 2µM V1+ H_2O_2, 6. DNA+ 0,5 µM V2+ H_2O_2, 7. DNA+ 1 µM V2+ H_2O_2, 8. DNA+ 2 µM V2+ H_2O_2, 9. DNA+ 0,5 µM V3+ H_2O_2, 10. DNA+ 1 µM V3+ H_2O_2, 11. DNA+ 2 µM V3+ H_2O_2

3.5. Antibacterial activity

Results of antibacterial activity of three *Verbascum* plant extracts against the test bacteria were qualitatively and quantitatively assessed by the presence and diameters of the inhibition zones, MIC, and MBC (Table 4). The ethanolic extracts obtained from the three *Verbascum* plants were strong antibacterial activities against the test bacteria with inhibition zones at 9.0-19.0 mm. *V. vacillans* extract was more effective than comparative antibiotic P10 against *P. aeruginosa* ATCC 27853, *B. subtilis* ATCC 6633 and *S. haemolyticus* ATCC 43252. But *V. mucronatum* and *V. bombyciferum* are obtained in similar strong antibacterial activity only against *P. aeruginosa* ATCC 27853. The extracts have shown the weaker activity against *E. coli* NRRL B-3704, *E. aerogenes* ATCC 13048, *P. vulgaris* ATCC 13315, *A. baumanii* ATCC 19606, *S. aureus* ATCC 6538P as compared to control antibiotic P10.

Table 4. Disc Diffusion, MIC, MBC, and MBC/MIC ratios of the extracts of strains

Test bacteria	Plant extracts *Disc Diffusion[a] V1	V2	V3	Control P10	MIC (µg/mL) V1	V2	V3	Control ST10	MBC V1	V2	V3	MBC/MIC V1	V2	V3
E. coli NRRL B-3704	10.3±0.1	9.6±0.1	10.0±0.1	16.0	10±0	5±0	10±0	4.0	10±0	20±0	10±0	1	4	1
E. aerogenes ATCC 13048	11.3±0.1	10.0±0.1	10.0±0.1	14.0	10±0	5±0	1.25±0.01	2.0	10±0	10±0	1.25±0.01	1	2	1
P. aeruginosa ATCC 27853	11.3±0.5	12.3±0.2	10.3±0.2	8.0	20±0	5±0	10±0	1.0	20±0	20±0	10±0	1	4	1
P. vulgaris ATCC 13315	12.6±0.2	9.3±0.1	9.0±0.5	13.0	10±0	5±0	10±0.1	4.0	10±0	10±0	20±0	1	2	2
A. baumanii ATCC 19606	10.4±0.2	10.0±0.2	11.0±0.2	12.0	2.5±0	10±0	1.25±0.01	2.0	5±0	20±0	1.25±0.01	2	2	1
B. subtilis ATCC 6633	9.6±0.2	10.0±0.2	15.0±0.2	14.0	5±0	5±0	2.5±0.0	4.0	5±0	5±0	5±0	1	1	2
S. aureus ATCC 6538P	14.0±0.4	10.3±01	9.3±0.3	15.0	10±0	10±0	10±0	4.0	10±0	10±0	10±0	1	1	1
S. haemolyticus ATCC 43252	13.0±0.2	12.3±0.1	19.0±0.6	14.0	20±0	10±0	20±0	5.0	20±0	20±0	20±0	1	2	1

V1: V. mucronatum; V2: *V. bombyciferum;* V3: *V. vacillans;* *Inhibition zone (mm); a includes diameter of disk (6 mm); P10 = Penicillin (10 ug/disc); ST10: *Streptomycin (10 ug/disc)*

V. vacillans extract demonstrated good inhibitory activity against *E. aerogenes* ATCC 13048, *A. baumanii* ATCC 19606, and *B. subtilis* ATCC 6633, with MICs values of 1.25 mg/mL, 1.25 mg/mL, 2.5 mg/mL as compared to control antibiotic ST10, respectively. However, the three *Verbascum* plant extracts have a weak antibacterial effect against the other test bacteria with MICs and MBCs ranged from 20 (20) to 5 (5) mg/mL. These values are far below the standard antibiotic-Streptomycin (ST10).

The results of the present investigation show that three different *Verbascum* ethanol extracts have antibacterial and antibiofilm potential against test bacteria. In Table 3, MBC/MIC ratio was calculated to establish bacteriostatic or bactericidal effects of the plant extracts. According to Ocampo et al. [53] and Azman et al. [54] bacteriostatic can be defined as the agent that inhibit the growth of bacteria without killing effects, while bactericidal means agents that kill bacteria. An extract is considered bactericidal when the ratio of MBC/MIC is ≤ 4 and bacteriostatic when this ratio is > 4 [55]. It appears that all plant extracts have bactericidal activity on the test bacteria. Our antibacterial activity findings confirmed the observations of some other investigations about various *Verbascum* species antimicrobial activity [12,14,15, 38,56].

When examining previous studies about *V. mucronatum*, *V. bombyciferum*, *V. vacillans*, we found that Dülger et al. [56], Dülger and Hacıoğlu [57] and Kahraman et al. [12] revealed antibacterial activity against Gram (+) bacteria, respectively. Our findings are distinct from previous studies because of strong antibacterial activity against *P. aeruginosa* ATCC 27853 of three plant extracts. Ethanol was chosen as the solvent since it was reported that ethanol was the best solvent in previous studies [58].

3.6. Results of biofilm inhibition

Inhibition biofilm activity was performed with MIC concentrations of plant extracts. Treatment with *V. mucronatum*, *V. bombyciferum*, *V. vacillans* extracts have shown significant reduction in biofilm formation in *E. coli* NRRL B-3704, *P. aeruginosa* ATCC 27853, *A. baumanii* ATCC 19606, *B.subtilis* ATCC 6633, *S. aureus* ATCC 6538P (Fig. 4a, 4b, 4c).

Biofilm is assessed as significant virulence factor because of increasing the resistance of bacteria to antibiotics and host defense systems [59]. This necessitated the screening of new and natural antibiotic sources in the fight against biofilm. Studies of antibiofilm activity of *Verbascum* species are very limited. Moghaddam et al. [60] reported that *V. thapsus* extracts have inhibitory effects on biofilm formation of three oral streptococci. The high the biofilm inhibition activity we obtain from three *Verbascum* species is very important in this respect. Therefore, comprehensive investigations about these three *Verbascum* species antibacterial and antibiofilm activity have become a new strategy for the treatment of these bacterial infections.

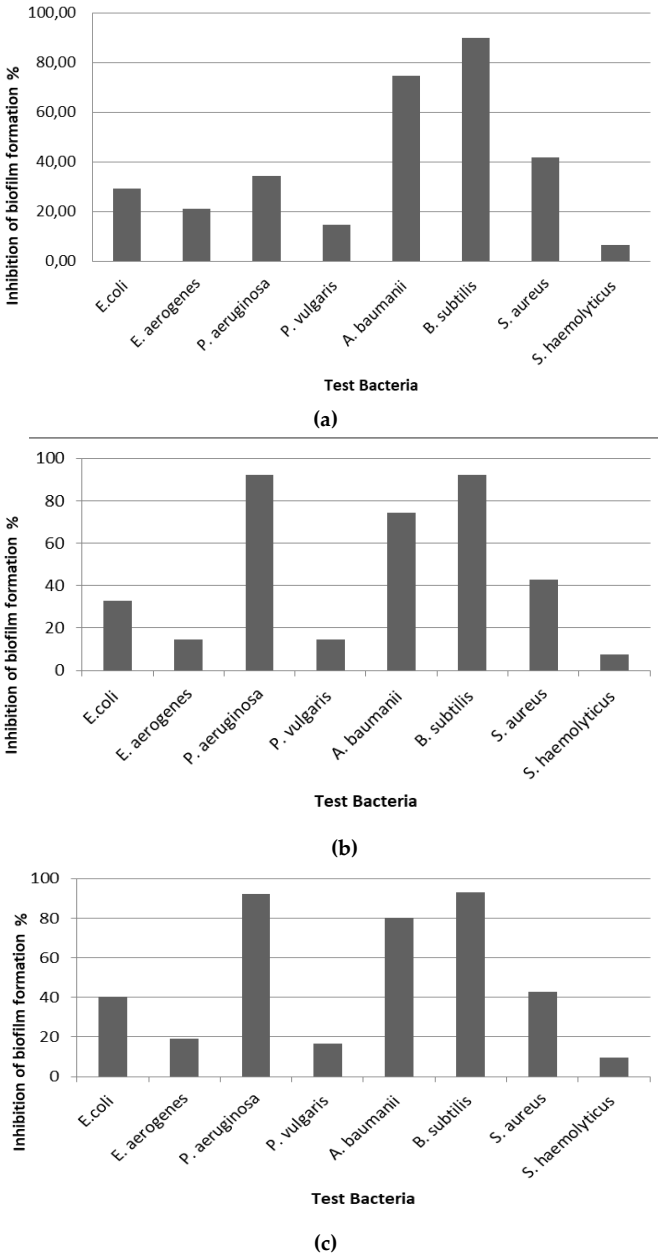

Figure 4. Inhibition of biofilms formation of three *Verbascum* plant extracts, **a)** *V. mucronatum* biofilm inhibition activity, **b)** *V. bombyciferum* biofilm inhibition activity, **c)** *V. vacillans* biofilm inhibition activity

4. Conclusion

Three *Verbascum* plant species demonstrated the presence of some phytochemical-especially flavonoids-as secondary metabolites with potential biological activities. It may be considered that these extracts are a mixture of substances with different characteristics and biological activities. Results reported in this study can be considered as the first comprehensive study on phytochemical contents, antioxidant, antimutagenicity, DNA damage protecting, the antibacterial and antibiofilm activity of ethanolic extracts of *V.*

mucronatum, *V. bombyciferum*, *V. vacillans*. Future studies should be done to define the biological active components of three *Verbascum* species, especially with different solvents.

Disclosure statement

No potential conflict of interest was reported by the author(s).

References

[1] E. Fischer, Scrophulariaceae, The Families and genera of vascular plants, Editor: K. Kubitzki, 2004, Germany, Springer.

[2] P.H. Davis, R.R. Mill, K. Tan, Flora of Turkey and the East Aegean Islands, 1988, England, Edinburgh University Press.

[3] F.A. Karavelioğulları, *Verbascum* L., Türkiye Bitkileri Listesi (Damarlı Bitkiler), Editors: A. Güner, S. Aslan, T. Ekim, M. Vural, M.T. Babaç, 2012, Turkey, Nezahat Gökyiğit Botanical Garden and Flora Research Association.

[4] F.A. Karavelioğulları, *Verbascum ibrahim-belenlii* (Scrophulariaceae), a new species from East Anatolia, Turkey, Phytotaxa, 212(3), 2015, 246-248.

[5] A. Huber-Morath, Die Turkischen Verbasceen, 1971, Switzerland, Kommissionsverlag von Gebrüder Fretz AG.

[6] A. Huber-Morath, *Verbascum* L., Flora of Turkey and the East Aegean Islands, Editor: P.H. Davis, 1978, England, Edinburgh University Press.

[7] T. Baytop, Türkiye'de Bitkiler ile Tedavi, 1999, Turkey, Nobel Medical Bookstores.

[8] M. Georgiev, K. Alipieva, I. Orhan, R. Abrashev, P. Denev, M. Angelova, Antioxidant and cholinesterases inhibitory activities of *Verbascum xanthophoeniceum* Griseb. and its phenylethanoid glycosides, Food Chem, 128, 2011, 100-105.

[9] A.U. Türker, E. Gürel, Common mullein (Verbascum Thapsus L.): Recent advances in research, Phytother Res, 19, 2005, 733-739.

[10] B. Dülger, N. Hacıoğlu, Activity of three endemic *Verbascum* species against hospital isolates methicillin-resistant Staphylococcus aureus, Biotechnol Biotec EQ, 23, 2009, 760-762.

[11] Ç. Kahraman, M. Ekizoğlu, D. Kart, Z.S. Akdemir, I.I. Tatlı, Antimicrobial activity of some *Verbascum* species growing in Turkey, FABAD J Pharm Sci, 36, 2011, 11-15.

[12] Ç. Kahraman, Z.S. Akdemir, I.I. Tatlı, Promising cytotoxic activity profile, biological activities and phytochemical screening of *Verbascum* L. species, Med Aromat Plant Sci Biotechnol, 6, 2012, 63-75.

[13] E. Kozan, I.T. Çankaya, Ç. Kahraman, E.K. Akkol, Z. Akdemir, The *in vivo* anthelmintic efficacy of some *Verbascum* species growing in Turkey, Exp Parasitol, 129, 2011, 211-214.

[14] B. Özcan, M. Esen, M. Calışkan, R.A. Mothana, A.C. Cihan, H. Yolcu, Antimicrobial and antioxidant activities of the various extracts of *Verbascum pinetorum* Boiss. O. Kuntze (Scrophulariaceae), Eur Rev Med Pharmaco, 15, 2011, 900-905.

[15] I.I. Tatlı, Z.S. Akdemir, Traditional uses and biological activities of *Verbascum* species, FABAD J Pharm Sci, 3, 2006, 85-96.

[16] P.E. Boissier, *Verbascum* L., Pp. 298-362. In: Celsia L., Staurophragma Fisch. and C A Mey in Boissier P.E. (editor) Flora orientalis, 1869, Switzerland.

[17] T. Ekim, *Verbascum* L., Flora of Turkey and the East Aegean Islands, Editors: A. Güner, N. Özhatay, T. Ekim, K.H.C. Başer, 2000, England, Edinburgh University Press.

[18] I.K. Ferguson, *Verbascum* L., Flora Europea, Editors: V.H. Heywood, G.T. Tutin, N.A. Burges, D.M. Moore, D.H. Valentine, S.M. Walters, D.A Webb, 1972, England, Cambridge University Press.

[19] R.D. Meiklei, *Verbascum* L., Flora of Cyprus, Editor: R.D. Meikle, 1985, England, Royal Botanic Gardens.

[20] S.S. Murbeck, Monographie der Gattung *Verbascum*, 1933, Sweden, Acta Universitatis Lundensis.

[21] A.M. Khan, R.A. Qureshi, S.A. Gillani, U. Faizan, Antimicrobial activity of selected medicinal plants of Margalla Hills, Islamabad, Pakistan, J Med Plants Res, 5, 2011, 4665-4670.

[22] W.C. Evans, Pharmacognosy, 2009, Singapore, W B Saunders Co. Ltd.

[23] J.B. Harborne, Phytochemical methods: A guide to modern techniques of plant analysis, 1973, England, Champman and Hall.

[24] N. Raaman, Phytochemical Techniques, 2006, India, New India Publishing Agency.

[25] W. Brand-Williams, M.E. Cuvelier, C. Berset, Use of a free radical method to evaluate antioxidant activity, LWT-Food Sci Technol, 28, 1995, 25-30.

[26] R. Apak, K. Güçlü, M. Özyürek, S.E. Karademir, E. Erçağ, The Cupric ion reducing antioxidant capacity and polyphenolic content of some herbal teas, Int J Food Sci Nutr, 57, 2006, 292-304.

[27] D.M. Maron, B.N. Ames, Revised methods for the Salmonella mutagenicity test, Mutat Res, 113, 1983, 173-215.

[28] C.E. Hong, S.Y. Lyu, Genotoxicity detection of five medicinal plants in Nigeria, J Toxicol Sci, 36(1), 2011, 87-93.

[29] Y. Ikken, P. Morales, A. Martinez, M.L. Marin, A.I. Haza, M.I. Cambero, Antimutagenic effect of fruit and vegetable ethanolic extracts against N-Nitrosoamines evaluated by The Ames Test, J Agr Food Chem, 47, 1999, 3257-3264.

[30] P.S. Negi, G.K. Jayaprakasha, B.S. Jena, Antioxidant and antimutagenic activities of Pomegranate peel extracts, Food Chem, 80, 2003, 393-397.

[31] A. Russo, A.A. Izzo, V. Cardile, F. Borrelli, A. Vanella, Indian medicinal plants as antiradicals and DNA cleavage protectors, Phytomedicine, 8(2), 2001, 125-132.

[32] C.H. Collins, P.M. Lyne, J.M. Grange, Microbiological Methods, 1989, England, Butterworths and Co Ltd.

[33] CLSI, Methods for dilution antimicrobial susceptibility tests for bacteria that grow aerobically (9. edition), CLSI Document M07-A9, 2012, USA.

[34] R. Teanpaisan, P. Kawsud, N. Pahumunto, J. Puripattanavong, Screening for antibacterial and antibiofilm activity in Thai medicinal plant extracts against oral microorganisms, J Tradit Complement Med, 7(2), 2017, 172-177.

[35] J.H. Merritt, D.E. Kadouri, G.A. O'toole, Growing and analysing static biofilms, Curr Protoc Microbiol, 1(1B), 2005, 1-17.

[36] A.A. Shad, S. Ahmad, R. Ullah, N.M. AbdEl-Salam, H. Fouad, N. Rehman, H. Hussain, W. Saeed, Phytochemical and biological activities of four wild medicinal plants, Sci World J, 2014, 857363.

[37] G. Pramila, D.B. Jirekar, M. Farooqui, S.D. Naikwade, Biological activity of aqueous extract of some medicinal plants, Der Chemica Sinica, 5(4), 2014, 65-70.

[38] N. Ali, S.W.A. Shah, I. Shah, G. Ahmed, M. Ghias, I. Khan, W. Ali, Anthelmintic and relaxant activities of *Verbascum thapsus* Mullein, BMC Complem Altern M, 12, 2012, 29-36.

[39] Ç. Kahraman, I.I. Tatlı, I.E. Orhan, Z.S. Akdemir, Cholinesterase inhibitory and antioxidant properties of *Verbascum mucronatum* Lam. and its secondary metabolites, Z Naturforsch, 65c, 2010, 667-674.

[40] N.H. Khan, M.S.A. Nur-E Kamal, M. Rahman, Antibacterial activity of *Euphorbia thymifolia* Linn, Indian J Med Res, 87, 1988, 395-397.

[41] R. Fillipini, A. Piovan, A. Borsarini, R. Caniato, Study of dynamic accumulation of secondary metabolites in three subspecies of Hypericum perforatum, Fitoterapia, 81, 2010, 115-119.

[42] J.C.M.S. Moura, C.A.V. Bonine, J.O.F. Viana, M.C. Dornelas, P. Mazzafera, Abiotic and biotic stresses and changes in the lignin content and composition in plants, J Integr Plant Biol, 52, 2010, 360-376.

[43] J.P.B. Sousa, M.F. Leite, R.F. Jorge, D.O. Resende, A.A. da Silva Filho, N.A.J.C. Furtado, A.E.E. Soares, A.C.C. Spadarom, PM. Magalhães, J.K. Bastos, Seasonality role on the phenolics from cultivated *Baccharis dracunculifolia*, Evid-Based Compl Alt, 2011, 464289.
[44] Z. Akdemir, C. Kahraman, I. Tatlı, E.K. Akkol, I. Suntar, H. Keles, Bioassay-guided isolation of anti-inflammatory, antinociceptive and wound healer glycosides from the flowers of *Verbascum mucronatum* Lam., J Ethnopharmacol, 136, 2011, 436-443.
[45] J.B. Harborne, H. Baxter, Handbook of Natural Flavonoids, 1999, England, Wiley.
[46] S. Phongpaichit, J. Nikom, N. Rungjindamai, J. Sakayaroj, N. Hutadilok-Towatana, V. Rukachaisirikul, K. Kirtikara, Biological activities of extracts from endophytic fungi isolated from Garcinia plants, FEMS Immunol Med Mic. 51(3), 2007, 517-525.
[47] A. Mahmood, A. Mahmood, M. Mahmood, *In vitro* biological activities of most common medicinal plants of family Solanaceae, World Appl Sci J, 17(8), 2012, 1026-1032.
[48] S. Alan, F.Z. Saltan, R.S. Göktürk, M. Sökmen, Taxonomical properties of three *Verbascum* L. species and their antioxidant activities, Asian J Chem, 21, 2009, 5438-5452.
[49] M. Boğa, A. Ertaş, M.A. Yılmaz, M. Kızıl, B. Çeken, N. Haşimi, T.Y. Özden, S. Demirci, İ. Yener, Ö. Deveci, UHPLC-ESI-MS/MS and GC-MS analyses on phenolic, fatty acid and essential oil of *Verbascum pinetorum* with antioxidant, anticholinesterase, antimicrobial and DNA damage protection effects, Iran J Pharm Res, 15(3), 2016, 393-405.
[50] T.J. Makhafola, E.E. Elgorashi, L.J. McGaw, L. Verschaeveand, J.N. Eloff, The correlation between antimutagenic activity and total phenolic content of extracts of 31 plant species with high antioxidant activity, BMC Complemen Altern M, 16, 2016, 490.
[51] C.C. Carneiro, J.H. Véras, B.R. Góes, C.N. Pérez, L. Chen-Chen, Mutagenicity and antimutagenicity of Salacia crassifolia (mart. Ex. Schult.) G. Don. evaluated by Ames test, Braz J Biol, 78(2), 2018, 345-350.
[52] S.S.B.N. Ntuli, W.C.A. Gelderblom, D.R. Katerere, The mutagenic and antimutagenic activity of Sutherlandia frutescens extracts and marker compounds, BMC Complemen Altern M, 18, 2018, 93.
[53] P.S. Ocampo, V. Lazar, B. Papp, M. Arnoldini, P.A. Wiesch, R. BusaFekete, G. Fekete, C. Pal, M. Ackermann, S. Bonhoeffer, Antagonism between bacteriostatic and bactericidal antibiotics is prevalent, Antimicrob Agents Ch, 58, 2014, 4573-4582.
[54] A. Azman, I. Othman, C. Fang, K. Chan, B. Goh, L. Lee, Antibacterial, anticancer and neuroprotective activities of rare actinobacteria from mangrove forest soils, Indian J Microbiol, 57(2), 2017, 177-187.
[55] G.A. Pankey, L.D. Sabath, Clinical relevance of bacteriostatic versus bactericidal mechanisms of action in the treatment of Gram-positive bacterial infections, Clin Infect Dis, 38, 2004, 864-870.
[56] B. Dülger, N. Hacıoğlu, Antimicrobial activity of some endemic *Verbascum* and *Scrophularia* species from Turkey, Asian J Chem, 20(5), 2008, 3779-3785.
[57] B. Dülger, S. Kırmızı, H. Arslan, G. Güleryüz, Antimicrobial activity of three endemic *Verbascum* species, Pharm Biol, 40(8), 2002, 587-589.
[58] S.G. Jonathan, I.O. Fasidi, Antimicrobial activities of two Nigerian edible macrofungi, Lycoperdon pusillum (Bat. Ex) and L. giganteum (Pers.), Afr J Biomed Res, 6, 2003, 85-90.
[59] S.S. Grant, D.T. Hung, Persistent bacterial infections, antibiotic tolerance, and the oxidative stress response, Virulence, 4(4), 2013, 273-283.
[60] H.K. Moghaddam, M. Mirzaii, M. Khaksari, M. Fazli, F. Rahimi, A.A. Behzadi, Antibacterial and anti-Adherent activity of great mullein (*Verbascum thapsus* L.) ethanolic extract on *in vitro* biofilm formation of three oral Streptococci, Int J Health Stud, 1(2), 2015, 34-37.

e-ISSN: 2687-6698 Research Article

Turkish Journal of Analytical Chemistry
TurkJAC
www.turkjac.org
2019

Solvent and molecular structure effects on acidity strength in non-aqueous medium

Şule Bahçeci[1], Zafer Ocak[2*], Nuri Yıldırım[3], Haydar Yüksek[4]

[1]Trabzon University, Fatih Education Faculty, Secondary Education Science and Mathematics Education, 61080, Trabzon, Turkey
[2]Kafkas University, Education Faculty, Mathematics and Science Education,36100 Kars, Turkey
[3]Karadeniz Technical University, Faculty of Science, Department of Chemistry, 61080, Trabzon, Turkey
[4]Kafkas University, Faculty of Science & Letters, Department of Chemistry, 36100 Kars, Turkey

Abstract

The acidic properties of ten 3-alkyl(aryl)-4-[3-hydroxy-4-methoxy benzylidenamino]-4,5-dihydro-1H-1,2,4-triazol-5-one derivatives were investigated. Amphiprotic solvents used in this study were isopropyl alcohol and *tert*-butanol. Acetone and N,N- dimethylformamide (DMF) were preferred as a dipolar aprotic solvent. Compounds were titrated with tetrabutylammonium hydroxide (TBAH) in isopropyl alcohol and titrimetric analyses were used potentiometric method determining the end-points, half-neutralization method determining acidity. Typical S-shaped titration graphs excepted were determined. The acidity strengths of 4,5-dihydro-1H-1,2,4-triazol-5-one derivatives in amphiprotic and dipolar aprotic solvents were calculated using tables and graphs. The pK_a values obtained in the solvents were found to be differentiated. The effects of solvent, molecular structure, autoprotolysis constant dielectric constant, and leveling-differentiation effects of the solvents upon acidity strength of the compounds were discussed.

Keywords: Triazole, amphiprotic solvent, pK_a, potentiometry

1. Introduction

Potentiometry, one of the electrochemical methods, is widely used due to its wide advantages. Potentiometric techniques have long been used in landmark determination. It is simple and inexpensive in potentiometric methods [1]. Potentiometric titrations are one of the most widely used methods for determining acidity constants due to their simple and low cost. In the course of time, many different methods such as spectrometry, conductimetry, electrophoresis, NMR, polarimetry, calorimetry, theoretical, etc. were developed [2]. However, the potentiometric method does not include the restrictions specified in the determination of the equivalent point, so it is the most widely used method among these methods due to its simplicity, accuracy, and precision [3].

Thousands of potentiometric sensors have been successfully developed and applied in many fields such as medicine, environmental monitoring, agriculture, industry and pharmaceutical sciences [4,5].

Among the electrochemical methods of the best techniques for antioxidant activity (AOA) assessment, potentiometry is where the potential shift of the platinum electrode, which is readily applicable and the source of information about AOA, is placed in a mediator system. Their advantages such as usability, speed, and easy measurement offer a direct evaluation of the electron-donor-acceptor properties of the system, ie the properties that determine the antioxidant status [6-8].

Using the dissociation constant, some thermodynamic parameters can be measured, such as enthalpy change (H°), Gibb's energy change (ΔG°), and entropy change (ΔS°). Enthalpy change of the decomposition process (ΔH°) Van't Hoff relation ($dlnK / dT = \Delta H° / RT^2$) Gibb's free energy (ΔG°) is calculated using the equation $\Delta G° = 2.303RTpK$. Using these calculated values of ΔH° and ΔG°, the entropy change (ΔS°) is determined by the equation $\Delta S° = (\Delta H° - \Delta G°) / T$ [9].

In this article, some 3-alkyl(aryl)-4-(3-hydroxy-4-methoxybenzylideneamino)-4,5-dihydro-1H-1,2,4-triazol-5-one derivates known to have biological

Citation: Ş. Bahçeci, Z. Ocak, N. Yıldırım, H. Yüksek, Solvent and molecular structure effects on acidity strength in non-aqueous medium, Turk J Anal Chem, 3(1), 2021, 27-32.

https://doi.org/10.51435/turkjac.939857

***Author of correspondence:** zafcak@gmail.com
Tel: +90 (474) 225 12 62
Fax +90 (474) 225 12 64
Received: May 20, 2021
Accepted: June 02, 2021

activities and acidic properties were used. The dissociation constants of the compounds were determined by the potentiometric titration method. [10-15]. Acidic properties in solvents were investigated with respect to solvent effect, structure effect, dielectric constant, and autoprotolysis constants. The study will contribute to the literature in the field of acid-bases and buffer solutions.

2. Materials and Methods

2.1. Reagents

Ten 3-alkyl(aryl)-4-(3-hydroxy-4-methoxybenzylidenamino)-4,5-dihydro-1H-1,2,4-triazol-5-ones which acidity strengths have been determined are shown in Fig. 1. Compounds 1 has been synthesized according to the literature [16].

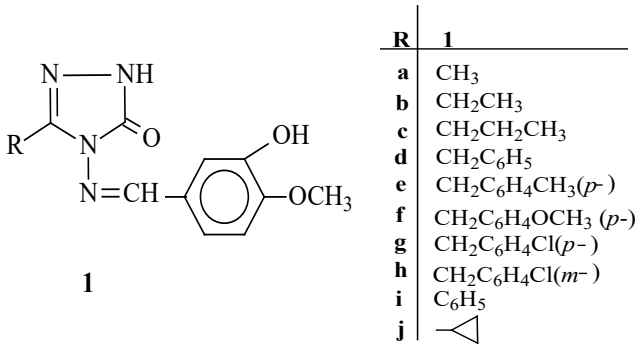

Figure 1. 3-Alkyl(Aryl)-4-(3-hydroxy-4-methoxybenzylidenamino)-4,5-dihydro-1H-1,2,4-triazol-5-one compounds

2.2. Solvents

Isopropyl alcohol as an amphiprotic solvent for the determination of acidity constants of 3-alkyl(aryl)-4-(3-hydroxy-4-methoxybenzylidenamino)-4,5-dihydro-1H-1,2,4-triazol-5-ones, *tert*-butanol, DMF from dipolar aprotic solvents, and acetone were used. The wide potential range of solvents, the solubility of TBAH and 3-alkyl(aryl)-4-(3-hydroxy-4-methoxybenzylidenamino)-4,5-dihydro-1H-1,2,4-triazol-5-ones in the solvents, and the working possibility under room conditions were important factors in the selection of solvents. A solution of 0.05 N of TBAH in isopropyl alcohol was preferred as a titrant. Isopropyl alcohol, acetone DMF, and *tert*-butanol were purchased from Merck.

2.3. Titrant

As a titrant, TBAH has been a widely used base against acids. The standard 0.05 N concentration of TBAH in isopropyl alcohol was preferred.

2.4. Apparatus

In the study, measurements were made with a Jenway 3040-model ion analyzer. The sensitivity of the pH meter used in pH readings is ± 0.002, while the sensitivity in mV measurement is ± 0.1, and the precision is ± 0.2. A combined pH electrode was used in the studies. A 50 µL micropipette was used for titrant addition.

2.5. Solutions

10^{-3} M solutions of 3-alkyl(aryl)-4-(3-hydroxy-4-methoxybenzylidenamino)-4,5-dihydro-1H-1,2,4-triazol-5-ones in acetone, *tert*-butanol, isopropyl alcohol, DMF has also been prepared. A 0.05 N solution of TBAH in isopropyl alcohol was prepared as a titrant.

2.6. Methods

Two buffer solutions of pH = 7,0 and pH = 10,0 were used for calibration of the pH meter used. Potentiometric titrations were carried out at 25,0 °C. 3-Alkyl(Aryl)-4-(3-hydroxy-4-methoxy benzyliden amino) -4,5-dihydro-1H-1,2,4-triazol-5-ones in amphiprotic and dipolar aprotic solvents 10^{-3} M 17,0 mL of its solution was taken. The acid solution was made homogeneous by mixing with a magnetic stirrer. With a micropipette, 0.05 mL of titrant each time was added to the stirring acid solution. 10^{-3} M of acid derivatives of 3-alkyl(aryl)-4-(3-hydroxy-4-methoxybenzylidenamino)-4,5-dihydro-1H-1,2,4-triazol-5-one in amphiprotic and dipolar aprotic solvents. Its solution was titrated with 0.05 N TBAH and the results are expressed as a graph of mV-mL TBAH.

2.7. Determination of acidity constants with Half-neutralization method

Titration graphs of mL TBAH-pH and mL TBAH-mV were drawn with the help of titration data. To determine the equivalent points, the graphs of TBAH - $\Delta E / \Delta V$ (first derivative) and mL TBAH - $\Delta^2 E / \Delta V^2$ (second derivative) were used (Fig. 2). From these values, half-neutralization points were calculated [17-21].

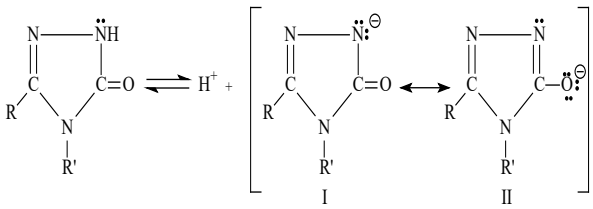

(1)

3. Result and Discussion

When the N-H hydrogen in the 4,5-dihydro-1H-1,2,4-triazol-5-one ring is protonated, the equilibrium shifts to the right because the remaining electron pair is delocalized to include oxygen and is easy to accommodate.; hence the acidity increases (Equation 1). This is evidence that the N-H proton in the 4,5-dihydro-1H-1,2,4-triazol-5-one ring system shows acidic properties.

10^{-3} M of 3-alkyl(aryl)-4-(3-hydroxy-4-methoxybenzylidenamino)-4,5-dihydro-1H-1,2,4-triazol -5-ones amphiprotic (isopropyl alcohol, *tert*-butyl alcohol) and dipolar aprotic, (DMF, acetone) as a titrant in solvent mediums, plotted from the data obtained by titration of 0.05 N TBAH solution in isopropyl alcohol, graphs as mV -mL (TBAH) are given in Fig. 3.

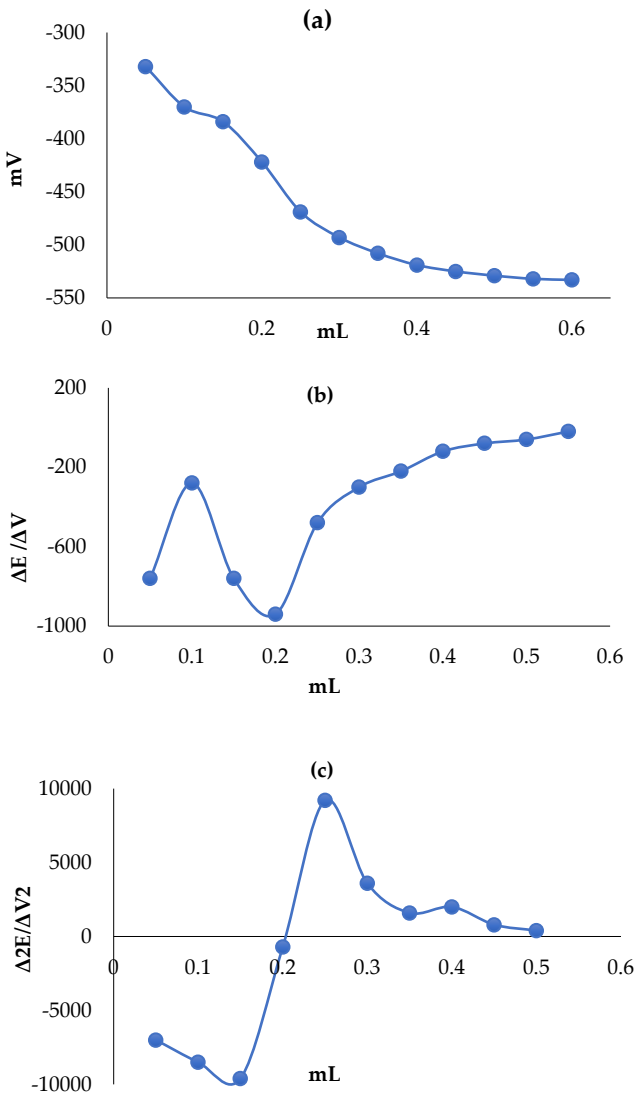

Figure 2. Compound **1b**: **a.** mL-mV curve **b.** ΔE/ΔV curve **c.** $\Delta^2E/\Delta V^2$ curve

Table 1. Acidity strengths of 3-alkyl(aryl)-4-(3-hydroxy-4-methoxybenzylidenamino)-4,5-dihydro-1H-1,2,4-triazol-5-ones in amphiprotic and dipolar aprotic solvents

Compound	Isopropyl alcohol		*tert*-butyl alcohol		Acetone		DMF	
	p*K*a	Hnp	p*K*a	Hnp	p*K*a	Hnp	p*K*a	Hnp
1a	15,09	-388	-	-	12,72	-274	15,20	-337
1b	10,23	-168	-	-568	12,72	-248	15,60	-370
1c	14,73	-346	12,77	-290	-	-	15,24	-341
1d	14,43	-317	-	-	16,49	-381	14,47	-307
1e	14,55	-391	-	-	15,38	-361	17,20	-415
1f	15,58	-351	14,20	-290	12,49	-225	14,12	-297
1g	16,02	-370	13,05	-295	15,40	-364	14,56	-313
1h	11,56	-226	-	-	15,85	-372	15,51	-355
1i	13,63	-271	-	-	16,75	-363	18,24	-460
1j	14,98	-331	14,23	-357	12,90	-249	16,50	-390

Half-neutralization potentials were calculated from the graphs obtained and plotted in the excel program. Calculated Hnp and p*K*a values are given in Table 1.

3-Alkyl(Aryl)-4-(3-hydroxy-4-methoxybenzyliden-amino)-4,5-dihydro-1H-1,2,4-triazol-5-ones determined by potentiometric titration in amphiprotic and dipolar aprotic solvents. Acidity strength (Fig. 4), functional groups, autoprotolysis constant, dielectric constant, and the leveling-differentiation effect was investigated.

Classification of acidity strength in different solvents can be made by the dielectric constant. It was stated that the theoretical increase in p*K*a values in four solvents should be *tert*-butyl alcohol < isopropyl alcohol < acetone < DMF. Experimental results suitable for the theoretical sequence were obtained for compounds **1a**, **1b**, **1d**, **1e**, **1h**, and **1i** in amphiprotic solvents. Since typical S-shaped curves for other compounds could not be obtained, acidity constants could not be determined in the *tert*-butanol solvent.

Theoretically, it has been stated that the p*K*a values of the compounds in the DMF medium from dipolar aprotic solvents are higher than that of acetone. The experimental results showed a result contrary to the theoretical order of compounds **1d**, **1g**, and **1h**. Typical S-shaped curves could not be obtained for compound **1** in acetone medium, so they could not be compared. For other compounds, theoretical order and experimental results were in agreement. This situation, which is similar to other studies, can be explained as follows.

Solvents such as acetone and N, N-dimethylformamide form lyonium ions but not lyate ions. HX is acid (molecular), S is a solvent and DMF (protophilic solvent) formed the following equilibrium.

$$HX + S \underset{1}{\leftrightarrow} S \cdots\cdots HX \underset{2}{\leftrightarrow} SH^+X^- \underset{3}{\leftrightarrow} SH^+ + X^- \qquad (2)$$

When protophilic solvents are used for the equilibrium given in Equation 1, the equilibrium number (1) and (2) mostly shifts to the direction in which it is written, while the equilibrium number (3) shifts slightly to the right. In equilibrium number (3), the strongest acid in the free environment is SH^+. This strain reacts directly with the titrant. However, in the case of protophobic solvent such as acetone, the equilibrium shifts slightly to the right in Equation 2. Equilibrium (3) shifts slightly to the right. In this case, SH^+ in protophobic solvent is a much stronger acid.

Considering the autoprotolysis constant, it was seen that the Hnp values of the compounds and the potential ranges of the solvents in *tert*-butyl alcohol, isopropyl alcohol, DMF, and acetone medium are weakly acidic when compared with the data in Table 2.

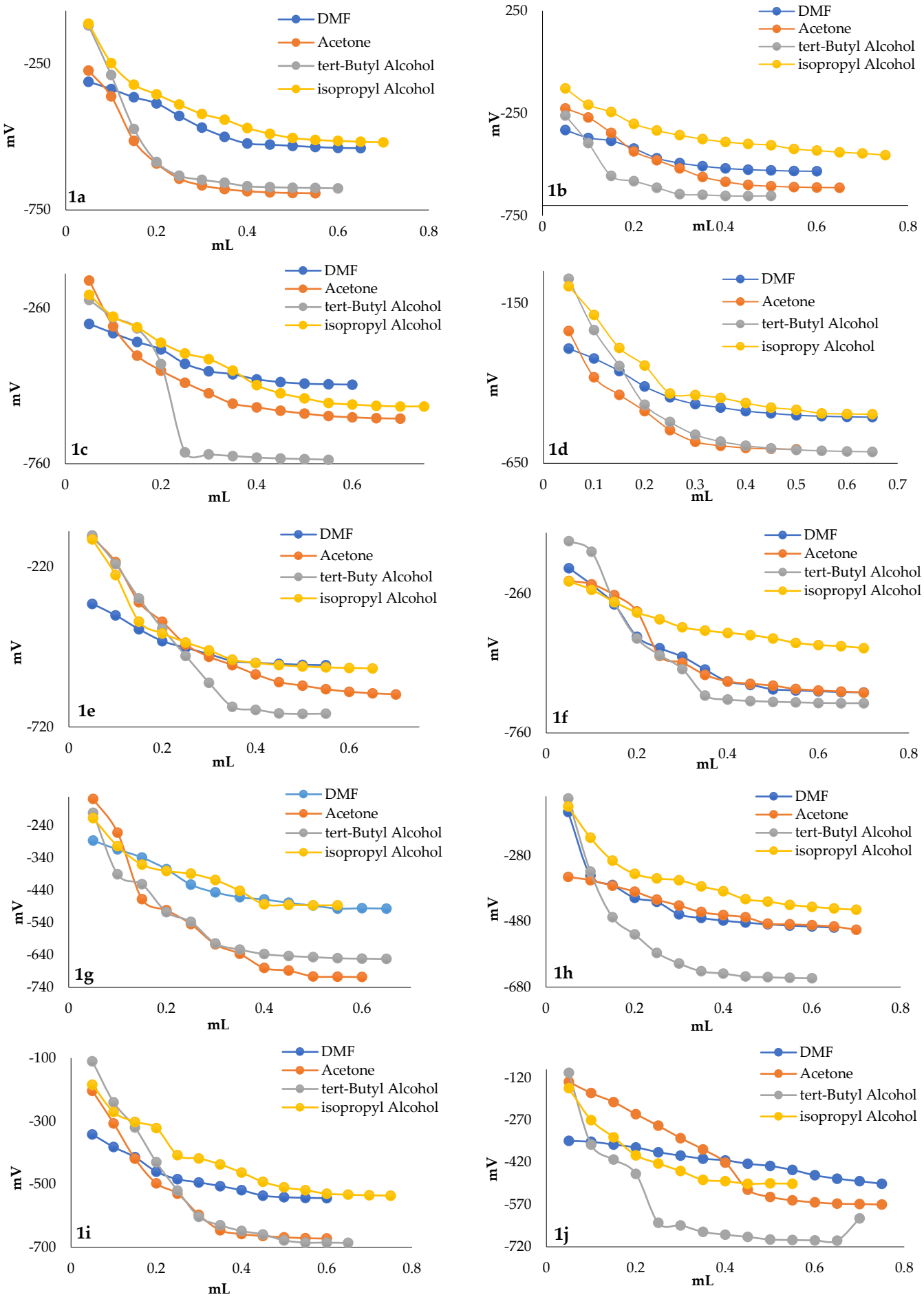

Figure 3. Potentiometric titration graphs of compounds **1a-j** with TBAH in isopropyl alcohol

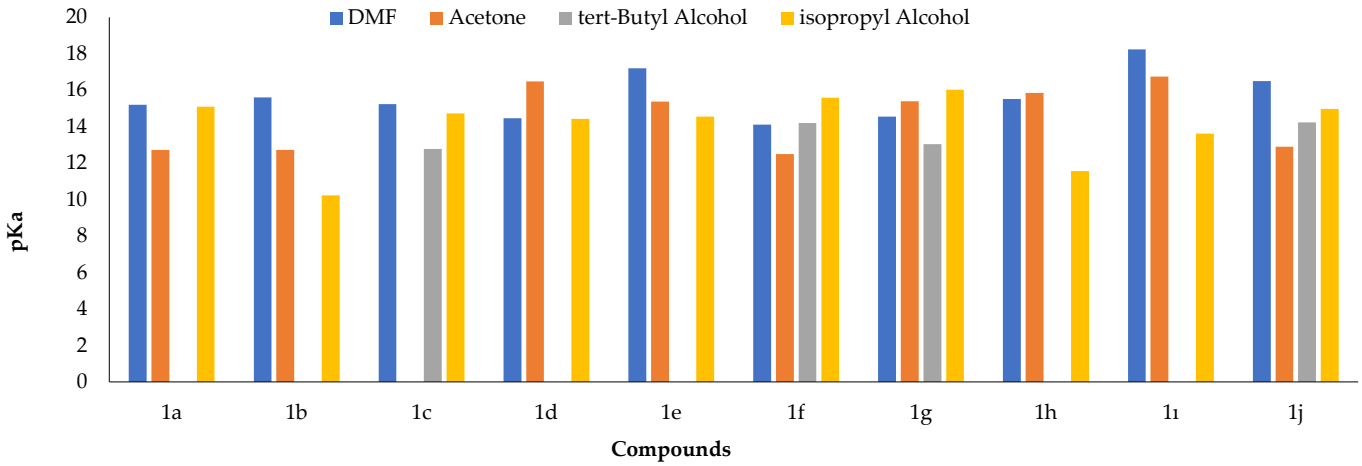

Figure 4. p*K*a-compounds plot for compound **1**

Table 2. Potential ranges of solvents and measured Hnp values of 3-alkyl(aryl)-4-(3-hydroxy-4-methoxybenzylidenamino)-4,5-dihydro-1H-1,2,4-triazol-5-ones

Solvents	Potential Range (mV)[a]		Potential Range (mV)[a]		Potential Range (mV)[b]	Measured Compounds of the Type 1 Hnp Range	
***tert*-butyl alcohol**	-	-	-	-	1200	-290	-568
Isopropyl alcohol	-750	+400	-720	+407	1000	-168	-391
Acetone	-970	+660	-965	+598	1550	-225	-381
DMF	-1000	+270	-900	+237	1300	-297	-460

4. Conclusion

Research results; 3-alkyl(aryl)-4-(3-hydroxy-4-methoxybenzylidenamino)-4,5-dihydro-1H-1,2,4-triazol-5-ones have proven to be weakly acidic in anhydrous media solvents. When the acidity strength is listed according to the dielectric constant and acidity constant, it has been determined that 1d, 1g, and 1h in DMF and acetone environments are not suitable for the theoretical order [24,25], but suitable for other environments. Compounds **1a** and **1b** were leveled in acetone medium. It has been differentiated in other solvents. However, the molecular effect was examined and it was concluded that there was no significant difference due to the distance of the functional groups to the acidic proton and the solvent effect.

Acknowledgments

This study was supported by a grant (Project Number: 2008.116.006.1) from the Scientific Research Projects Coordination Unit of Karadeniz Technical University.

References

[1] D.A. Skoog, D.M. West, F.J. Holler, S.R. Crouch, Analitik Kimya Temel İlkeler, Translators: E. Kılıç, H. Yılmaz, 2007, Turkey, Bilim Yayıncılık.

[2] J. Reijenga, A. Hoof, A. Loon, B. Teunissen, Development of methods for the determination of p*K*a values, Anal Chem Insights, 8, 2013, 53-71.

[3] S. Zafar, S. Akhtar, T. Tariq, N. Mushtag, A. Akram, A. Ahmed, M. Arif, S. Naeem, S. Anwar, Determination of p*K*a values of new phenacyl-piperidine derivatives by potentiometric titration method in aqueous medium at room temperature (25 ± 0.5 °C), Pak J Pharm Sci, 27(4), 2014, 925-929.

[4] S. Sharif Manesh, M. Masrournia, Carbon nitride nanoparticles modifed carbon paste electrodes as potentiometric sensors for determination of nickel(II) and chromium(III) ions in tap water samples, J Iran Chem Soc, 18, 2021,1219-1229.

[5] Ö. Işıldak, O. Özbek, Application of potentiometric sensors in real samples, Crit Rev Anal Chem, 2020, doi:10.1080/10408347.2019.1711013.

[6] K. Braininaa, N. Stozhko, M. Bukharinova, E, Khamzina, M. Vidrevich, Potentiometric method of plant microsuspensions antioxidant activity determination, Food Chem, 278, 2019, 653-658.

[7] Kh.Z. Brainina, E.L. Gerasimova, D.P. Varzakova, S.L. Balezin, I.G. Portnov, V.A. Makutina, E.V. Tyrchaninov, Potentiometric method for evaluating the oxidant/ antioxidant activity of seminal and follicular fluids and clinical significance of this parameter for human reproductive function, Open Chem Biomed Methods J, 5, 2012, 1-7.

[8] Kh.Z. Brainina, A.V. Ivanova, E.N. Sharafutdinova, E.L. Lozovskaya, E.I. Shkarina, Potentiometry as a method of antioxidant activity investigation, Talanta, 71, 2007, 13-18.

[9] K.D. Bhesaniya, S. Baluja, Potentiometric determination of dissociation constant and thermodynamic parameters of dissociation process of some newly synthesized pyrimidine derivatives in MeOH/DMF-water medium at different temperatures, J Mol Liq, 190, 2014, 190-195.

[10] Z. Farkas, M. Posa, V. Tepavcevic, Determination of p*K*a values of oxocholanoic acids by potentiometric titration, J Surfactants Deterg, 17, 2014, 609-614.

[11] V.R. Almeida, B. Szpoganicza, S. Bonnevilleb, Potentiometric titration and out-of-equilibrium pH response of the biotite-water system, J Brazil Chem Soc, 26(9), 2015, 1848-1860.

[12] A.S. Katea, K.C. Basavaraju, A simple potentiometric titration method for estimation of maleic anhydride in high molecular weight styrene-maleic anhydride copolymer, Polym Test, 65, 2018, 369-373.

[13] M. Lakubowska, B. Bas, E. Niewiara, W. Reczynski, W.W. Kubiak, Potentiometric titration of industrial samples-end-point detection by means of wavelets, AIP Conference Proceedings, 1148, 2009, 613-616.

[14] T. Lisa, D. Chansyanah, S. Marina, K. Nina, S. Andrian, Using potentiometric acid-base titration to determine p*K*a from

Mangosteen Pericarps Extract, Periód Tchê Quím, 16, 2019, 768-773.

[15] N. Demirbaş, R. Uğurluoğlu, A. Demirbaş, Synthesis of 3-Alkyl(Aryl)-4-Alkylidenamino-4,5-dihydro-1H-1,2,4-Triazol-5-Ones as Antitumor Agents, Bioorgan Med Chem, 10, 2002, 3717-3723.

[16] Ş. Bahçeci, N. Yıldırım, Ö. Gürsoy-Kol, S. Manap, M. Beytur, H. Yuksek, Synthesis, characterization and antioxidant properties of new 3-alkyl(aryl)-4-(3-hydroxy-4-methoxy-benzylidenamino)-4,5-dihydro-1H-1,2,4-triazol-5-ones, Rasayan J Chem, 9, 2016, 494-501.

[17] E. Kılıc¸ O. Atakol, E. Canel, Z. Alibeşeoğlu, T. Gunduz, F. Köseoğlu, Potentiometric investigation of the effects of several substituents on the basicity of benzilidene-o-hydroxyaniline, Turk J Chem, 22, 1998, 387-391.

[18] H. Yüksek, E. Koca, Ö. Gürsoy-Kol, O, Akyıldırım, M. Çelebier, Synthesis, in vitro antioxidant activity, and physicochemical properties of novel 4,5-dihydro-1H-1,2,4-triazol-5-one derivatives, J Mol Liq, 206, 2015, 359-366.

[19] M. Kurtoğlu, N. Birbiçer, Ü. Kimyonsen, S. Serin, Determination of pK_a values of some azo dyes in acetonitrile with perchloric acid, Dyes Pigments, 41, 1999, 143-147.

[20] N. Gündüz, T. Gündüz, M. Havyalı, Titrations in non-aqueous media: Potentiometric investigation of symmetrical and unsymetrical tetra-aryl porphyrins with 4- nitrophenyl and 4-aminophenyl substituents in nitrobenzene solvent, Talanta, 48, 1999, 71-79.

[21] Z. Ocak, Amfiprotik ve dipolar aprotik çözücülerde 3-(4-Aril) propiyonik asit türevlerinin asitlik kuvvetleri, Iğdır Üniversitesi Fen Bilimleri Enstitüsü Dergisi, 10(3), 2020, 1876-1885.

[22] O. Hakli, K. Ertekin, M.S. Ozer, S. Aycan, Determination of pK_a values of clinically important perfluorochemicals in nonaqueous media, J Anal Chem, 63(11), 2008, 1051-1056.

[23] R.H. Loeppert, L.W. Zelazny, B.G. Volk, Titration of pH-dependent sites of kaolinite in water and selected nonaqueous solvents, Clay Clay Miner, 27 (1), 1979, 57-62.

[24] H. Yüksek, M. Küçük, M. Alkan, Ş. Bahçeci, S. Kolaylı, Z. Ocak, U. Ocak, E. Şahinbaş, M. Ocak, Synthesis and antioxidant activities of some new 4-(4-hydroxy-benzylidenamino)-4,5-dihydro-1H-1,2,4-triazol-5-one derivatives with their acidic properties, Asian J Chem, 18(1), 2006, 539-550.

[25] A. Arslantaş, H. Yüksek, Ö. Gürsoy Kol, Z. Ocak, Z. Tomruk, M. Calapoğlu, Study of antioxidant properties and DNA interaction of some novel 4,5-dihydro-1*H*-1,2,4-triazol-5-one derivates, Asian J Chem, 24(8), 2012, 3327-3334.

e-ISSN: 2687-6698 Research Article

Turkish Journal of Analytical Chemistry
TurkJAC
www.turkjac.org
2019

New octa-benzothiazole substituted metal-free and metallophthalocyanines: Synthesis, characterization and electrochemical studies

Gülsev Dilber[1], Asiye Nas[1]*, Zekeriya Biyiklioglu[2]

[1]Karadeniz Technical University, Macka Vocational School, 61750, Macka, Trabzon, Turkey
[2]Karadeniz Technical University, Faculty of Science, Department of Chemistry, 61080 Trabzon, Turkey

Abstract

The synthesis of novel phthalonitrile (**3**) and synthesis, spectroscopic and electrochemical properties of the following octa-benzothiazole substituted metal-free (**4**), cobalt(II) (**5**), and zinc(II) (**6**) phthalocyanines are reported for the first time in this work. The novel phthalonitrile (**3**) has been characterized by FT-IR, ^{1}H NMR, ^{13}C NMR, and mass spectroscopy and the novel phthalocyanines (**4-6**) have been characterized by FT-IR, electronic spectroscopy, and mass spectroscopy. Voltammetric analysis of benzothiazole group substituted phthalocyanines (MPc) were determined by cyclic voltammetry (CV) and square wave voltammetry (SWV). According to the results, phthalocyanines revealed metal and ligand-based quasi-reversible reduction and oxidation processes. While the CoPc **5** showed one metal-based and one Pc-based reduction reactions, H_2Pc **4** and ZnPc **6** gave two Pc-based reduction reactions.

Keywords: Phthalocyanine, zinc, electrochemistry, squarewave, cyclic voltammetry

1. Introduction

Phthalocyanines, planar aromatic macrocycles constituted by four isoindole units linked together through nitrogen atoms, were serendipitously discovered in 1928. These synthetic analogs of the naturally occurring porphyrins have been the subject of extensive research in many different fields such as lithium batteries, optical data storage, solar energy conversion, catalysis, and so on [1-6]. Apart from the use in materials science, phthalocyanines are also highly promising for their applications as magnetic resonance imaging (MRI) and photodynamic therapy (PDT) [7-9].

Many functions of metallophthalocyanine derivatives resulted from electron transfer occurring in these macromolecules. Determination of electrochemical behavior is required for the development of functional materials carrying metallophthalocyanine. MPc having Pc^{2-}, phthalocyanine dianion, does not show redox activity at the ring. Two successive one-electron oxidations may happen by the removal of electrons from a_{1u} forming Pc^{-1} and Pc^{0} species. Reductions happen by adding electrons to e_g to form Pc^{3-}, Pc^{4-}, Pc^{5-} and Pc^{6-} species. Each oxidation and reduction species has a definite spectrum that can be employed for its characterization. The presence of the electroactive central metal causes additional redox processes to occur, resulting in unique electronic spectral behavior [10].

Also, phthalocyanines can be used as electrochemical sensors. The use of metallophthalocyanines as electrochemical sensors has become widespread and new sensors are being produced day by day [11,12].

In our previous papers, we reported electrochemical and spectroelectrochemical properties of various tetra substituted metal-free and metallophthalocyanines which have electroactive and non-electroactive centers. [13-16]. As seen in the literature, the electrochemical properties of tetrasubstituted metal-free and metallophthalocyanines have worked in recent years [17-19], but there is not much work on the electrochemical properties of octa-substituted metal-free and metallophthalocyanines [20-22]. So in this study, the electrochemical properties of the octa-substituted metal-free phthalocyanine (4) and zinc(II) phthalocyanine (6) having the non-electroactive center, and cobalt(II) phthalocyanine (5) carrying an electroactive center have been investigated.

Citation: G. Dilber, A. Nas, Z. Biyiklioglu, New octa-benzothiazole substituted metal-free and metallophthalocyanines: synthesis, characterization and electrochemical studies, Turk J Anal Chem, 3(1), 2021, 33-38.
https://doi.org/10.51435/turkjac.935057

***Author of correspondence:** asiyenas@ktu.edu.tr
Tel: +90 462 377 76
Fax: +90 462 512 35 52
Received: May 10, 2021
Accepted: June 04, 2021

2. Experimental

The used materials and equipment were provided as supplementary information.

2.1. Synthesis

2.1.1. *Synthesis of 4,5-bis(2-(benzo[d]thiazol-2-yl)phenoxy) phthalonitrile* ***(3)***

The mixture of 2-(benzo[d]thiazol-2-yl) phenol (**1**) (2.00 g, 8.80 mmol) and 4,5-dichlorophthalonitrile (**2**) (0.86 g, 4.40 mmol) were dissolved in dry DMF (30 ml) under nitrogen atmosphere and this mixture was stirred at 65 °C for 10 min. After stirring, finely ground anhydrous K_2CO_3 (2.42 g, 17.60 mmol) was added over a period of 2 h and it was stirred under the nitrogen atmosphere at 65 °C for 3 days. The reaction mixture was added crushed ice. The forming white precipitate was filtered off, washed with distilled water, and then dried in vacuo. Yield: 1.33 g (52%), m.p.: 109.2-110.3 °C. $C_{34}H_{18}N_4O_2S_2$. FT-IR ν_{max}/cm^{-1}: 3061 (Ar-H), 2237 (C≡N), 1482, 1381, 1270, 1197, 1010, 969, 757, 727, 694. ^{1}H NMR ($CDCl_3$) (δ: ppm): 8.57-8.56 (d, H, Ar-H), 8.07-8.05 (d, H, Ar-H), 8.02-8.00 (d, H, Ar-H), 7.93 (s, H, Ar-H), 7.91-7.88 (m, 2H, Ar-H) 7.72-7.70 (d, H, Ar-H), 7.65-7.62 (t, H, Ar-H), 7.53-7.50 (m, 3H, Ar-H), 7.45-7.40 (m, 3H, Ar-H), 7.19-7.17 (d, H, Ar-H), 7.14-7.12 (d, H, Ar-H), 7.09 (s, H, Ar-H), 7.00-6.96 (t, H, Ar-H). ^{13}C NMR ($CDCl_3$) (δ: ppm): 169.39, 160.68, 157.94, 157.29, 152.61, 151.84, 150.42, 135.62, 135.54, 132.80, 132.66, 131.39, 129.84, 128.45, 127.55, 126.73, 126.61, 125.75, 125.59, 123.49, 122.20, 121.72, 121.56, 121.50, 119.94, 119.57, 117.87, 116.79, 115.62, 114.28, 114.22, 110.36. MS (ES$^+$), *m/z*: Calc.: 578.68; Found: 578.66 [M]$^+$.

2.1.2. *Synthesis of metal-free phthalocyanine H_2Pc* ***(4)***

Compound **3** (0.20 g, 0.34 mmol) and three drops of DBU were stirred in dry *n*-pentanol (3 mL) under reflux in a nitrogen atmosphere at 160 °C in a sealed glass tube for 24 h. Then, the mixture was degassed several times before it was left to cool to room temperature. 20 mL of ethanol was added to the mixture to be precipitated the green crude product and filtered off. The obtained green product was filtered off again after the refluxing with 40 mL of ethanol for 4 h. The solid product was successively washed several times with hot ethanol, distilled water, and diethyl ether to removing the organic impurities. Column chromatography using chloroform-methanol (96:4) solvent system as eluent was applied to purification of the product after it dried in vacuo. Yield: 70 mg (35%), m.p.: >300 °C. $C_{136}H_{74}N_{16}O_8S_8$. FT-IR ν_{max}/cm^{-1}: 3286 (N-H), 3061 (Ar-H), 1497, 1422, 1239, 1100, 1012, 871, 749, 726. UV/vis (chloroform): λ, nm (log ε): 712 (5.40), 675 (5.26), 645 (4.79), 611 (4.62), 384 (4.92). MS (ES$^+$), *m/z*: Calc.: 2316.72; Found: 1550.480 [M-6C_7H_4NS+K]$^+$.

2.1.3. *General procedures for metallophthalocyanine derivatives (**5**, **6**)*

The mixture of compound **3** (0.40 g, 0.68 mmol), anhydrous metal salt [$CoCl_2$ (88 mg, 0.68 mmol) or $Zn(CH_3COO)_2$ (124 mg, 0.68 mmol)] and three drops of 1,8-diazabicyclo[5.4.0]undec-7-ene was stirred at 160 °C with dry *n*-pentanol (3 mL) in a sealed tube for 24 h. Then, the mixture was left to cool to room temperature. The green crude product was precipitated with 10 mL of ethanol and then filtered off. The green-colored product was filtered off again after refluxing with 40 mL of ethanol for 4 h. It was successively washed several times with hot ethanol, distilled water, and diethyl ether to remove the organic impurities. Column chromatography using a chloroform-methanol (96:4) solvent system as eluent was applied to purify the product after it dried in vacuo.

*2.1.3.1. Cobalt (II) phthalocyanine (**5**)*

Yield: 27 mg (7%), m.p.: >300 °C. $C_{136}H_{72}N_{16}O_8S_8Co$. FT-IR ν_{max}/cm^{-1}: 3058 (Ar-H), 1497, 1432, 1399, 1242, 1195, 1098, 1004, 967, 888, 750, 725. UV/vis (chloroform): λ, nm (log ε): 682 (5.15), 613 (4.48), 305 (5.15). MS (ES$^+$), *m/z*: Calc.: 2373.63; Found: 1607.901 [M-6C_7H_4NS+K]$^+$.

*2.1.3.2. Zinc (II) phthalocyanine (**6**)*

Yield: 102 mg (25%), m.p.: >300 °C. $C_{136}H_{72}N_{16}O_8S_8Zn$. FT-IR ν_{max}/cm^{-1} (KBr pellet): 3061 (Ar-H), 1727, 1428, 1388, 1239, 1195, 1094, 990, 877, 753, 744. UV/vis (chloroform): λ, nm (log ε): 691 (5.25), 619 (4.52), 358 (4.86), 317 (5.06). MS (ES$^+$), *m/z*: Calc.: 2380.09; Found: 1614.725 [M-6C_7H_4NS+K]$^+$.

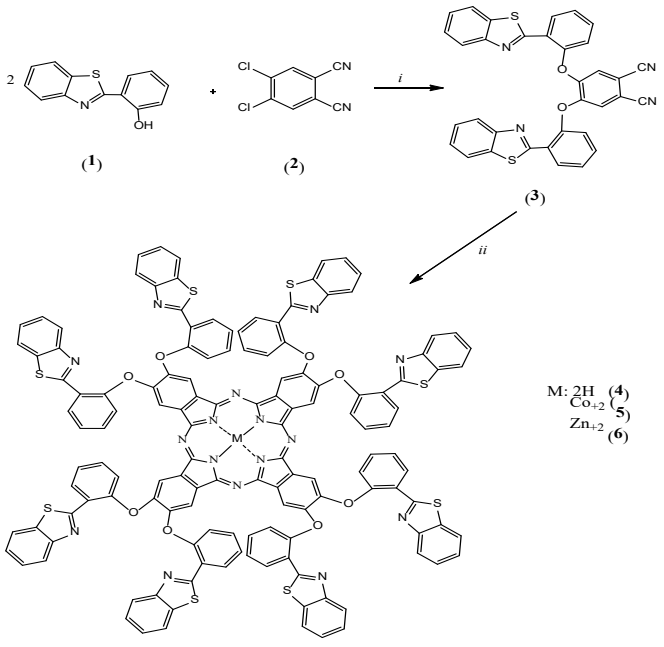

Scheme 1. Synthesis of **3**, **4**, **5** and **6**. *i*: K_2CO_3, DMF, 50 °C, 5 days. *ii*: 1-pentanol, DBU, related metal salts ($CoCl_2$, $Zn(ac)_2$), 24h, 160 °C

3. Results and discussion

3.1. Synthesis and characterization

The octa-benzothiazole substituted phthalonitrile derivative **3** was obtained by the reaction of 2-(benzo[d]thiazol-2-yl)phenol **1** with 4,5-dichlorophthalonitrile **2** in 52% yield (Scheme 1). The nucleophilic substitution reaction was performed in the presence of anhydrous K_2CO_3 in dry DMF at 65 °C [23].

Octa-substituted zinc(II) and cobalt(II) phthalocyanines (**5** and **6)** were syntheses by treatment of phthalonitrile derivatives **3** in the presence of related anhydrous metal salts ($Zn(CH_3COO)_2$ and $CoCl_2$ respectively) as a metal source in dried *n*-pentanol at 160 °C [24]. The yields of the reactions for compounds **5** and **6** were determined as 7% and 25%, respectively. Starting phthalonitrile derivatives **3**, metal-free phthalocyanine compound **4** was synthesized under the same conditions without using metal salt in a 52% yield. The general synthetic procedures of the novel phthalocyanine compounds (**4-6**) were shown in Scheme 1. Purification of the crude products was carried out by column chromatography using the chloroform-methanol solvent system as an eluent.

The structures of novel compounds were characterized by FT-IR, ^{1}H NMR, ^{13}C NMR, UV-vis spectroscopies, and mass spectra.

For compound **3**, the appearance of vibration bands at 2223 C≡N, 1283 (Ar-O-C) in the FT-IR spectrum showed the formation of **3**. In the ^{1}H NMR spectrum of this phthalonitrile **3**, the proton signal of OH group of 2-(benzo[d]thiazol-2-yl)phenol disappeared as expected. The resonances for the compound 3 in the ^{1}H NMR were observed between 8.57-6.96 ppm integrating for a total of 18 aromatic protons. In the ^{13}C NMR spectrum of **3,** the characteristic signals of nitrile carbon atoms were observed at δ = 11.79, 115.62 ppm. The mass spectrum of phthalonitrile **3** showed a molecular ion peak at *m/z* = 578.66 $[M]^+$.

For the new phthalocyanine compounds, cyclotetramerization of phthalonitrile 3 was evidenced by the loss of the -C≡N signal in the FT-IR spectrum of compounds **4**, **5**, and **6** after the formation of the phthalocyanine rings. Mass spectra of phthalocyanine compounds **4**, **5**, and **6** reasonably supported the expected structures when observing molecular ion peaks at 1550.480 as $[M\text{-}6C_7H_4NS+K]^+$ for **4**, 1607.901 as $[M\text{-}6C_7H_4NS+K]^+$ for **5** and 1614.725 as $[M\text{-}6C_7H_4NS+K]^+$ for **6** (Fig. 1, Fig. 2 and Fig. 3), respectively.

3.2. Electronic absorption spectra

The electronic spectra of phthalocyanines exhibit several bands which are due to π-π* and n-π* transitions. In the near UV region, there is the B band or Soret band at approximately between 300-400 nm and finally, there is the strongest Q band at approximately between 600-700 nm. While the Q bands of the H_2Pcs are observed as split two bands, because of D_{2h} symmetry and the lifting of the degeneracy of the LUMO (eg) level, as Qx and Qy bands that of MPcs are observed as a single intense band because of D_{4h} symmetry [10, 25].

Fig. 4 shows the UV-Vis absorption spectra of complexes **4-6** in chloroform. Table 1 contains a summary of the Q band maxima of the complexes (**4-6**). In UV-vis spectra of metal-free (**4**) phthalocyanine gave a split two Q band absorptions at 712 and 675 nm with shoulders 645 and 611 nm, respectively as expected.

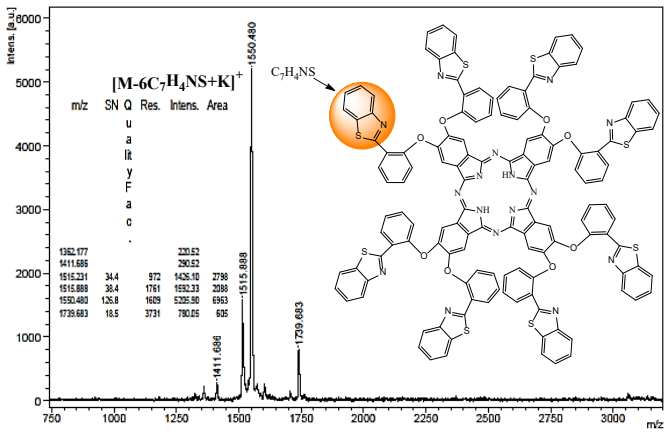

Figure 1. Mass spectrum of phthalocyanine **4**

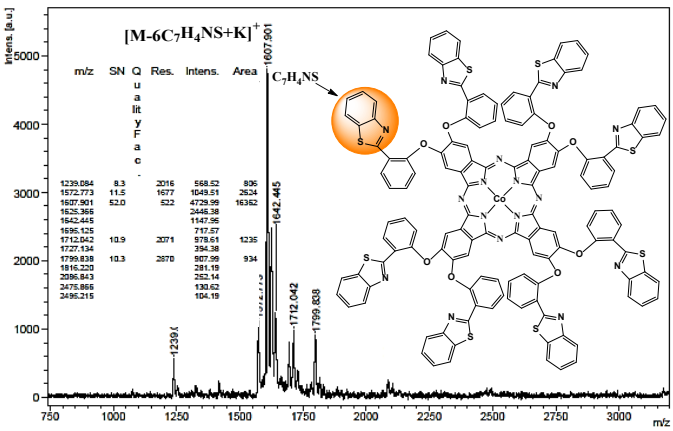

Figure 2. Mass spectrum of phthalocyanine **5**

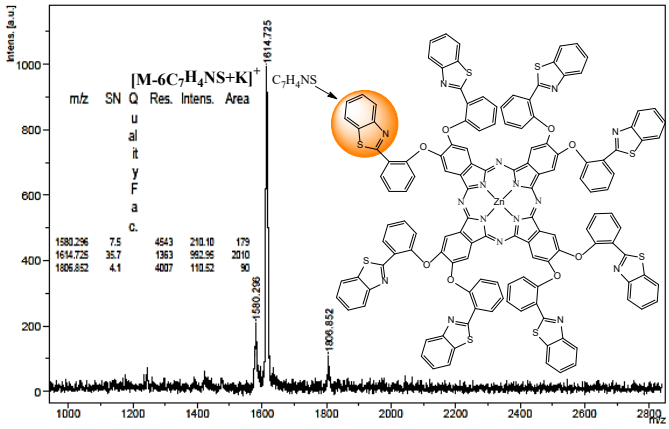

Figure 3. Mass spectrum of phthalocyanine **6**

Table 1. Absorption spectral data for **4**, **5**, and **6** in chloroform

	Solvent	Q band, λmax (nm)	log ε	B band, λmax (nm)	log ε
H_2Pc (4)	Chloroform	712	5.40	384	4.92
		675	5.26		
		645	4.79		
		611	4.62		
CoPc (5)	Chloroform	682	5.15	305	5.15
		613	4.48		
ZnPc (6)	Chloroform	691	5.25	358	4.86
		619	4.52	317	5.06

The cobalt(II) (**5**) and zinc(II) (**6**) phthalocyanines gave an intense single Q band absorption of the π-π* transitions at 682 and 691 nm with shoulders 613 and 619 nm, respectively. The B bands of complexes were observed at 384 nm for **4**, 305 nm for **5**, and (358, 317) nm for **6**, respectively.

3.3. Electrochemical Studies

Electrochemical studies of H_2Pc, ZnPc, CoPc were achieved in DCM using a (DCM)/(TBAP) electrolyte system on a Pt working electrode. The results are shown in Table 2. Fig. 5 shows the CV and the SWV of H_2Pc in DCM. H_2Pc gave two ring-based and quasi-reversible reductions (R_1 = -0.55 V, R_2 = -0.91 V) and one oxidation (O_1 = 1.22 V) process. This data of the H_2Pc is compatible with H_2Pc behavior in literature [26]. Fig. 6 shows the CV and the SWV of ZnPc. Similarly, ZnPc gave two ring-based and quasi-reversible reductions (R_1 = -0.92 V, R_2 = -1.17 V) and one oxidation (O_1 = 0.93 V) process. But, CoPc showed different electrochemical behavior than H_2Pc and ZnPc. Fig. 7 shows the CV and the SWV of CoPc. As shown in Fig. 7, CoPc gave one metal-based and one ring based quasi-reversible reductions (R_1 = -0.20 V, R_2 = -1.24 V), two oxidation (O_1 = 0.92 V, O_2 = 1.29 V) processes.

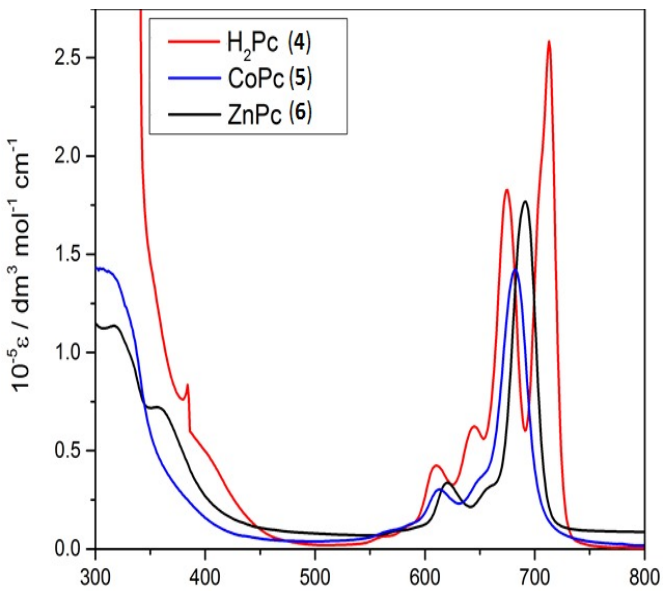

Figure 4. Absorption spectra of novel synthesized octa-substituted phthalocyanines (**4-6**) in chloroform

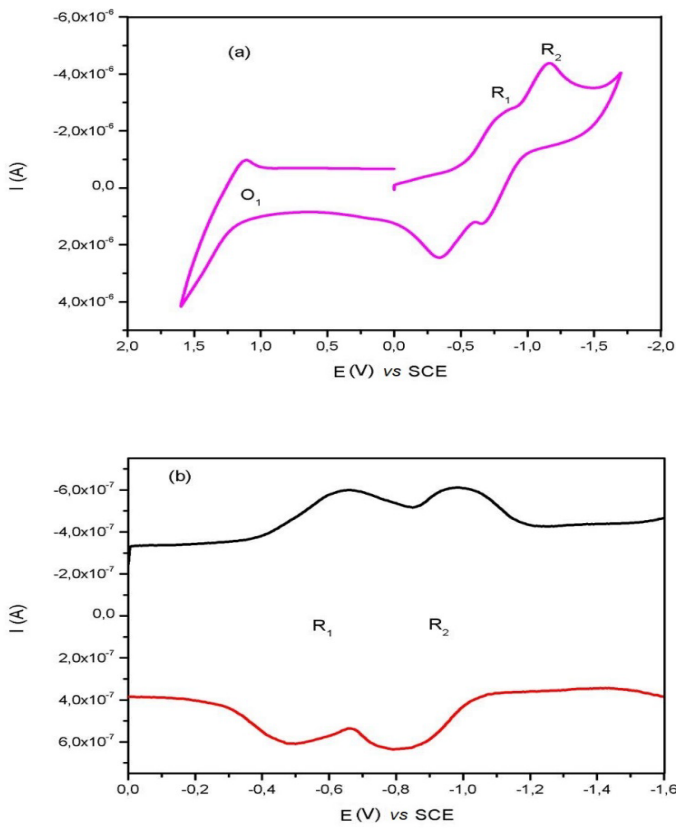

Figure 5. (**a**) CV of **H_2Pc** recorded at 0.100 Vs^{-1} scan rate on a Pt electrode in DCM/TBAP. (**b**) SWV of **H_2Pc** recorded at 0.100 Vs^{-1} scan rate on a Pt electrode in DCM/TBAP

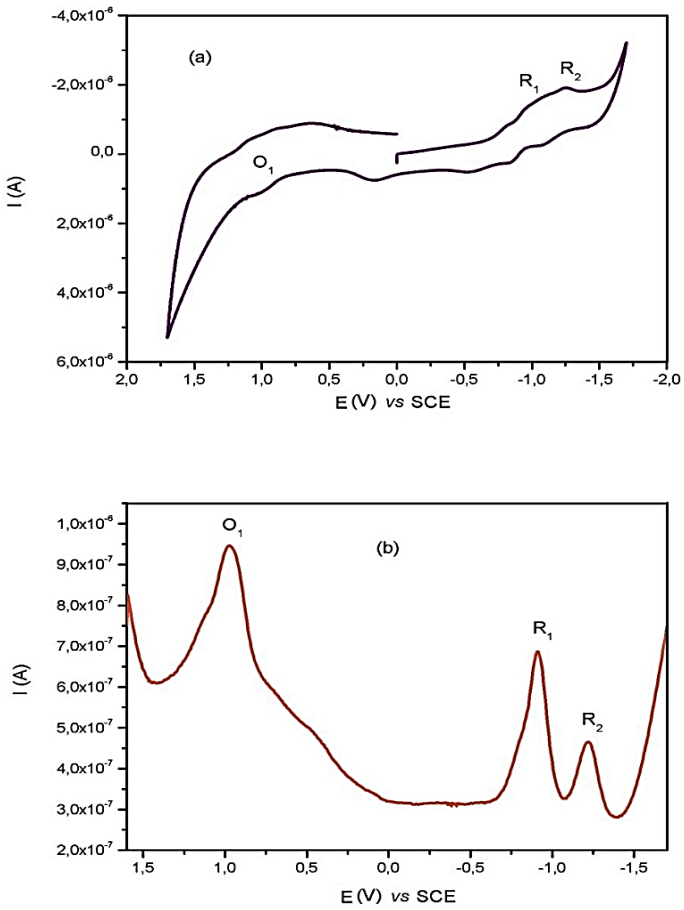

Figure 6. (**a**) CV of **ZnPc** recorded at 0.100 Vs^{-1} scan rate on a Pt electrode in DCM/TBAP. (**b**) SWV of **ZnPc** recorded at 0.100 Vs^{-1} scan rate on a Pt electrode in DCM/TBAP

Table 2. Voltammetric data of the **4-6**. The voltammetric data were given versus SCE

Phthalocyanines	Label	[a]$E_{1/2}$	[b]ΔE_p (mV)	[c]$\Delta E_{1/2}$
	R_1	-0.55	161	
H_2Pc (4)	R_2	-0.91	156	1.77
	O_1	1.22	170	
	R_1	-0.92	178	
ZnPc (5)	R_2	-1.17	166	1.85
	O_1	0.93	180	
	R_1	-0.20	173	
CoPc (6)	R_2	-1.24	151	1.12
	O_1	0.92	144	
	O_2	1.29	163	

[a]: $E_{1/2}$ values ((E_{pa}+E_{pc})/2) were given versus SCE at 0.100 Vs^{-1} scan rate.
[b]: ΔE_p= E_{pa}-E_{pc}. [c]: $\Delta E_{1/2}$ = $E_{1/2}$ (first oxidation)-$E_{1/2}$ (first reduction)

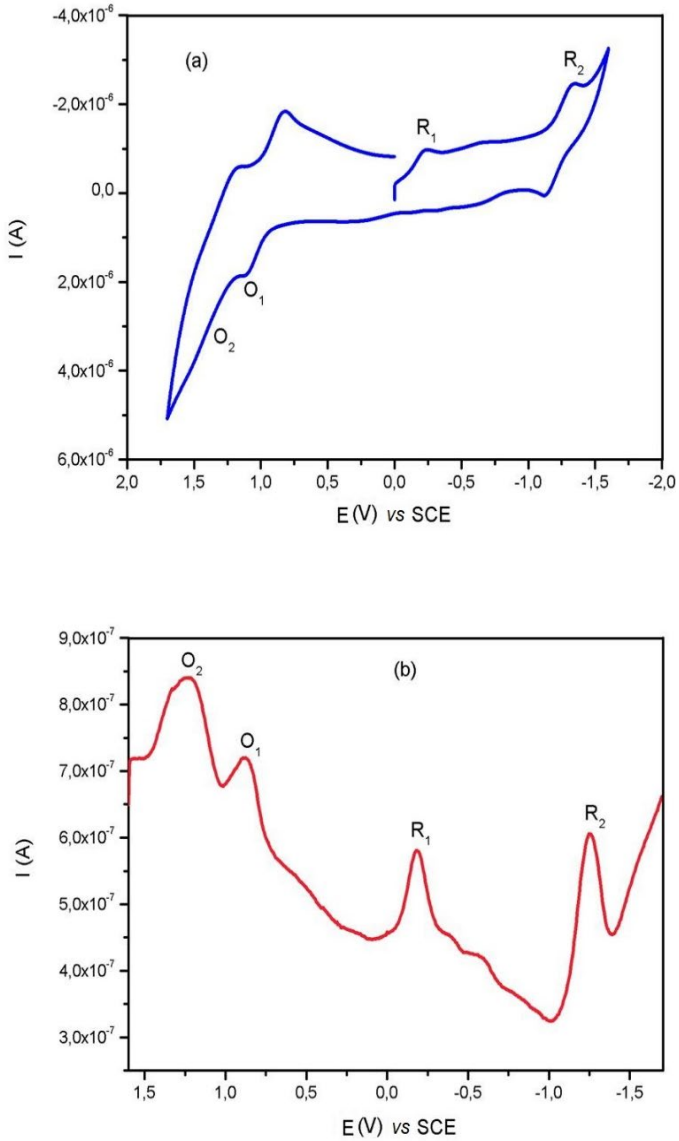

Figure 7. (**a**) CV of **CoPc** recorded at 0.100 Vs^{-1} scan rate on a Pt electrode in DCM/TBAP. (**b**) SWV of **CoPc** recorded at 0.100 Vs^{-1} scan rate on a Pt electrode in DCM/TBAP

4. Conclusions

Octa-benzothiazole substituted H_2Pc, CoPc, and ZnPc phthalocyanines were synthesized in moderate yields and fully characterized by general spectroscopic techniques such as FT-IR, UV-Vis, ^{1}H-NMR, and MS. The obtained novel compounds exhibited excellent solubility in most organic solvents such as $CHCl_3$, $CHCl_2$, THF, DMSO, and DMF. CV and SWV were used to determine the electrochemical properties of the H_2Pc, the ZnPc, and the CoPc. Electrochemical responses of the H_2Pc, the ZnPc, and the CoPc verified the proposed structure. The H_2Pc and the ZnPc showed only ring-based redox processes. But CoPc exhibited one metal-based and one ring-based redox reactions. These properties increase their possible usage in different electrochemical applications.

Acknowledgement

This study was supported by the Research Fund of Karadeniz Technical University, Project no: FHD-2018-7631 (Trabzon-Turkey).

References

[1] A. Arul, M. Christy, M. Y. Oh, Y. S. Lee, K. S. Nahm, Nanofiber carbon-supported phthalocyanine metal complexes as solid electrocatalysts for lithium-air batteries, Electrochim Acta, 218, 2016, 335-344.
[2] Y. Xuan, L. Xie, X. Huang, B. Su, Molecular electrocatalysis of oxygen reduction by iron(II) phthalocyanine at the liquid/liquid interface, J Electroanal Chem, 766, 2016 37-43.
[3] H. Karaca, Redox chemistry, spectroelectrochemistry and catalytic activity of novel synthesized phthalocyanines bearing four Schiff bases on the periphery, J Organomet Chem, 822, 2016, 39-45.
[4] I. A. Tarasyuk, I. A. Kuzmin, Y. S. Marfin, A. S. Vashurin, A. A. Voronina, E. V. Rumyantsev, Synthesis and catalytic properties of hybrid materials based on organically modified silica matrix with cobalt phthalocyanine, Synthetic Met, 217, 2016, 189-196.
[5] N. Li, Z. Sun, R. Liu, L. Xu, K. Xu, X.-M. Song, Enhanced power conversion efficiency in phthalocyanine-sensitized solar cells by modifying TiO_2 photoanode with polyoxometalate, Sol Energ Mat Sol C, 157, 2016, 853-860.
[6] Y. Baygu, T. Soganci, N. Kabay, Y. Gök, M. Ak, Phthalocyanine-cored conductive polymer design: effect of substitution pattern and chalcogen nature on optical and electrical properties of Zn(II)-phthalocyanine–cored polycarbazoles, Mater Today Chem, 18, 2020, 100360.
[7] A. Günsel, P. Taslimi, G. Yaşa Atmaca, A. T. Bilgiçli, H. Pişkin, Y. Ceylan, A. Erdoğmuş, M. N. Yarasir, İ. Gülçin, Novel potential metabolic enzymes inhibitor, photosensitizer and antibacterial agents based on water-soluble phthalocyanine bearing imidazole derivative, J Mol Struct, 1237, 2021,130402.
[8] B. Barut, C. Ö. Yalçın, Ü. Demirbaş, The water soluble Zn(II) and Mg(II) phthalocyanines: Synthesis, photochemical, DNA photodamage and PDT effects against A549 cells, J Photoch Photobio A, 405, 2021, 112946.
[9] B. Köksoy, M. Durmuş, M. Bulut, Potential photosensitizer candidates for PDT including 7-oxy-3-thiomethylphenyl coumarino-phthalocyanines, Inorg Chim Acta, 498, 2019, 119137.
[10] T. Nyokong, Electronic Spectral and Electrochemical Behaviour of Near Infrared Absorbing Metallophthalocyanines, Structure and Bonding: Functional Phthalocyanine Molecular Materials, Editor: J. Jianzhuang, 2010, Germany, Springer.

[11] E. Demir, H. Silah, B. Uslu, Phthalocyanine modified electrodes in electrochemical analysis, Crit Rev Anal Chem, 2020, in press, doi:10.1080/10408347.2020.1806702.
[12] O. Inam, E. Demir, B. Uslu, Voltammetric pathways for the analysis of ophthalmic drugs, Curr Pharm Anal, 16, 2020, 367-391.
[13] Z. Biyiklioglu, O. Bekircan, Synthesis and electrochemical properties of axially disubstituted silicon phthalocyanine and peripherally tetra substituted manganese(III) phthalocyanine bearing 1,2,4-triazole substituents, Synthetic Met, 200, 2015, 148-155.
[14] A. Nas, H. Kantekin, A. Koca, Novel 4-(2-(benzo[d]thiazol-2-yl)phenoxy) substituted phthalocyanine derivatives: Synthesis, electrochemical and in situ spectroelectro-chemical characterization, J Organomet Chem, 757, 2014, 62-71.
[15] Z. Bıyıklıoğlu, V. Çakır, D. Çakır, H. Kantekin, Crown ether-substituted water soluble phthalocyanines and their aggregation, electrochemical studies, J Organomet Chem, 749, 2014, 18-25.
[16] E. T. Saka, G. Sarkı, H. Kantekin, A. Koca, Electrochemical, spectroelectrochemical and catalytical properties of new Cu(II) and Co(II) phthalocyanines, Synthetic Met, 214 ,2016, 82-91.
[17] E. T. Saka, R. Z. U. Kobak, H. Alp, G. Sarkı, A. Koca, H. Kantekin, Electrochemical and spectroelectrochemical properties of new metal free, nickel(II), lead(II) and zinc(II) phthalocyanines, Synthetic Met, 217, 2016, 295-303.
[18] Ö. İpsiz, H. Y. Yenilmez, K. Kaya, A. Koca, Z. A. Bayır, Carbazole-substituted metallo-phthalocyanines: Synthesis, electrochemical, and spectroelectrochemical properties, Synthetic Met, 217, 2016, 94-101.
[19] Ü. Demirbaş, R. Z. U. Kobak, H. T. Akçay, D. Ünlüer, A. Koca, F. Çelik, H. Kantekin, Synthesis, characterization, electrochemical and spectroelectrochemical properties of novel peripherally tetra-1,2,4-triazole substituted phthalocyanines, Synthetic Met, 215, 2016, 68-76.
[20] A. Koca, H. A. Dinçer, H. Çerlek, A. Gül, M. B. Koçak, Spectroelectrochemical characterization and controlled potential chronocoulometric demetallation of tetra- and octa-substituted lead phthalocyanines, Electrochim Acta, 52, 2006, 1199-1205.
[21] A. L. Uğur, A. Erdoğmuş, A. Koca, U. Avcıata, Synthesis, spectroscopic, electrochemical and spectroelectrochemical properties of metal free, manganese, and cobalt phthalocyanines bearing peripherally octakis-[4-(thiophen-3-yl)-phenoxy] substituents, Polyhedron, 29, 2010, 3310-3317.
[22] H. R. P. Karaoğlu, A. Koca, M. B. Koçak, The synthesis and electrochemistry of novel, symmetrical, octasubstituted phthalocyanines, Synthetic Met, 182, 2013, 1-8.
[23] A. Nas. The photo-physicochemical properties of an octa-substituted zinc phthalocyanine containing 1,2,4-triazole moieties, J Coord Chem, 69, 2016, 1326-1336.
[24] G. Dilber, H. Altunparmak, A. Nas, H. Kantekin, M. Durmuş, The peripheral and non-peripheral 2H-benzotriazole substituted phthalocyanines: Synthesis, characterization, photophysical and photochemical studies of zinc derivatives, Spectrochim Acta A, 217, 2019, 128-140.
[25] M. J. Stillman, T. Nyokong, Phthalocyanines: Properties and Applications, Editor: C. C. Leznoff, 1989, USA, VCH Publishers.
[26] G. G. Köse, G. K. Karaoğlan, S. N. Işık, D. Akyüz, A. Koca, The synthesis, characterization, electrochemical and spectroelectrochemical properties of novel unsymmetrical phthalocyanines containing naphthoic acid and di-tert-butylphenoxy, Synthetic Met, 264, 2020, 116386.

Supplementary Information

1. Materials

All solvents and reagents were dried and purified according to the known methods [1]. 4,5-dichlorophthalonitrile (2) was prepared according to the reported procedure [2]. Reagent grade chemicals and solvents were used obtained from commercial suppliers.

2. Equipment

Infrared and electronic spectra were recorded on a Perkin-Elmer FT-IR spectrometer and Unicam UV2-100 Shimadzu 2101 spectrophotometers using 1 cm path length cuvettes at room temperature, respectively. All of the reactions were carried in a standard Schlenk system under a dry nitrogen atmosphere. ^{1}H NMR and ^{13}C NMR spectra were recorded on a Varian Mercury 200 MHz spectrometer by using $CDCl_3$ as a solvent, and chemical shifts were reported (δ) relative to TMS as an internal standard. Mass spectra were recorded on a Brucker Microflex LT MALDI-TOF MS spectrometer (Gebze Technical University, Turkey). An electrothermal apparatus was used to determine the melting points. Column chromatography processes was carried out with silica gel 60 (particle size: 0.04-0.063 mm).

Gamry Interface 1000 potentiostat/galvanostat with a three-electrode configuration was employed for all electrochemical measurements at 25 °C. The working electrode was a Pt disc having a surface area of 0.071 cm^2. A Pt wire was employed as the counter electrode and the saturated calomel electrode (SCE) was used as the reference electrode and separated from the bulk of the solution by a double bridge. Electrochemical grade tetrabutylammonium perchlorate (TBAP) in extra pure dichloromethane (DCM) was used as the supporting electrolyte at a concentration of 0.10 mol/dm^3.

References

[1] D. D. Perrin, W.L.F. Armarego, Purification of Laboratory Chemicals. 2nd ed. 1989, Oxford, Pergamon Press.
[2] D. Wöhrle, M. Eskes, K. Shigehara, A. Yamada, A simple synthesis of 4,5-disubstituted 1,2-dicyanobenzenes and 2,3,9,10,16,17,23,24-octasubstituted phthalocyanines, Synth, 2, 1993, 194-196.